

DRUG DISCOVERY AND DEVELOPMENT OF RESISTANCE IN *NAEGLERIA FOWLERI* IDENTIFIES POTENT COMPOUNDS AND NOVEL TARGETS TO TREAT PRIMARY AMOEBIC MENINGOENCEPHALITIS

by

BEATRICE LOURDES COLON

(Under the Direction of Dennis Kyle)

ABSTRACT

Primary amoebic meningoencephalitis (PAM) is >97% fatal disease caused by the brain-eating amoeba, *Naegleria fowleri*. The amoeba can infect immunocompetent individuals when it enters the nasal cavity and begins feeding on the nasal epithelium and olfactory nerves as it travels towards the frontal lobe of the brain. In this study, we developed a high-throughput assay to identify active compounds that inhibit amoebic growth. With this assay, we screened a library of amidines and diamidines that were known to be active against other infectious diseases such as *Trypanosoma* spp. and *Leishmania* species. We found that the bis-benzimidazole amidines and diamidines were the most potent compounds against the pathogenic *N. fowleri*. Additionally, we screened a library of FDA-approved compounds to identify the potential of repurposing drugs for PAM. In this study, we identified posaconazole to be among the fastest compounds that inhibit amoebic growth *in vitro*. In addition, In the murine PAM

model we found 33% of *Naegleria*-infected mice treated with 3 doses of posaconazole survived. Moreover, when testing posaconazole in combination with azithromycin, we found a 40% increased survival of mice when compared to the fluconazole-azithromycin combination. From the results of this study, we propose to include posaconazole in PAM treatments instead of fluconazole. In the last portion of this project, we developed resistance to a potent bis-benzimidazole amidine, DB 2518, to elucidate a potential mechanism of action. We characterized multiple phenotypic differences to compare with the genotypic variations identified through whole-genome sequencing. We hypothesize from the decreased size of trophozoites and number of lysosomes in the resistant clones, that ion binding, lyase or hydrolase mutated genes may be likely targets for the bis-benzimidazole, DB 2518.

INDEX WORDS: *Naegleria fowleri*, primary amoebic meningoencephalitis, drug discovery, bis-benzimidazoles, posaconazole, drug repurposing, animal studies, drug-resistance, whole genome sequencing, drug targets

DRUG DISCOVERY AND DEVELOPMENT OF RESISTANCE IN *NAEGLERIA*  
*FOWLERI* IDENTIFIES POTENT COMPOUNDS AND NOVEL TARGETS TO  
TREAT PRIMARY AMOEBIC MENINGOENCEPHALITIS

by

BEATRICE LOURDES COLON

BS, University of Illinois at Urbana-Champaign, 2011

MSc, University of South Florida, 2012

A Dissertation Submitted to the Graduate Faculty of The University of Georgia in  
Partial Fulfillment of the Requirements for the Degree

DOCTOR OF PHILOSOPHY

ATHENS, GEORGIA

2018

© 2018

Beatrice Lourdes Colon

All Rights Reserved

DRUG DISCOVERY AND DEVELOPMENT OF RESISTANCE IN *NAEGLERIA*  
*FOWLERI* IDENTIFIES POTENT COMPOUNDS AND NOVEL TARGETS TO  
TREAT PRIMARY AMOEBIC MENINGOENCEPHALITIS

by

BEATRICE LOURDES COLON

Major Professor: Dennis Kyle  
Committee: Silvia Moreno  
David Peterson  
Rick Tarleton  
Adrian Wolstenholme

Electronic Version Approved:

Suzanne Barbour  
Dean of the Graduate School  
The University of Georgia  
December 2018

## DEDICATION

I would like to dedicate this work to my mom, dad, and brother: Lourdes, Vince and Matthew. The unwavering support and love from each of you is what has fueled this work on the most difficult of days.

## ACKNOWLEDGEMENTS

There are many individuals to thank for the completion of this study. First and foremost, I would like to thank my mentor, Dr. Dennis Kyle, for the opportunity to be one of the first “amoeba wranglers” in the lab. The mentorship and opportunities you have provided have truly shaped me into an independent scientist and I am truly grateful for the experience. I would also like to thank Dr. Christopher Rice for your support, patience, guidance, and feedback throughout my PhD. You have taught me so much in the lab, but also in “The University of Life.” I would also like to thank the many chemists over the years that we have collaborated with for their interest and effort to find a treatment for this disease, especially Dr. David Boykin and his lab.

Many thanks to my committee from the University of Georgia and my previous committee from the University of South Florida: Drs. Silvia Moreno, David Peterson, Rick Tarleton, and Adrian Wolstenholme and Drs. Robert Deschenes, Andreas Seyfang, and Lynn Wecker. The guidance and advice over the years has truly been invaluable.

I would like to thank all of the past and present Kyle Lab members for their feedback with this project throughout the years. I would like to specifically thank: Adonis, Amanda, Chris, Emma, Marvin, and Sasha. You have all helped in different ways, but each of you have left such an impression on this work and my scientific development. I would like to thank our lab neighbors, the members of

the Moreno lab and the Docompo lab, especially Stephen Vella and Ciro Cordeiro for all of their help and support while I was finishing my project. I would like to thank Rodrigo de Paula Baptista for the incredible amount of work he has done in the minimal amount of time we had to finish the genotype analysis. Lastly, I would like to thank our funding, the work in this project would not have been possible without the support from NIH (R21AI103664 and R21AI119787) and the Georgia Research Alliance.



## TABLE OF CONTENTS

	Page
ACKNOWLEDGEMENTS .....	v
LIST OF TABLES .....	ix
LIST OF FIGURES .....	xi
CHAPTER	
1 INTRODUCTION AND LITERATURE REVIEW .....	1
Pathogenic free-living amoebae .....	1
Primary amoebic meningoencephalitis .....	4
Diagnosis and treatment .....	6
Amphotericin B .....	6
Miltefosine.....	8
Azithromycin .....	9
Fluconazole .....	11
Drug discovery.....	13
Focus of study .....	14
2 BIS-BENZIMIDAZOLE HITS AGAINST <i>NAEGLERIA FOWLERI</i> DISCOVERED WITH NEW HIGH-THROUGHPUT SCREENS.....	15
Abstract.....	16
Introduction .....	17
Materials and methods.....	21

Results.....	25
Discussion .....	28
3 PHENOTYPIC SCREENS REVEAL POSACONAZOLE AS RAPIDLY CIDAL COMBINATION PARTNER FOR TREATMENT OF PRIMARY AMOEBIC MENINGOENCEPHALITIS .....	46
Abstract.....	47
Introduction.....	47
Materials and Methods.....	50
Results.....	54
Discussion .....	60
4 DB 2518-RESISTANT <i>NAEGLERIA FOWLERI</i> ELUCIDATES POTENTIAL TARGETS FOR DRUG DISCOVERY .....	79
Introduction.....	79
Materials and Methods.....	81
Results.....	86
Discussion .....	89
5 CONCLUSION .....	110
REFERENCES.....	114
APPENDICES	
A American Society for Microbiology Copyright .....	128
B Oxford University Press Copyright .....	129

## LIST OF TABLES

	Page
Table 2.1: Susceptibility of <i>Naegleria fowleri</i> to amphotericin B, miltefosine, and diamidines <i>in vitro</i> .....	34
Table 2.2: Bis-benzimidazole amidines evaluated for activity against <i>N. fowleri in vitro</i> .....	35
Table 2.3: Bis-benzimidazole diamidines evaluated for activity against <i>N. fowleri in vitro</i> .....	36
Table 2.4: <i>In vitro</i> activity of furamide derivatives against <i>N. fowleri</i> .....	37
Table 2.5: <i>In vitro</i> activity of linear benzimidazole types against <i>N. fowleri</i> .....	38
Table 2.6: <i>In vitro</i> activity of central indole ring diamidines against <i>N. fowleri</i> .....	39
Table 2.7: <i>In vitro</i> activity of arylimidamide derivatives against <i>N. fowleri</i> .....	40
Table 2.8: <i>In vitro</i> activity of additional arylimidamide derivates.....	41
Table 2.9: Comparative potency and cytotoxicity of amidino derivatives against <i>Naegleria fowleri</i> , bacteria, fungi and rat myoblast <i>in vitro</i> . .....	42
Table 3.1: Primary amoebic meningoencephalitis patient isolates .....	66
Table 3.2: Active FDA-approved compounds identified from the St. Jude Children’s Research Hospital library.....	67
Table 3.3: Active compounds from the Medicines for Malaria Venture (MMV) Pathogen Box .....	68
Table 3.4: Dose-response data from a collection of anti-parasitics (n=2). .....	69

Table 4.1: Comparison of the structurally similar bis-benzimidazole amidines with Hoechst stain.....	94
Table 4.2: Cross-resistance among resistant clones .....	95
Table 4.3: Mutated sequences identified in the resistant clone, AB7 .....	96

## LIST OF FIGURES

	Page
Figure 2.1: Quantitative dose-response data for <i>Naegleria fowleri</i> demonstrating similar activities of amidino compounds in the alamarBlue (AB) and CellTiter-Glo (CTG) assay formats. ....	43
Figure 2.2: Structural classes of amidino compounds screened against <i>Naegleria fowleri</i> .....	44
Figure 2.3: Optimization of AB and CTG assays for <i>N. fowleri</i> drug discovery....	45
Figure 3.1: Single point assays of FDA-approved compounds from the St. Jude Children’s Hospital Library .....	70
Figure 3.2: Standard curve displaying the linearity between the number of amoeba per well and relative luminescent units (RLUs) for the RealTime-Glo assay that was used to identify the rate of inhibition .....	71
Figure 3.3: Rate of inhibition at 1x-IC <sub>50</sub> for drugs in the current PAM treatment..	72
Figure 3.4: Rate of inhibition at 5x-IC <sub>50</sub> for drugs in the current PAM treatment..	73
Figure 3.5: Isobolograms of posaconazole with azithromycin .....	74
Figure 3.6: Kaplan-Meier survival curves for female ICR mice dosed intravenously with posaconazole .....	75
Figure 3.7: Kaplan-Meier survival curves for female ICR mice dosed intravenously with posaconazole replicate .....	76

Figure 3.8: Survival curves of mice infected with <i>N. fowleri</i> and dosed with combinations of azithromycin and conazoles.....	77
Figure 3.9: IC <sub>50</sub> s of multiple CDC isolates and NF69.....	78
Figure 4.1: Development of resistance for <i>N. fowleri</i> to DB 2518.....	102
Figure 4.2: Work flow describing the identification of potential genes that are mutated in AB7 in comparison to DD8 and the clones. ....	103
Figure 4.3: Dose-response curves for DB 2518 with NF69 and NF69 cultures grown with 50x-IC <sub>50</sub> of DB 2518 .....	104
Figure 4.4: Half maximum inhibitory concentrations of DB 2518 with clones of <i>N. fowleri</i> grown under DB 2518 drug pressure and grown under normal conditions .....	105
Figure 4.5: Growth rate differences DB 2518-resistant clones, sensitive clones, and the reference strain .....	106
Figure 4.6: Area of trophozoites from resistant clones and sensitive clones .....	107
Figure 4.7: Nuclear staining with Hoechst 33342 of resistant clone and sensitive clone .....	108
Figure 4.8: Fluorescent imaging with DAPI and LysoTracker Red identifies a decrease in acidic vacuoles in resistant clones. ....	109

## CHAPTER 1

### INTRODUCTION AND LITERATURE REVIEW

#### **PATHOGENIC FREE-LIVING AMOEBAE**

*Naegleria fowleri*, *Acanthamoeba* spp., and *Balamuthia mandrillaris* are free-living amoebae that are found ubiquitously in the environment within the soil, saltwater or freshwater. While these amoebae most often feed on bacteria and detritus in the environment, they are capable of invading hosts and feeding on the tissue. These amoebae have been termed amphizoic amoebae because of their ability to live freely in the environment, but also within hosts if the opportunity arises [1].

*Naegleria* is unique among these pathogenic free-living amoebae because they are able to form flagella [1]. Most commonly *Naegleria* exists as a trophozoite or cyst. The trophozoite stage is the metabolically active stage where they feed and reproduce by binary fission. The cyst stage is a protective form that can be induced in low-nutrient environments or colder temperatures [2]. Both the trophozoite and flagellate forms are known to cause infection, however it is plausible that cysts could enter the nasal passage and then excyst into trophozoites to cause infection.

These flagellate amoebae were first discovered by Schardinger in 1899 who classified them as *Amoeba gruberi* [3]. By 1912 Alexeieff proposed to name

the genus *Naegleria* after Nägler, who described replication of *Amoeba limax* to be “promitotic” [4]. It was not until decades later that pathogenic *Naegleria* species were discovered to cause the fatal human disease, primary amoebic meningoencephalitis [5]. These amoebae were then classified as *Naegleria fowleri* after the physician Malcolm Fowler, who first described the infection [6]. Although species such as *N. australiensis* and *N. italica* have been found to be pathogenic in experimental animals, only *N. fowleri* has been identified in human infections and is the only pathogen to cause primary amoebic meningoencephalitis (PAM) [3].

*Acanthamoeba* spp. are less motile than *Naegleria* and exists either in the metabolically active trophozoite stage or as a resilient, dormant cyst [1,2]. *Acanthamoeba* was first isolated in 1913 by Puschkarew, but these amoebae were not known to cause pathogenesis until 1958 [7–9]. Decades later over 24 species have been identified and categorized into three classes based on cyst shape and size. Pathogenic *Acanthamoeba* spp. are known to cause either granulomatous amoebic encephalitis (GAE) or cutaneous acanthamoebiasis in immunocompromised individuals and amoebic keratitis (AK) in immunocompetent individuals [2,10,11]. *Balamuthia mandrillaris* was later isolated in 1986 from a mandrill baboon, but was not classified until 1993 [2,12]. To date, *Balamuthia mandrillaris* is the only species identified to cause balamuthiasis, a similar disease to GAE [2,12].

When *B. mandrillaris* or pathogenic *Acanthamoeba* spp. are introduced into an immunocompromised individual, these amoebae can systemically spread



and can cross the BBB causing an encephalitis with multiple hemorrhagic and necrotic lesions [13]. Both of these amoebae are able to form lesions outside of the brain and have been identified in organ transplant patients [14,15]. GAE is an insidious disease taking weeks to months to form hemorrhagic lesions throughout the brain. Patients exhibit many CNS symptoms such as headache, nausea, vomiting, stiff neck, seizures, and coma [2,11,16].

More commonly, pathogenic *Acanthamoeba* spp. are able to cause AK in immunocompetent individuals. AK cases are most often associated with poor contact lens care [2,17,18]. In these cases, the amoebae feed on the cornea causing a corneal ulcer and ultimately blindness, if left untreated. Patients may undergo an extensive drug therapy and corneal transplant but is often not curative because *Acanthamoeba* spp. are able to form resilient cysts that withstand many of the prescribed therapeutics [19,20].

Since treatments are harsh and maintained for weeks to eliminate *Acanthamoeba*, the therapies differ among patients and depend on various factors including CNS involvement, immunocompetency and renal function. Drug therapy of GAE survivors includes a combination of ketoconazole, trimethoprim-sulfamethoxazole and rifampin [21], or sulfadiazine, pyrimethamine, and fluconazole [22]. Survivors of cutaneous amoebiasis have been treated with combinations of pentamidine, chlorhexidine, ketoconazole, itraconazole [23,24], amphotericin B, fluorocytosine, azithromycin, and clarithromycin [24]. Beyond corneal transplants, AK patients undergo a vigorous treatment of

polyhexamethylene biguanide (PHMB) [25–29], chlorhexidine [29,30] and propamidine [28–30] as either mono-therapy or combinatorial therapy [11].

## **PRIMARY AMOEBIC MENINGOENCEPHALITIS**

*Naegleria fowleri* is the only species that is known to cause primary amoebic meningoencephalitis (PAM), a fulminant disease that is 97% fatal in healthy individuals [31]. PAM is associated with exposure to untreated warm freshwater in either aquatic recreational activities, sinus irrigations or nasal ablation, which is a ritual cleansing of the nasal cavity [31–34]. From a study collating case reports in the US, there were 44 PAM cases that had a single exposure to warm fresh water prior to onset of symptoms. Of those patients, the median time period of inoculation before patients experienced symptoms was 5 days. Furthermore, once patients experienced symptoms, there was an average of 5 days until patients succumbed to death (n=103) [31].

Unlike other encephalitides, *N. fowleri* trophozoites do not need to cross the blood-brain barrier (BBB) in order to cause disease. Early studies have aimed to identify the route by which the amoebae cause disease by inoculating mice with *N. fowleri* trophozoites and monitoring disease progression with microscopy [35–37]. Within the first 8 hours post-inoculation, some amoebae are seen to penetrate the mucosal layer and adhere to the olfactory epithelium [35]. Amoebae are then seen to penetrate the sustentacular cells of the olfactory epithelium and continue migration to the submucosal nervous plexus and lamina propria [37]. Interestingly, Rojas-Hernandez et al. report a potential secondary

mechanism of entry through the respiratory epithelium [35]. At 30 hours post-inoculation, trophozoites are seen to traverse the cribriform plate of the ethmoid bone and invade the olfactory bulb, which rests directly above the plate. Severe tissue damage is not seen until 96 hours post-infection. At this time, inflammatory cells are abundantly seen in the olfactory bulb and there is an increase in number of trophozoites [35]. Once the amoebae reach the neuronal tissue, they are localized to the olfactory bulb and frontal lobe [38]. Five days post-infection, hemorrhages, edema, and swelling are seen in the olfactory bulb and cerebral hemispheres [37].

The murine model of primary amoebic meningoencephalitis is thought to be a close representation of disease in humans [36]. In both instances, amoebae are introduced through the nasal cavity and migrate to the olfactory bulb and frontal lobe of the brain affecting similar nasal and neuronal structures. Similarly in both mice and humans, there is a short incubation time and death within a week post-infection [36,37].

The mechanisms by which *N. fowleri* digests tissue are not well understood. However, recent studies have begun looking at the capability of *N. fowleri* to degrade various proteins. Cysteine proteases, in particular, have been shown to be essential in degrading human hololactoferrin, hemoglobin, and human holotransferrin [39]. Interestingly, other human pathogens, such as *Entamoeba histolytica*, have also been identified to use hololactoferrin to acquire iron [40].

## **DIAGNOSIS AND TREATMENT**

Unfortunately, 27% of PAM patients from 1951-2013 (n=89) were discharged when they presented with symptoms suggesting a severe lack of PAM awareness amongst clinics, primary care providers and hospitals. [31]. According to the Centers for Disease Control and Prevention (CDC), approximately 75% of PAM patients in the United States are diagnosed in autopsy. For those who are diagnosed prior to autopsy, *N. fowleri* can be detected in the cerebrospinal fluid (CSF) or in biopsy samples with polymerase chain reaction (PCR), microscopy, antigen detection, or culture [31].

Many of the treatments for PAM have been used to treat other infections and empirically chosen to treat PAM patients, rather than using drugs that have experimental evidence of inhibiting amoebae growth *in vitro* or *in vivo*. The current PAM therapy is based from the recent successful cure, which includes: amphotericin B, miltefosine, azithromycin, fluconazole, rifampin, dexamethasone and therapeutic hypothermia [41].

### **AMPHOTERICIN B**

Amphotericin B is a broad spectrum antifungal that has been used to treat fungal diseases such as histoplasmosis, coccidiomycosis, cryptococcosis, *Candida* infections, aspergillosis [42]. Amphotericin B works in fungi by irreversibly binding to ergosterol, which creates a leaky membrane. Amphotericin B has been shown to bind more stably to ergosterol and forms wider channels than with the binding of cholesterol [43]. There is serious renal toxicity with

chronic use of amphotericin B [44]. This is a potential problem for PAM patients since a recent survivor was treated for 28 days on a combination of antimicrobials, though amphotericin was decreased after 2 days and removed after 8 days [41].

Amphotericin B was first used for a PAM case in 1969 because of its success with CNS fungal diseases and preliminary data with *N. fowleri* patient isolates [31]. However, the first PAM survivor was nearly a decade later in 1978 with a combination of intravenous and intrathecal amphotericin B and miconazole, rifampin orally, intravenous sulfisoxazole, dexamethasone, and phenytoin [31,45]. Samples from this patient were cultured to identify which treatments were successful at inhibiting the growth of amoebae. Seidel et al. identified amphotericin B with miconazole to be synergistic with this patient isolate, but rifampin showed no inhibition [45].

Although PAM case evidence does not show amphotericin B to be an effective treatment, with over the 97% fatality in cases, there is some evidence for amphotericin B in both *in vitro* and *in vivo* models [31]. An early study with a *N. fowleri* patient isolate showed amphotericin B to inhibit the amoebae with 0.075 $\mu$ g/ml *in vitro*. Additionally, 7.5mg/kg amphotericin B dosed for 14 days protected 60% of mice (n=20) infected with *N. fowleri*. Unrealistically, these mice received their first dose of amphotericin B 24 hours prior to inoculation with the amoebae [46]. The protection seen with amphotericin B in this study is most likely due to treating the animals before they have been infected. Unlike in

human PAM cases where many patients do not seek treatment until 5 days post-infection [31].

Additional studies have also verified the activity of amphotericin B *in vitro* by using a patient isolate passaged through mice to keep virulence (Lee M67 strain). Goswick and Brenner also found 0.1 µg/ml of amphotericin B to inhibit the growth on amoebae in a culture flask after 72 hours of drug exposure [47]. In their *in vivo* model, mice began treatment 72 hours after infection and were dosed for 5 consecutive days. Goswick and Brenner found 7.5mg/kg of amphotericin B protected 50% of mice [47]. However, when evaluating the efficacy of amphotericin B with a different clinical isolate (ATCC 30215) in a high-throughput luminescence assay or absorbance assay, the IC<sub>50</sub> of amphotericin B was found to be 47 µM [48].

## **MILTEFOSINE**

Miltefosine is an alkylphosphocholine drug that was originally registered as an anti-cancer therapeutic for cutaneous metastasis of breast cancer, although activity of trypanosomatids was also indicated [49,50]. In 2002, miltefosine was approved as the only oral drug treatment for visceral leishmaniasis [51]. Many studies have looked at the mechanism of action of miltefosine in *Leishmania* spp. and have found varying results, suggesting miltefosine most likely acts on multiple targets. As shown by the differences in lipid biochemical pathways between miltefosine-resistant *Leishmania donovani* and wildtype, lipid metabolism may be a likely target [52]. Specifically,

miltefosine-resistant *L. donovani* were found to have a lower amount of unsaturated fatty acids than wildtype, indicating resistant parasites may have less fluid membranes [52]. Additional significant differences between length of alkyl chains in resistant and wildtype clones suggest miltefosine may target fatty acid alkyl chain elongation [52]. In *Leishmania infantum*, Moreira et al. showed that miltefosine-resistant parasites were able to evade apoptosis by measuring reactive oxygen species (ROS) levels, gDNA degradation, and decrease in mitochondrial membrane potential [53]. Furthermore, resistant parasites also showed cross-tolerance to trivalent antimony, miltefosine and amphotericin B that caused apoptosis in sensitive parasites [53].

Since 2009, miltefosine has been used to treat free-living amoebae infections [54]. However, it was not until 2013 that two PAM patients survived with the recommended therapy [31,55,56]. Much of the success in the 2015 PAM case was in part to the familiarity of disease within the hospital, which led to a quick identification, diagnosis and administration of treatments.

## **AZITHROMYCIN**

Azithromycin is a 15-membered ring azalide antibiotic that was derived from erythromycin in the 1980s [57]. In bacteria, azithromycin is known to inhibit mRNA translation by binding to the 50s subunit of the ribosome and not allowing proper formation of the large ribosomal subunit [58]. The mechanism of action of azithromycin in *N. fowleri* is unknown. Importantly, azithromycin is known to cross the BBB. In a human study sampling brain biopsies 24, 48, 72, or 96 hours

after a single oral dose of azithromycin (500mg) found concentrations of 2.63, 3.64, 0.74, and 0.41 $\mu$ g/g, respectively [59].

In a 6 day assay with clinical strains of *Acanthamoeba* isolated from brain biopsy samples at autopsy, azithromycin was found to be active at 5 $\mu$ g/ml [60]. In contrast, within the same assay clarithromycin and erythromycin were found to be inactive against the isolates [60]. In the same study, various *Acanthamoeba* isolates were screened at 1, 5 and 10 $\mu$ g/ml. All isolates tested showed >80% inhibition suggesting azithromycin is not species specific. However, when removing drug from cells to identify if azithromycin was amoebicidal, the amoebae continued to grow similar to controls, suggesting azithromycin is amoebastatic [60].

Due to the activity of azithromycin with *Acanthamoeba*, Goswick and Brenner tested 1, 10 and 100 $\mu$ g/ml over a 7 day period against *N. fowleri* [47]. They found 1 $\mu$ g/ml to be inactive, but 10 $\mu$ g/ml began inhibiting growth at 24 hours [47]. Additionally, azithromycin was tested in the murine PAM model at 25mg/kg and 75mg/kg. Goswick and Brenner found 75mg/kg of azithromycin to cure 100% of infected mice, while 25mg/kg of azithromycin cured 40% of mice. Interestingly, the remaining 60% mice that did succumb to death survived an average of 7.3 days longer than control mice [47].

Once azithromycin was found to be active *in vivo*, Soltow and Brenner investigated the synergistic potential when in combination with amphotericin B. They found the sum of the fractional inhibitory concentration ( $\Sigma$ FIC) from *in vitro*



combinations to be between 0.3-0.7 with either 48 or 72 hours of drug exposure, suggesting that amphotericin B and azithromycin are mildly synergistic *in vitro* against the Lee M67 strain of *N. fowleri* [61]. Moreover, *in vivo* combination studies showed 100% survival of infected mice that were treated with 2.5mg/kg of amphotericin B and 25mg/kg of azithromycin. Whereas, only 45% of mice survived with 2.5mg/kg of amphotericin B and only 55% survived with 25mg/kg of azithromycin [61].

With mounting experimental evidence, azithromycin was given in combination with miltefosine, fluconazole, amphotericin B, and rifampin to two PAM patients in 2013; both patients survived [31,55]. Since 2013, azithromycin has been suggested by the CDC to be added into the PAM treatment regimen [31].

## **FLUCONAZOLE**

Fluconazole is an antifungal that affects ergosterol by blocking the precursor, lanosterol, from being catalyzed by 14- $\alpha$ -demethylase (CYP51). CYP51 belongs to the cytochrome P-450 enzyme family. NfCYP51 has been identified in the *Naegleria* genome, which validates the importance of CYP51 as a potential drug target [62]. Furthermore, there was approximately a 35% similarity to the human CYP51 and a greater similarity to *Acanthamoeba* and *N. gruberi* [62]. As shown with multiple *Candida* spp., different conazoles have different affinities to inhibiting CYP51 [63]. A recent study used UV-vis spectroscopy to identify the interactions between different conazoles and

NfCYP51. Debnath et al. found that conazoles with a greater molecular weight interacted more with NfCYP51 than the smaller molecular weight conazoles, such as fluconazole [62].

Conazoles have been used since the 1978 PAM case [31]. Moreover, fluconazole or miconazole have been included in the extensive combination therapy of PAM survivors [31,41,45,64]. Fluconazole has been chosen as the conazole of choice because it is thought to cross the BBB more efficiently due to its low molecular weight and logP value [62]. However, in a disease such as PAM where the BBB is likely leaky due to the destruction and inflammation, amoebicidal activity should be given precedence.

Although fluconazole and miconazole have been used in PAM survivors, there is little *in vitro* or *in vivo* evidence of rapid, potent amoebicidal activity for fluconazole or miconazole. An early study using multiple *Naegleria* patient isolates identified miconazole to have little to no effect within 24 hours, but averaged 1 µg/ml MIC at 48 hours [65]. With a fulminant disease such as PAM, identifying drugs that have a rapid inhibition of trophozoites is crucial. The lack of potency with fluconazole is further shown with Thai patient and environmental isolates to have an MIC<sub>50</sub> > 0.50-2mg/ml and 1.75mg/ml, respectively [66,67]. Furthermore, a recent study found fluconazole to be the least potent conazole against the KUL *N. fowleri* strain (EC<sub>50</sub> = 13.9 µM); the most potent conazoles identified were itraconazole and posaconazole with an EC<sub>50</sub> <0.01 µM [62].

## DRUG DISCOVERY

Much of the drug discovery in the free-living amoebae field has been accomplished through biased, low-throughput methods. Many of the studies use large culture volumes (10-30ml per flask) to determine efficacy of drugs [47,61,68]. Considering the large volumes, the amount of amoebae needed to test the compounds is approximately 10,000 amoebae/ml [47,61,69]. Similarly, the amount of drug needed is increased to maintain the same concentrations in the larger volumes in comparison to a small volume assay. Additionally, the methods used to measure inhibition of drugs are based on manual cell counts, which can be time-consuming and biased [47,61,69–71]. With the use of large volumes of media, cells and compounds, and manual cell counts, it is understandable that only a handful of compounds reported per study rather than large library screens.

Most importantly, the experimental design of these studies does not provide a sensible opportunity to identify an effective PAM treatment. Many studies have assay lengths beyond 72 hours, which does not identify compounds that are inhibiting the amoebae growth rapidly [47,68,71]. It is important to identify rapid-acting compounds when 5 days is the median days from hospitalization to death [31]. Furthermore, many studies are using the non-pathogenic *N. gruberi* to identify compounds that would inhibit the pathogenic *N. fowleri* [69,72–75].

## **FOCUS OF STUDY**

This study has been created to identify compounds that could be used to treat PAM. First, we developed high-throughput methods using *N. fowleri* to identify potent compounds that inhibit the pathogenic amoebae. This method allowed us to screen large libraries to identify potent compounds in a quick and unbiased manner. The second goal was to further characterize potent compounds by how quickly they inhibited the amoebae, how they interacted in combination with the current treatments, and if they provided cures in the murine PAM model. After identifying a compound through structure-activity relationship studies to possess potent and rapid inhibition of amoebae, we developed resistance to identify the potential mechanism of action for the novel compound.

## CHAPTER 2

### BIS-BENZIMIDAZOLE HITS AGAINST *NAEGLERIA FOWLERI* DISCOVERED WITH NEW HIGH-THROUGHPUT SCREENS<sup>1</sup>

---

<sup>1</sup>Rice CA, \*Colon BL, Alp M, Göker H, Boykin DW, Kyle DE. (2015). Bis-benzimidazole hits against *Naegleria fowleri* discovered with new high-throughput screens. *Antimicrobial Agents and Chemotherapy*, 59:2037–2044. doi:10.1128/AAC.05122-14.

\* These authors contributed equally to this work

Reprinted here with permission from the American Society for Microbiology

## ABSTRACT

*Naegleria fowleri* is a pathogenic free-living amoebae (FLA) that causes an acute fatal disease known as primary amoebic meningoencephalitis (PAM). The major problem for infections with any pathogenic FLA is a lack of effective therapeutics, since PAM has a case mortality rate approaching 99%. Clearly, new drugs that are potent and have rapid onset of action are needed to enhance the treatment regimens for PAM. Diamidines have demonstrated potency against multiple pathogens, including FLA, and are known to cross the blood-brain barrier to cure other protozoan diseases of the central nervous system. Therefore, amidino derivatives serve as an important chemotype for discovery of new drugs. In this study, we validated two new *in vitro* assays suitable for medium- or high- throughput drug discovery and used these for *N. fowleri*. We next screened over 150 amidino derivatives of multiple structural classes and identified two hit series with nM potency that are suitable for further lead optimization as new drugs for this neglected disease. These include both mono- and diamidino derivatives, with the most potent compound (DB173) having a 50% inhibitory concentration (IC<sub>50</sub>) of 177 nM. Similarly, we identified 10 additional analogues with IC<sub>50</sub>s of < 1 μM, with many of these having reasonable selectivity indices. The most potent hits were > 500 times more potent than pentamidine. In summary, the mono- and diamidino derivatives offer potential for lead optimization to develop new drugs to treat central nervous system infections with *N. fowleri*.

## INTRODUCTION

The first report of animal pathogenicity by free-living amoebae (FLA) was by Culbertson et al., who identified *Acanthamoeba* in necrotic lesions of monkeys and mice [8]. He later suggested that FLA causes similar disease in humans. Fowler and Carter reported the first cases of an acute fatal disease caused by *Naegleria fowleri* in four victims in Australia in 1965 [76]. Since the identification of primary amoebic meningoencephalitis (PAM), hundreds of cases have been reported worldwide, including 142 cases in the United States [16,31,33]. Most infections with *N. fowleri* occur during the summer months, victims usually are symptomatic within 5 days and the disease is almost always fatal. Infection usually occurs after the victim swam in warm, fresh, or brackish water or from exposure to contaminated tap water associated with use of Neti pots for nasal irrigation[16,31,77,78]. Amoebic invasion occurs via disruption of the olfactory mucosa, penetration of organisms into the submucosal nervous plexus, and ultimately passage through the cribriform plate to the frontal lobes of the brain [37,79]. Although most cases of PAM occur in warm climates, such as the southern tier states of the United States, pathogenic amoebae found in thermally polluted water sources, hot springs, and poorly chlorinated pools have been linked to infections [70,80]. Interestingly, most of the PAM cases have been diagnosed in developed countries, including the United States, Australia, and Europe. Although sporadic cases have been diagnosed in tropical regions of the world, it is likely that many cases in these areas go undetected or misdiagnosed as bacterial or viral meningitis [31,77]. Recent evidence to support this

hypothesis includes the large number of cases reported from Pakistan that appear to be related to poor chlorination of water used for ablution, a ritual cleansing that includes nasal passages [77]. The prevalence of FLA in warm climates, the advent of global warming, and the use of immunosuppressive drugs combine to threaten expansion of the spatial distribution of pathogenic FLA with an increased incidence of disease.

The major problem for infections with any of the pathogenic FLA is the lack of effective therapeutics [31,81,82]. PAM has a case fatality rate approaching 99%, even if the infection is diagnosed promptly and treated with the best available drug regimens. For *N. fowleri* infections in the United States, only three cases have been successfully treated; all other documented cases were fatal [31]. Treatment of PAM is empirical and based upon the first few cases of successful treatment. Amphotericin B is the drug of choice for PAM and is administered intravenously and intrathecally, usually in combination with rifampin, miltefosine, other antibiotics, or antifungals. A broader array of drugs has been used to treat systemic infections with *Acanthamoeba* spp. [81]. For central nervous system (CNS), nasopharyngeal, and disseminated infections a variety of azole antifungals (e.g., ketoconazole, itraconazole), pentamidine, and cotrimoxazole are used. Despite the slower, more insidious onset of disease in systemic *Acanthamoeba* infections, the outcome of systemic *Acanthamoeba* infections is death in these (usually) immunocompromised patients. Substantially more data is available on treatment of amoebic keratitis than any other FLA infection. Most of the regimens include the topical use of microbicides



(chlorhexidine, polyhexamethylene biguanide (PHMB), and hexamidine) with or without neomycin, azoles, or antibiotics. Despite moderate success with chlorhexidine and PHMB for amoebic keratitis, both granulomatous amoebic encephalitis (GAE) and keratitis are difficult to treat due to the presence and persistence of both trophozoites and cysts of *Acanthamoeba* spp. Cysts are refractory to most drugs used to treat CNS infections; therefore, prolonged therapy is required due to this poor efficacy, prompting concerns for emergence of drug resistance. Clearly, new drugs that can be administered parenterally for neurological disease or topically for keratitis are urgently needed.

Pentamidine and propamidine are diamidines with demonstrated potency against several pathogens, including pathogenic FLA [70,81]. Both of these are reported to be active against trophozoites of *Naegleria fowleri* and *Acanthamoeba* spp. *in vitro* [70,83] and pentamidine has been used clinically in combination with other drugs for FLA infections. Brolene, a topical formulation of propamidine isothionate plus neomycin, is the first line treatment for amoebic keratitis in Europe [2]. These diamidino derivatives suffer from poor bioavailability, narrow therapeutic indices, and poor selectivity, yet they serve to validate the potential utility of the amidino chemotypes as anti-FLA drugs. In the past decade, an extensive series of amidino derivatives have been synthesized and assessed for activity as antiparasitic and antimicrobial agents. These include more than 2,000 derivatives that include dozens of structural classes with various linkers, prodrug moieties, and physiochemical properties [84–100]. Many of these compounds have potency *in vitro* and *in vivo* against a variety of parasitic

protozoa, including *Leishmania* spp., *Plasmodium falciparum*, *Trypanosoma cruzi*, and *T. brucei*. Recent data demonstrate diamidines cross the blood-brain barrier (BBB) and have efficacy in late stage animal models of human African trypanosomiasis (HAT) [101]. Several of these pyridyl diamidine derivatives achieve steady-state levels of 10 to 40  $\mu\text{M}$  in the brain of rodents dosed orally, and in recent studies DB820 cured Vervet monkeys of late stage HAT disease [84,102]. DB844, a prodrug that is rapidly converted to DB820, dosed at 5 mg/kg of body weight once a day for 5 days, cured monkeys infected with *T. brucei rodiesense* in the late-stage disease model [103]. In yet another model of CNS disease, two arylimidamides were active in BALB/c mice infected with the apicomplexan parasite *Neospora caninum* and significantly reduced the cerebral parasite burden [104]. Given the demonstrated susceptibility of FLA to diamidines and efficacy for CNS protozoal diseases, the amidino analogs are a very promising series for discovery of a new drug for the most severe forms of FLA-induced disease.

The focus of our work is to discover and develop a new drug to treat the usually fatal CNS infections caused by *N. fowleri* and *Acanthamoeba* spp. Here, we report the development and validation of new *in vitro* drug susceptibility assays for *N. fowleri*; we then used these models to screen over 150 amidino derivatives of multiple structural classes and have identified two hit series with nM potency that are suitable for further lead optimization as new drugs for these neglected diseases.

## **MATERIALS AND METHODS**

### Amoebae culture

We used an isolate of *Naegleria fowleri* (ATCC 30215) originally collected from a child that died of PAM in South Australia in 1969. Trophozoites were grown axenically at 34°C in Nelsons complete medium (NCM). NCM is composed of 0.17% liver infusion broth (BD, Sparks, MD), 0.17% D-(+)-glucose, 0.0012% sodium chloride, 0.00136% potassium phosphate monobasic, 0.00142% sodium phosphate dibasic, 0.0004% calcium chloride, 0.0002% magnesium sulfate, supplemented with 10% fetal bovine serum (FBS) and 125µg of penicillin-streptomycin. All reagents were obtained from Sigma-Aldrich (St. Louis, MO), and all experiments were performed using logarithmic-phase trophozoites.

### Development of *in vitro* drug susceptibility assays

Most previous drug susceptibility assays for *N. fowleri* are not amenable for medium- or high-throughput due to requirements of large culture volumes, long incubation periods with drug, and assay endpoints not easily optimized for automated, quantitative assessment. Therefore, we first assessed the potential for new *in vitro* assays with the goal of validating assays that could run in 96- and 384-well formats, which require no longer than 72 h of drug exposure and provided robust, quantitative endpoints for the assessment of drug response. The alamarBlue colorimetric microtiter plate assay was first described by McBride et al. for *Acanthamoeba* species [105], but has not been used previously for *N.*

*fowleri*. The assay is based upon the reduction of resazurin, a non-fluorescent dye, to resorufin by metabolically active cells. The second assay we used was the CellTiter-Glo (CTG) 2.0 luminescent cell viability plate assay that was first used with amoebae by Debnath et al. to screen for compounds active against nonpathogenic *Naegleria gruberi* [69]. The CTG assay is a quantitative assay that assesses the presence of ATP in lysed cells.

Since neither of these assays had been used with *N. fowleri* previously, we first established the optimal seeding density and length of assay (hours) for each assay in both 96- and 384-well microtiter plate formats. In brief, trophozoites of *N. fowleri* grown in NCM were seeded in triplicate at concentrations ranging from  $1 \times 10^5$  cells/ml to  $2 \times 10^6$  cells/ml for 96- and 384-well plates to determine the concentration of cells that best reduce alamarBlue at 24, 48, 72 and 96 hours (Figure 2.1). From these studies, the alamarBlue assay period was established at 72 h with the reagent added at 48 h. The optimal seeding density for the 72-h assays was determined to be 100,000 cells/well and 3,000 cells/well for 96- and 384-well formats, respectively. We similarly optimized the seeding density for 72 h in the CTG assay, determining 4,000 and 3,000 cells/well for 96- and 384-well plates formats, respectively (Figure 2.1).

#### *In vitro* drug susceptibility methods

All compounds were prepared as 5mg/ml stock solutions in dimethylsulfoxide (DMSO). A Biomek 3000 automated liquid-handling workstation (Beckman Coulter) was used to serially dilute the compounds in 2-

fold dilutions 6 or 11 times, yielding a concentration range of 24ng/ml to 50µg/ml in NCM with a final concentration of 1% DMSO. The Biomek workstation was used to transfer 10µl or 6µl of diluted compounds, followed by the addition of 100,000 or 3,000 *N. fowleri* trophozoites/well in 96- or 384-well screening plates, respectively, for alamarBlue colorimetric assays. For the CTG assays, 4,000 or 3,000 cells/well were used in white 96- or 384-well plates. The total volume for 96- and 384-well plates was 100µl and 60µl, respectively. Positive-growth control wells in the screening plates contained *N. fowleri* trophozoites in NCM, and negative growth control wells contained *N. fowleri* trophozoites in the presence of 135µM amphotericin B (Sigma, St. Louis, MO). All assay plates were incubated for 72 h at 34°C. For the alamarBlue assays, 10% of the total well volume of reagent was added 24 h before the end of incubation, and the plates were incubated a final 24 hours in complete darkness. At the end of incubation, all CellTiter-Glo 2.0 luminescent cell viability assay white plates were equilibrated to room temperature for 10 min, and 25µl or 15µl of CellTiter-Glo 2.0 reagent (Promega, Madison, WI) was added to all wells of the 96- and 384-well plates, respectively, using the Biomek 3000 workstation. The plates were placed on an orbital shaker at room temperature for 2 min to induce cell lysis. After shaking, the plates were equilibrated at room temperature for 10 min to stabilize the luminescent signal. The resulting absorbance from the alamarBlue assay was determined at 570nm and 600nm using a SpectraMax M2é (Molecular Devices, Sunnyvale, CA). The ATP bioluminescence signal was measured at 490nm using a SpectraMax L (Molecular Devices, Sunnyvale, CA). Curve fitting using

nonlinear regression was carried out using DataAspects Plate Manager analysis software to determine 50 and 90% inhibitory concentrations (IC<sub>50</sub> and IC<sub>90</sub>).

### Cytotoxicity

The cytotoxicity of compounds for J774 murine macrophages was determined by using the CellTiter 96 AQueous one-solution cell proliferation assay (Promega, Madison, WI). In brief, J774 cells were seeded at  $5 \times 10^5$  cells/well in a 96-well tissue culture plate (Corning, NY) in the presence of the serial dilutions of active drugs against *N. fowleri*. Positive-control wells contained cells and media; negative-control wells contained media alone. Cells were grown in RPMI 1640 at a pH of 7.2 supplemented with 10% fetal bovine serum and 1% penicillin-streptomycin (all supplied from Invitrogen Corp., Carlsbad, CA). The inhibitor concentration started at 50µg/ml and was diluted in doubling dilutions to assess cytotoxicity compared to that of *Naegleria fowleri*. The total volume of each well was 100µl and plates were incubated at 37°C, 5% CO<sub>2</sub> for 72 h. Four h before the assessment time point, 20µl of 3-(4,5-dimethylthiazol-2-yl)-5-(3-carboxymethoxyphenyl)-2-(4-sulfophenyl)-2H-tetrazolium (MTS; Promega, Madison, WI) was added to each well. Inhibition of J774 growth was assessed at the 72-h time-point, measuring the optical density (OD) values determined at 490nm using a SpectraMax M2é. Curve fitting using nonlinear regression was carried out using DataAspects Plate Manager analysis software to obtain IC<sub>50</sub> and IC<sub>90</sub> values.

## Compounds

Miltefosine was purchased from Cayman Chemical Company (Ann Arbor, MI), whereas other standard drugs were obtained from Sigma-Aldrich (St. Louis, MO). The amidino derivatives studied have been reported previously, and their purity was verified by elemental analysis and nuclear magnetic resonance spectroscopy. Representative references to their synthesis are the following: type I [90,106], type II [86,99,100], type III [96], type IV [97], type V [87], and type VI [93]. Hexamidine and octamidine were synthesized by using established methods.

## **RESULTS**

### Validation of drug susceptibility assays

Two drug assays, alamarBlue and CTG were assessed in both 96- and 384-well plate formats to enable medium- and high-throughput applications for *N. fowleri* drug discovery. Since the overall goal of our efforts was to discover new drugs that are potent and have rapid onset of action, we validated the assays with 72 h of drug exposure. Quantitative dose-response data in the alamarBlue and CTG assays for standard drugs as well as new amidino inhibitors were similar regardless of the method used (Figures 2.1 and 2.2). Compared with previous methods, the efficacies of amphotericin B, pentamidine, and miltefosine in the alamarBlue and CTG assays were reduced (Table 2.1) yet consistent between the two new methods and in 96-or 384-well format.

### Screening results for amino series

Previous studies demonstrated activity of diamidino derivatives (e.g., pentamidine and propamidine) against pathogenic FLA [70,83] with octamidine and hexamidine found to be the most active derivatives against *Acanthamoeba* spp. *in vitro* [83]. Against *N. fowleri in vitro*, pentamidine, hexamidine, and propamidine were inactive, and octamidine was only moderately active ( $IC_{50} = 89.1\mu\text{M}$ ; Table 2.1), suggesting an inherent difference in susceptibility to diamidines between different pathogenic free-living amoebae.

Multiple furamidine derivatives were shown to cross the BBB and possess efficacy against several parasitic protozoa [84]. Therefore, amidino derivatives possess potential for discovery of novel, more potent derivatives as leads for the development of new drugs to treat CNS infections with *N. fowleri*. We evaluated over 150 amidino derivatives and related compounds that represent six major focused structural classes (summarized in Figure 2.3) and two miscellaneous groups of cationic compounds (diamidines and diguanidines; structures not shown). Our objective was to identify compounds with  $IC_{50}$  values of  $\leq 1\mu\text{M}$  and selectivity indices (SI)  $> 10$  as hits for further development. Two of the six groups of compounds (types I and II) presented in Figure 2.3 yielded compounds that met this standard. Three of the other four groups (IV-VI) yielded at least one compound that produced an  $IC_{50}$  near  $10\mu\text{M}$ . Consequently, we selected types I and II for further lead optimization, since several compounds were identified in each group with  $IC_{50}$ s  $< 1\mu\text{M}$  against *N. fowleri* and involved structures which



could be readily modified in an effort to improve activity, selectivity, and physical properties.

#### SAR studies of type I monoamidino compounds

In the initial screens of amidino compounds, we identified the bis-benzimidazole monoamidines as hits with remarkable potency compared to pentamidine. Five of the type I series (DB173, DB183, DB210, HG17 and HG24 in Table 2) exhibited  $IC_{50}$ s  $<1\mu\text{M}$  and provided reasonable SI. The most active compound was DB173, with an  $IC_{50}$  of  $0.177\mu\text{M}$  (Table 2.2). Six additional type I analogs produced  $IC_{50}$ s between 1 and  $10\mu\text{M}$ . The structure-activity relationship (SAR) of the type I compounds was not obvious given the divergent results obtained with fairly minor changes in structures; however, the set represents a significant hit that merits further optimization.

#### Optimization of type II diamidino compounds

Five compounds of the type II series produced  $IC_{50}$ s below  $1\mu\text{M}$ ; however, only one of those (DB1766) exhibited an acceptable SI value ( $\geq 10$ ). Three other active compounds (DB1684, DB1734 and DB1736) exhibit reasonable SI values (8.4 to 9.8) for early lead compounds. For the type II class, we have data for approximately 15 analogues (Table 2.3) that allow limited SAR conclusions to be drawn. Clearly, with type II compounds, we must diligently seek compounds with improved SI values. Often, cytotoxicity SARs are not obvious, and diamidines are no exception; however, we have found excellent SIs for numerous classes of

diamidines [96,98,107], and we expect that we can successfully achieve similar results with type II compounds. Future studies will explore several approaches to determine the minimum size of the bis-benzimidazole diamidines (type II) that retain activity in an effort to identify a lead with physical properties that allow penetration of the BBB.

#### Screening results for type III-VI amidino analogs

The furamidine analogs (Type III; Table 2.4) produced IC<sub>50</sub>s ranging from 31 to 84 μM. The reduced potency of the furamidine analogs was disappointing, given this series contained four compounds known to penetrate the BBB in both mice and monkey models for late-stage HAT disease. The linear benzimidazoles (type IV; Table 2.5) and the indoles (type V; Table 2.6) each yielded at least one compound with IC<sub>50</sub>s near 10 μM, although most compounds in these series were not potent against *N. fowleri* amoebae. Similarly, the arylimidamides (type VI; Table 2.7) had only one compound with an IC<sub>50</sub> near 10 μM. Finally, a series of miscellaneous amidino derivatives, mostly diamidines and diguanidnes, were uniformly inactive against *N. fowleri in vitro*. Other miscellaneous amidino derivatives (>50 μM) were found to be inactive and were not considered for lead optimization (Table 2.8).

## **DISCUSSION**

The drugs that are currently used for treating pathogenic FLA infections have not been discovered and developed prospectively. Amphotericin B,

antifungals, antibiotics, and microbicides available for other indications have been applied to the treatment of FLA in an empirical approach to find curative drugs [81]. Amphotericin B, pentamidine, propamidine, miltefosine, and azoles are drugs that were developed originally against other pathogens but also were found to possess limited to moderate *in vitro* or *vivo* efficacy against pathogenic FLA infections. Since no large-scale drug-screening programs have been initiated for pathogenic FLA and there have not been any hit expansion or lead optimization of new chemotypes, a strategy for drug discovery for FLA had to be established. In this study, we aimed to develop a discovery paradigm to identify, evaluate, optimize, and advance new molecules towards the clinic for use as new therapies for pathogenic FLA. The primary enabling technology is new, quantitative *in vitro* methods for whole-cell phenotypic screens. This is the primary tool that enhances early drug discovery by supporting screens of large libraries of compounds and quantitative assessment of antiparasitic efficacy sufficient for structure-activity relationship studies. Secondly, animal models of disease are required that mimic human disease, are amenable to infection with the human pathogen, and are validated by efficacy of known curative or partially efficacious drugs. These tools then are used to provide quantitative efficacy data required to fuel medicinal chemists' efforts to optimize structure-activity properties. Similar strategies and drug discovery pathways are used for novel antimalarial and antileishmanial drugs [108,109].

Most previous *in vitro* assays for the assessment of anti-FLA drug screening are not amenable for high- or even medium-throughput screening.

Endpoints for growth usually include morphology and visual counting of amoebae, assessment of viability that requires days to weeks, or release of lactate dehydrogenase [47,68,70,71,110]. In addition, these methods use large volumes of culture media (e.g., > 10ml) in flasks and require extended incubation periods up to 6 days [47,68,70,71,110]. These methods are simply too cumbersome to support modern drug discovery requirements. Given the lack of *in vitro* assays for medium- to high-throughput drug susceptibility testing, we developed and validated two methods for HTS in 96- and 384-well plates and used the methods for the first time with pathogenic *N. fowleri* (rather than nonpathogenic *N. gruberi*) [105].

The potencies of amphotericin B and pentamidine were significantly lower in the two new assays used in this study than in previous experience (Table 2.1). These differences likely are due to a much longer exposure to drug, since some assays were up to 6 days compared to the 72-h assays used in this report. Second, the number of amoebae used per ml was higher in the alamarBlue assay than in some previously published methods (Table 2.1). Despite any differences, the reduced efficacy observed in the 72-h assay formats was similar regardless of the end point used (alamarBlue or CTG); therefore, it is likely that the new assays reflect the inherent lack of potency and slow onset of action of most of the drugs currently used to treat FLA infections. Another factor that may reduce potency in all assay formats is the requirement for highly complex media (e.g., NCM) with multiple components that can serve as a sink for drugs and reduce the free concentration needed to affect the parasite. Regardless, the

72-h assay format we used successfully enabled the discovery of compounds with potency more than 500 times that of previously described diamidines. The 72-h assays we used have multiple advantages, including reproducible, quantitative endpoints that are important for medicinal chemistry optimization, as well as enabling the detection of compounds with a more rapid onset of action. Given the rapidly progressive, fatal disease caused by *N. fowleri*, it is important to focus drug discovery efforts on compound series with rapid onset of action and to prioritize these over other scaffolds for lead optimization.

By using the new quantitative assays for assessing efficacy against *N. fowleri in vitro*, we have identified compounds that appear to be much more potent than currently used drugs for PAM. Our predetermined criteria for a hit was potency ( $IC_{50} \leq 1\mu M$ ) and a SI  $> 10$ . By using these criteria, we identified three monoadimino analogs (DB173, DB183, and DB210) and one diamidino derivative (DB1766) that are validated hits. In addition, we identified 5 derivatives deemed marginal hits, as defined by potency of approximately  $1\mu M$  (DB1684 and DB1736) or SI  $> 8$  (HG17, HG24, DB1734). It is important to note that the hits we identified do not appear to be promiscuous inhibitors. Many of the hits and marginal hits have been screened previously for antiparasitic, antifungal, or antibacterial activities, and none appear to have indiscriminate activity across the spectrum of biological activities examined thus far (see Table 2.9). Furthermore, many of the compounds we tested that were not potent against *N. fowleri in vitro*, in particular type II derivatives, have broad activities in other biological systems (Table 2.9). These results lead us to propose inhibitors for *N.*

*fowleri* that have an encouraging degree of specificity that can be exploited in lead optimization. Therefore, from this study we identified nine compounds (hits and marginal hits in Table 2.9) that warrant further evaluation and optimization to identify lead compounds. For each of the hit compounds identified, the lead optimization process will require enhanced physiochemical properties to permit BBB penetration and improved selectivity. A partial list of some of the properties to be optimized include lower molecular weight, log of distribution coefficient (logD) of approximately 2, and efficacy *in vivo* (*N. fowleri* infected mouse model).

While all the screened compounds initially were designed to be DNA minor groove binders, we have no evidence to suggest that the activity of the compounds against *N. fowleri* involves binding to DNA. Consequently, we consider the hit compounds as ones with an unknown target(s). Furthermore, the two classes with best potency, bis-benzimidazole amidines (type I) and bis-benzimidazole diamidines (type II; Figure 2.3), may not have a common mode of action, since the two structural types have significant differences. Type I is a monocation and type II is a dication; while the overall geometry of both is curved, the type II compounds are more acutely curved, and the two types may be unable to fit the same binding site. In addition, it is possible that each of the hits has more than one target and inhibit their targets with different potencies depending upon the structural modifications in the series. Once a lead compound is identified, specific mechanism of action studies will be warranted. Both type I and II cations are likely to be very hydrophilic (ACD estimated logD for DB183 = -0.65); therefore, to have a reasonable chance of passing the BBB, it will be

essential to focus on modifications that lead to compounds with  $\log D = 2 \pm 1$ . Future studies should systematically vary the structures of type I and II to reduce their size and polarity in an attempt to optimize activity for *N. fowleri*, to develop reasonable selectivity, and to achieve the desired physiochemical properties. In addition, the type I and II derivatives should be assessed against multiple isolates of *Acanthamoeba* spp. Diamidino derivatives appear to be more potent against *Acanthamoeba* spp. than *N. fowleri*, therefore, the new hits identified in this study may be even more potent against *Acanthamoeba* and could be useful for developing new drugs to treat keratitis, GAE, or systemic infections with these important pathogens.

Advances in drug discovery for emerging infectious and tropical diseases have begun to deliver a pipeline of new chemotypes that are optimized for clinical development by academic and industrial scientists [107,108]. In comparison, pathogenic FLA have been ignored and early discovery studies have focused on a small number of drugs already approved for other indications or screens with non-pathogenic species of FLA. In this study, we have applied the tenets of modern drug discovery by using high-throughput phenotypic screens with pathogenic *N. fowleri*. To accomplish this goal, we validated two robust methods for quantitative dose-response and high-throughput screening of compounds for anti-FLA activity and applied these to conduct the first large-scale application of SAR to optimize new anti-FLA drugs. The mono- and diamidino compounds we discovered are synthetically tractable and highly attractive for hit-to-lead optimization.

**Table 2.1** Susceptibility of *Naegleria fowleri* to amphotericin B, miltefosine, and diamidines *in vitro*.

Drug	Isolate	MIC (μM)	IC50 (μM)	Assay Duration	Media	Assay Volume (ml)	No. of Amoeba/ml	Assay Endpoint	Reference
Amphotericin B	Lee (M67)	0.11		7 d	Mix	30	10 <sup>4</sup>	Cell counts	[47]
	ATCC 30808		0.84	60 hr	Bactocasten	40	25 x 10 <sup>6</sup>	Cell counts	[70]
			1.6	2, 4, 6 d	NCM	0.1	10 <sup>4</sup>	LDH release	[71]
	ATCC 30215		47	72 hr	NCM	9	10 <sup>6</sup>	Absorbance/luminescence	Current study
Miltefosine	CDC V511	40		1-4 d	NCM	10	9.6 x 10 <sup>4</sup>	Viability on recovery	[68]
			62	2, 4, 6 d	NCM	0.1	10 <sup>4</sup>	LDH release	[71]
	ATCC 30215		>122.7	72 hr	NCM	9	10 <sup>6</sup>	Absorbance/luminescence	Current study
Pentamidine	ATCC 30808		>54	60 hr	Bactocasten	40	25 x 10 <sup>6</sup>	Cell counts	[70]
	ATCC 30215		>84.4	72 hr	NCM	9	10 <sup>6</sup>	Absorbance/luminescence	Current study
Propamidine			>160.1						
Hexamidine	ATCC 30215		>117.3	72 hr	NCM	9	10 <sup>6</sup>	Absorbance/luminescence	Current study
Octamidine			89.1						

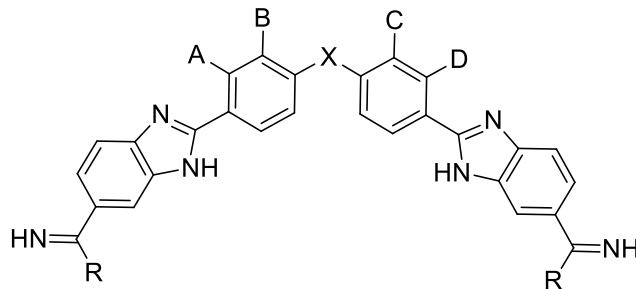


**Table 2.2** Bis-benzimidazole amidines evaluated for activity against *N. fowleri* *in vitro*.

Code	R	Ar	IC <sub>50</sub> (μM)		SI
			<i>N. fowleri</i> <sup>a</sup>	J774	
DB183	Am	4-hydroxyphenyl	0.458	6.47	14.2
DB158	Im	4-hydroxyphenyl	8.45	>96	>11
DB173	THP	4-hydroxyphenyl	0.177	7.89	44.6
DB210	Am	4-methoxyphenyl	0.795	64.9	81.6
DB164	Im	4-methoxyphenyl	2.26	5.06	2.39
DB221	Am	4-ethoxyphenyl	1.32	4.17	3.1
DB165	Im	4-ethoxyphenyl	4.13	13.6	3.3
HG11	Am	3,4-difluorophenyl	17.2	31.8	1.84
HG12	Am	4- <i>t</i> -butylphenyl	41.3	23.9	0.58
HG13	Am	2-hydroxy-3- <i>t</i> -butylphenyl	61.4	>17.0	~0.3
HG16	Am	3,5-dimethoxyphenyl	>88.2	>88.2	~1
HG17	Am	3,4-dimethoxyphenyl	0.318	2.91	9.2
HG19	Am	3-methoxy-4-benzyloxyphenyl	5.27	49.3	9.4
HG20	Am	3,4-dibenzyloxyphenyl	>79.3	>79.3	~1
HG22	Am	2-(4-chlorophenoxy)-5-fluorophenyl	>79.4	>79.4	~1
HG23	Am	4-(4-chlorophenoxy)phenyl	>80.0	28.4	~0.35
HG24	Am	4-(3,4-dimethoxyphenoxy)phenyl	0.462	2.54	9.15
HG25	Am	naphthalen-1-yl	9.59	>86.9	>9.1

<sup>a</sup> Mean of at least two independent alamarBlue assays; SI= selectivity index.

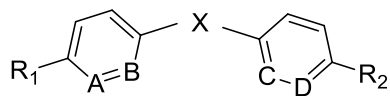
**Table 2.3** Bis-benzimidazole diamidines evaluated for activity against *N. fowleri* *in vitro*.



Code	X	A	B	C	D	R	IC <sub>50</sub> (μM)		SI
							<i>N. fowleri</i> <sup>a</sup>	J774	
DB325	(CH <sub>2</sub> ) <sub>2</sub>	H	H	H	H	<i>N-i</i> Pr	20.7	15.2	0.7
DB1736	O	H	H	H	H	<i>N-i</i> Pr	1.04	10.2	9.8
DB1774	S	H	H	H	H	<i>N-i</i> Pr	>50	55.8	~ 1
DB1765	NH	H	H	H	H	<i>N-i</i> Pr	1.28	7.0	5.5
DB1766	NMe	H	H	H	H	<i>N-i</i> Pr	0.43	6.92	16.1
DB1684	NPh	H	H	H	H	<i>N-i</i> Pr	1.04	9.58	9.2
DB1687	O	H	H	H	H	<i>N-c</i> -pentyl	1.11	6.65	6.0
DB1735	O	H	H	H	H	<i>N</i> -pent-3-yl	1.01	31.4	5.2
DB1768	O	H	H	H	H	4-Me-piperidyl	9.44	24.2	2.6
DB1754	O	H	H	H	H	azepanyl	10.2	15.5	1.5
DB1753	O	H	H	H	H	morpholine	4.14	ND	ND
DB1767	O	H	H	H	H	thiomorpholine	7.06	37.1	5.3
DB1734	O	H	Cl	H	H	<i>N-i</i> Pr	0.39	3.22	8.4
DB1682	O	Cl	H	H	H	<i>N-i</i> Pr	1.85	1.87	1.0
DB1690	O	OMe	H	H	H	<i>N-i</i> Pr	0.47	0.35	0.74
DB1683	O	Cl	H	H	MeO	<i>N-i</i> Pr	0.66	2.95	4.5
DB1685	O	CF <sub>3</sub>	H	H	H	<i>N-i</i> Pr	0.94	2.34	2.5

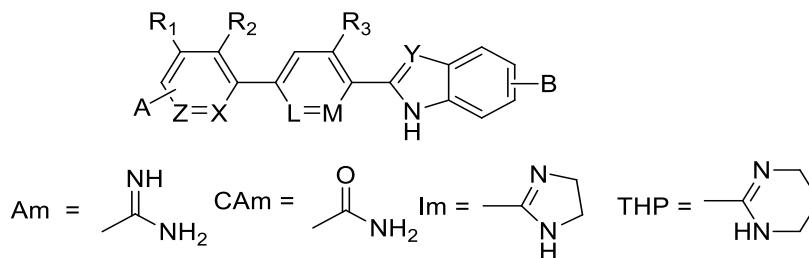
<sup>a</sup>Mean of at least two independent alamarBlue assays; SI= selectivity index.

**Table 2.4** *In vitro* activity of furamide derivatives against *N. fowleri*.



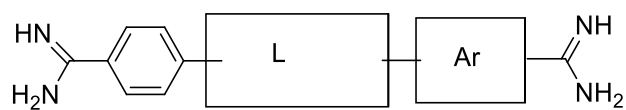
Code	X	A	B	C	D	R <sub>1</sub>	R <sub>2</sub>	<i>N. f.</i> IC <sub>50</sub> (μM)
DB75		CH	CH	CH	CH	Am	Am	69.8
DB103		CH	CH	CH	CH	THP	THP	47.4
DB569		CH	CH	CH	CH	<i>N</i> -Ph-Am	<i>N</i> -Ph-Am	46.9
DB568		CH	CH	CH	CH	<i>N</i> -4-MeOPh-Am	<i>N</i> -4-MeOPh-Am	83.3
DB573		CH	CH	CH	CH	<i>N</i> -Me <i>N'</i> -4-MeOPh-Am	<i>N</i> -Me <i>N'</i> -4-MeOPh-Am	31.7
DB574		CH	CH	CH	CH	<i>N</i> -4-MePh-Am	<i>N</i> -4-MePh-Am	32.6
DB820		CH	N	CH	CH	Am	Am	84.2
DB829		CH	N	N	CH	Am	Am	>50
DB351		CH	CH	CH	CH	Am	Am	68.6
DB1213		CH	CH	CH	CH	Am	Am	74.9
DB1237		CH	N	N	CH	Am	Am	62.5
DB1404		CH	CH	CH	CH	Am	Am	55.7
DB1210		CH	CH	CH	CH	Am	Am	77.1
DB1044		CH	CH	CH	CH	Am	Am	45.8

**Table 2.5** *In vitro* activity of linear benzimidazole types against *N. fowleri*.



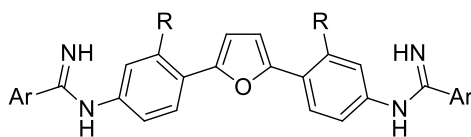
Code	X	Y	Z	L	M	R <sub>1</sub>	R <sub>2</sub>	R <sub>3</sub>	A	B	<i>N. f.</i> IC <sub>50</sub> ( $\mu$ M)
DB921	CH	N	CH	CH	CH	H	H	H	<i>p</i> -Am	3-Am	58.7
DB1055	CH	N	CH	CH	CH	H	H	H	<i>m</i> -Am	3-Am	41.6
DB1963	CH	N	CH	CH	CH	H	H	H	<i>p</i> -CAm	3-Am	78.5
DB1964	CH	N	CH	CH	CH	H	H	H	<i>p</i> -CAm	3-Im	ND
DB988	CH	N	CH	CH	CH	H	Me	H	<i>p</i> -Am	3-Am	13.4
DB1236	CH	N	CH	CH	CH	H	H	F	<i>p</i> -Am	3-Am	59.4
DB1883	CH	CH	CH	CH	CH	H	H	H	<i>p</i> -Am	3-Am	61.8
DB1944	CH	CH	CH	CH	CH	H	H	H	H	3-Am	55.5
DB1803	CH	CH	CH	CH	CH	H	H	H	<i>p</i> -Im	3-Im	55.7
DB1804	CH	CH	CH	CH	CH	H	H	H	<i>p</i> -THP	3-THP	17.3
DB1798	CH	CH	CH	CH	CH	H	H	H	<i>p</i> -Am	4-Am	36.6
DB1780	CH	CH	CH	CH	CH	H	H	H	<i>p</i> -Im	4-Im	66.5
DB1781	CH	CH	CH	CH	CH	H	H	H	<i>p</i> -THP	4-THP	8.66

**Table 2.6** *In vitro* activity of central indole ring diamidines against *N. fowleri*.



Code	L	Ar	<i>N. f.</i> IC <sub>50</sub> ( $\mu$ M)
DB1884			43.2
DB1902			50.8
DB1885			>50
DB1887			10.3
DB1476			25.5
DB2285			>50

**Table 2.7** *In vitro* activity of arylimidamide derivatives against *N. fowleri*.

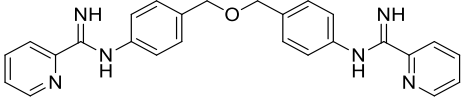
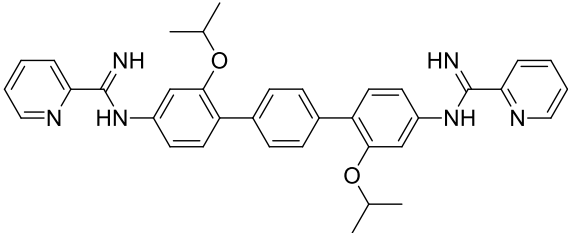
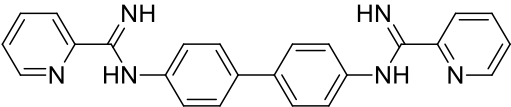


Code	R	Ar	<i>N. f.</i> IC <sub>50</sub> (μM)
DB745	OEt		18.6
DB766 <sup>a</sup>	O- <i>i</i> -Pr		12.5
DB1960 <sup>b</sup>	O- <i>i</i> -Pr		22.7
DB1852 <sup>a</sup>	O- <i>c</i> -pentyl		25.7
DB1955 <sup>b</sup>	O- <i>c</i> -pentyl		37.9
DB1831	O- <i>i</i> -Pr		>50
DB1931	O- <i>i</i> -Pr		>50
DB1850	O- <i>i</i> -Pr		47.5
DB1858	O- <i>i</i> -Pr		>50
DB1857	O- <i>i</i> -Pr		57.6
DB1848	O- <i>i</i> -Pr		50.6

<sup>a</sup> Hydrochloride salt

<sup>b</sup> Mesylate salt

**Table 2.8** *In vitro* activity of additional arylimidamide derivatives.

Code	Structure	<i>N. f.</i> IC <sub>50</sub> (μM)
DB1835		>50
DB1969		>50
DB1832		>50

**Table 2.9** Comparative potency and cytotoxicity of amidino derivatives against *Naegleria fowleri*, bacteria, fungi and rat myoblast *in vitro*.

Compounds*	Current Study			Bacteria (MIC, µg/ml)			Fungi (IC50, µg/ml)		Parasites (IC50, µg/ml)		Rat Myoblast	Ref.
	<i>N. f.</i> IC50 (µM)*	J774 IC50 (µM)*	SI	<i>Staphylococcus aureus</i> ATCC 29213	<i>Staphylococcus pneumoniae</i> ATCC 6301	<i>E. faecalis</i> ATCC 51575	<i>Candida albicans</i>	<i>Cryptococcus neoformans</i>	<i>Trypanosoma brucei</i>	<i>Plasmodium falciparum</i>	L6 IC50 (µg/ml)	
<b>Hits</b>	DB173	0.177	7.89	44.6			3.12	1.56				46
	DB183	0.458	6.47	14.2			0.78	3.12	0.017	0.013	4.2	38,46
	DB210	0.795	64.9	81.6			>100	3.12	0.017	0.013	4.2	38,46
	DB1766	0.43	6.92	16.1	1	0.12	0.25					25
<b>Marginal Hits</b>	HG17	0.318	2.91	9.2			25		0.06	0.008	>90	38
	HG24	0.462	2.54	9.15			3.12		0.036	0.015	29.4	38
	DB1684	1.04	9.58	9.2	1	0.12	.5					25
	DB1734	0.385	3.22	8.4	0.25	≤0.06	0.25					23
	DB1736	1.035	10.2	9.8	0.25	≤0.06	0.12					25
<b>Compounds not active against <i>Nf</i></b>	DB1754	10.2	15.5	1.5	0.25	0.12	0.5	4				23
	DB1767	7.06	37.1	5.3	0.5	0.25	0.5	16				23
	DB1768	9.44	24.2	2.6	0.25	0.12	0.5	4				23
	HK11	17.2	31.8	1.84				25	0.33	0.015	29.8	38
	HK12	41.3	23.9	0.58				1.56	1.06	0.031	13	38
	HK16	>88.2	>88.2	~1				50	0.59	0.017	25.5	38
	HK23	>80.0	28.4	-0.35				25	0.708	0.028	46	38

<sup>a</sup>Hits are defined as compounds having an IC<sub>50</sub> < 1µM for *Naegleria fowleri* (*N.f.*) and a selectivity index (SI) ≥ 10

<sup>b</sup>Marginal hits are defined as having an IC<sub>50</sub> ~1 for *N.f.* and an SI > 8 and < 10

<sup>c</sup>Inactive compounds have an IC<sub>50</sub> > 1 µM for *N.f.*



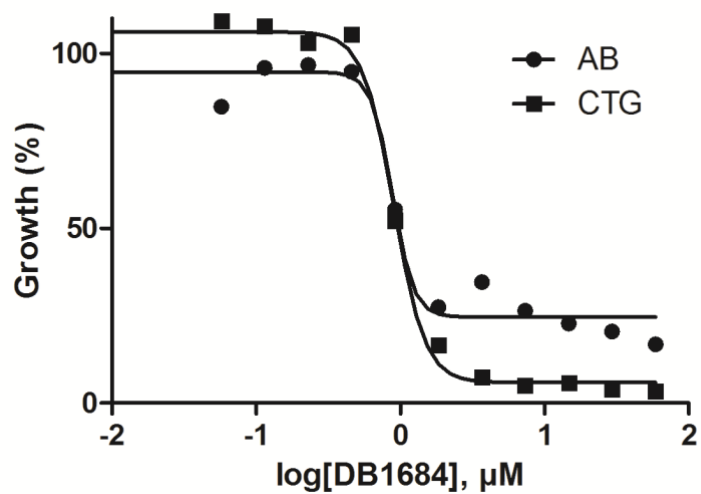


**Figure 2.1** Quantitative dose-response data for *Naegleria fowleri* demonstrating similar activities of amidino compounds in the alamarBlue (AB) and CellTiter-Glo (CTG) assay formats.

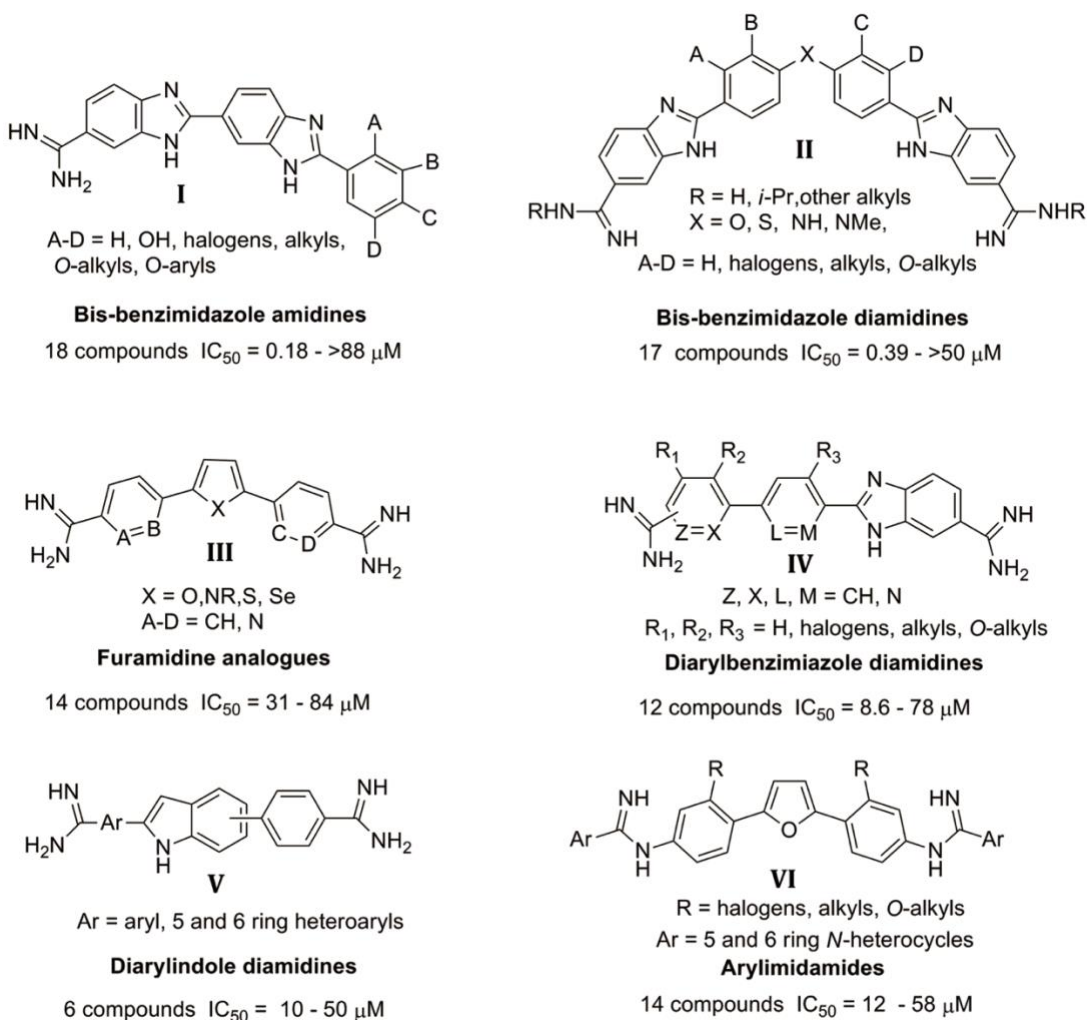


**Figure 2.2** Structural classes of amidino compounds screened against *Naegleria fowleri*.

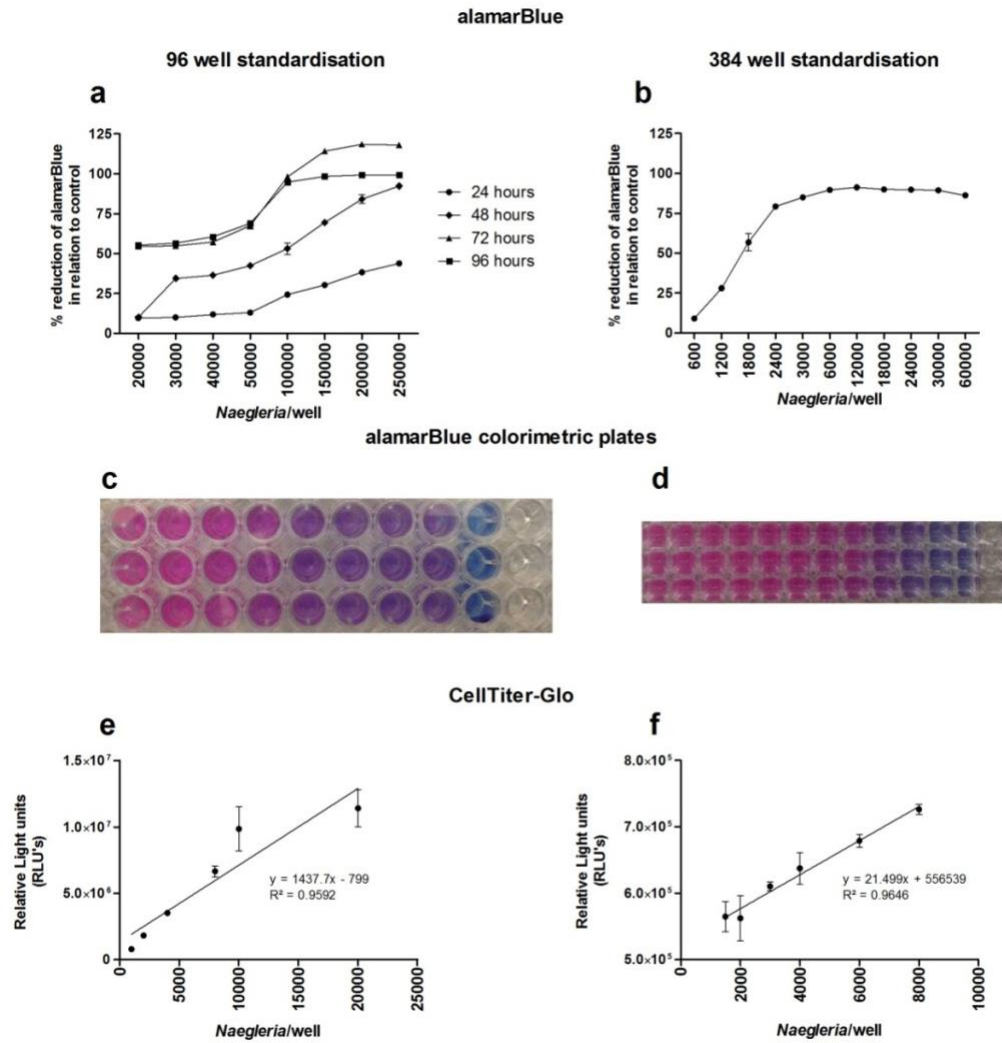


**Figure 2.3** Optimization of AB and CTG assays for *N. fowleri* drug discovery. A,B) the optimal seeding density of amoebae/well was determined in 96- and 384-well plates. C,D) The AB colorimetric readout was robust and reproducible. E,F) There was a strong correlation between relative luminescence units (RLUs) in CTG assay with number of amoebae/well.

### CHAPTER 3

## PHENOTYPIC SCREENS REVEAL POSACONAZOLE AS RAPIDLY CIDAL COMBINATION PARTNER FOR TREATMENT OF PRIMARY AMOEBIC MENINGOENCEPHALITIS<sup>1</sup>

---

<sup>1</sup>Colon BL, Rice CA, Guy RK, and Kyle DE (2018). Phenotypic screens reveal posaconazole as rapidly cidal combination partner for treatment of Primary Amoebic Meningoencephalitis. Accepted in *Journal of Infectious Diseases*, doi:10.1093/infdis/jiy622.

Reprinted here with permission from the Oxford University Press

## ABSTRACT

*Naegleria fowleri*, is the causative agent of primary amoebic meningoencephalitis (PAM), which is fatal in >97% of cases. Low survival rates are attributed in part to poor diagnostics and ineffective treatments. In this study, we aimed to identify new drugs to increase survival rates. We conducted phenotypic screens of libraries of FDA-approved compounds and the MMV Pathogen Box and validated 14 hits ( $IC_{50}s < 1\mu M$ ). The hits were then prioritized by assessing the rate of action and efficacy in combination with current drugs used to treat PAM. Posaconazole was found to inhibit amoebae growth within the first 12 hours of exposure, which was faster than any currently used drug. In addition, posaconazole cured 33% of *N. fowleri* infected mice at 20mg/kg and in combination with azithromycin increased survival further by 20%. Fluconazole, which is currently used for PAM therapy, was ineffective and showed 40% less survival in vivo.

## INTRODUCTION

*Naegleria fowleri* is a free-living amoebae that is the causative agent of a rapidly, fulminant disease known as primary amoebic meningoencephalitis (PAM). This amoebae is ubiquitous in the environment and can cause disease when an individual inhales warm freshwater through their nose. Most patients come in contact with *N. fowleri* through recreational water activities, use of Neti pot, or religious customs such as ritual ablutions [32–34]. *N. fowleri* migrates from the nasal cavity by feeding on the nasal epithelium and olfactory nerves

where they migrate along the olfactory nerves to cross the cribriform plate until they reach the olfactory bulb in the brain [112]. Once the amoebae reach the neuronal tissue, the pathology is mostly localized to the frontal lobe of the brain, unlike the dispersed lesions in granulomatous amoebic encephalitis caused by *Acanthamoeba spp.* and *Balamuthia mandrillaris* [2,38].

PAM has a worldwide presence with most cases reported in developed countries that have resources to properly identify cases [16]. In the United States from 1969 through 2017 there have been only 4 survivors from 143 reported cases of PAM [31,113]. However, the number of cases is most likely an underrepresentation since PAM is not a notifiable disease in the United States and may easily be misdiagnosed as bacterial meningitis or viral meningitis [114]. Under-reporting of PAM is likely in tropical climates. For example, in Karachi, Pakistan, there has been an increased number of diagnosed cases in the Aga Khan University Hospital after instituting policies to process CSF samples for amoebae diagnostics from patients that had symptoms of bacterial meningitis [32].

When patients are diagnosed with PAM, they receive a combination of drugs including amphotericin B, fluconazole, azithromycin, rifampin, and miltefosine [31]. The two main concerns with this treatment regimen are toxicity and efficacy. For example, amphotericin B is an antifungal that is used to treat leishmaniasis and is known to cause severe renal toxicity. Regardless, amphotericin B has been given to PAM patients since 1969 following the report of a PAM survivor, even though efficacy on *N. fowleri* in vitro is limited [31,48].

Additionally, miltefosine, initially developed as a breast cancer drug, has been repurposed for treating leishmaniasis and *N. fowleri* [54,68]. There is experimental evidence for azithromycin efficacy in vitro and in animal models [47,61], yet rifampin and fluconazole are used despite the lack of any experimental evidence with the amoebae. Steroids (e.g., dexamethasone) also are used to manage the increased intracranial pressure caused by the host's immune response to the amoebae. Recently, patients have been placed in a hypothermic coma because of the neuroprotective effects by reducing intracranial pressure and reducing reactive oxygen species, proinflammatory cytokines, and neuronal apoptosis [115,116]. Given that labs grow *N. fowleri* in vitro at 34°C [48], the mild-moderate hypothermic comas that are being used for PAM patients are likely to have little effect on the amoeba's ability to proliferate. Although the addition of miltefosine and hypothermic coma appear to have been beneficial in recent cases, the high fatality rates with similar treatments, as well as toxicity of current drugs, still drives the need to identify more safe and effective treatments [56].

Drug discovery for pathogenic free-living amoebae is not an active area of research and all drugs currently used for treatment of PAM were selected empirically. Many previous studies used low throughput methods with non-pathogenic or pathogenic amoebae to evaluate a few drugs in each study. More recently higher throughput methods have been developed and have been used to screen compound libraries or to evaluate potential drug targets [48,69,117]. While the shift to high-throughput methods with pathogenic amoebae may yield

success, a suitable candidate to treat PAM has not yet been identified. The only recent candidate has been corifungin, the sodium salt of amphotericin B, that received orphan drug status approval from the FDA in 2011, but has yet to be used to treat a PAM case [69]. This may be due to the risk of removing amphotericin B from treatment or adding corifungin due to concerns of additive toxicity.

In this study, we aimed to discover a drug that can be repurposed to treat PAM cases successfully. To do so, we used our previously developed high-throughput phenotypic screening method [48] to evaluate several compound libraries and we identified 14 potent compounds that inhibit pathogenic *N. fowleri* at nanomolar concentrations. In addition, we developed new methods for assessing rate of action and found that posaconazole has a more rapid onset of action than currently used drugs, possessed additive activity in vitro in combination with azithromycin, miltefosine, and amphotericin B, and produced a 33% cure rate in vivo. Most importantly, when posaconazole was combined with azithromycin, we report a 40% increase in survival in a murine model of PAM when compared to fluconazole in combination.

## **MATERIALS AND METHODS**

### Amoebae culture

The *Naegleria fowleri* isolate (NF69) used as a reference strain in these studies was isolated from a 9-year old boy in Adelaide, Australia, that died of PAM in 1969 (ATCC 30215). Additional strains from the Centers for Disease



Control and Prevention (CDC; Table 3.1) were used for comparison of in vitro drug susceptibility. All isolates were grown axenically as trophozoites at 34°C in Nelson's complete medium (NCM). Reagents for media were purchased from Sigma-Aldrich (St. Louis, MO).

#### In vitro drug susceptibility assay

Drug susceptibility assays were performed as previously described [3]. Initially a collection of 1,134 FDA-approved drugs assembled at the St. Jude Children's Research Hospital (SJ) was used for phenotypic screening of activity against NF69 using the CellTiter-Glo 2.0 (CTG) assay (Promega, Madison, WI). These compounds were prepared in 384-well plates at starting concentrations ranging from 1-17mM. We initially screened plates as a single-point assay at both 1:100 and 1:1000 dilutions with 3,000 amoebae/well. We also screened the Medicines for Malaria Venture (MMV) Pathogen Box, which is a collection of 400 drug and probe-like molecules that are active against various pathogens [118]. Compounds were prepared in 96-well plates at a 1mM concentration in dimethyl sulfoxide (DMSO). We first screened this collection as a single point assay in 96-well plates at 10 and 1µM. To verify active hits from both collections, compounds were cherry picked from the original plates and serially diluted in duplicate from 10µM to 10nM in a 96-well plate with 4,000 amoebae/well to generate dose-response curves with the CTG assay. Curve fitting using non-linear regression was analyzed using DataAspects Plate Manager analysis software [48].

### Drug combination assay

Miltefosine was purchased from Cayman Chemical (Ann Arbor, MI). Posaconazole, amphotericin B, and azithromycin were purchased from Sigma Aldrich (St. Louis, MO). Isobolar combination studies with drugs were conducted by combining compounds in ratios of their IC<sub>50</sub>s (5:1, 3:1, 1:1, 1:0, 0:1, 1:3, and 1:5) and serially diluted. Plates were prepared with 10µl of drug and 90µl of NCM with 4,000 cells/well. Positive growth controls were cells and media; negative growth controls were amoebae with 135µM of amphotericin B. CTG assay methods and analysis were followed as previous described [48].

### Rate of action assay

RealTime-Glo MT Cell Viability Assay (RTG; Promega, Madison, WI) was used to assess the rate of action of active compounds against *N. fowleri*. Compounds were plated at 1x and 5x their IC<sub>50</sub> with 4 replicates per plate. The 96-well plates were prepared with 10µl of drug, 40µl with 4,000 cells, and 50µl of RTG reagent. The positive growth control was cells in media with RTG reagent; the negative growth control was media and RTG reagent. Plates were incubated at 34°C for 72 hours in a SpectraMax i3x plate reader (Molecular Devices; Sunnyvale, CA). Relative luminescence units were recorded every hour for 72 hours and analyzed using Prism 7 (GraphPad Software; La Jolla, CA).

### Animal studies

In vivo efficacy studies were performed in accordance with the protocols approved by the Institutional Animal Care and Use Committees of the University of South Florida and University of Georgia. In a stringent model of PAM, female ICR mice were intranasally infected with 10 $\mu$ l of 10,000 *N. fowleri* trophozoites. Drug treatments began 3 days post-infection and were administered once per day for 3 consecutive days. Posaconazole (Noxafil; Merck) was obtained from SJ and was given intravenously (IV) through tail vein injections once daily at 20, 10, or 5mg/kg. Phosphate-buffered saline (PBS) and 20mg/kg of miltefosine were given intraperitoneally (IP) as vehicle and drug control, respectively, for the monotherapy study. Animals displaying symptoms (papilledema, hunched, ataxic, stiff neck, 20% decrease in body weight, shallow breathing) were euthanized to relieve suffering per the approved protocols. Mice were monitored twice daily, but deaths were pooled and recorded per day, in the monotherapy study.

A similar protocol was followed for infection and dosing schedule of the combination study. Mice in single drug groups were dosed with 20mg/kg of posaconazole IV, 30mg/kg of fluconazole IP, 25mg/kg ketoconazole IP or 25mg/kg azithromycin IP. Mice in combination groups were dose with 25mg/kg of azithromycin IP and either 20mg/kg of posaconazole IV, 30mg/kg of fluconazole IP or 25mg/kg of ketoconazole IP. IV PBS and IP 0.5% HEC/0.1% Tween 80 with 10% DMSO were used as vehicle controls. Mice were monitored twice daily and

survival data (deaths or compassionate euthanasia) were recorded twice per day (morning and evening).

## RESULTS

### Phenotypic screen of bioactive compound libraries

Following the development of new quantitative methods for high-throughput screening with *N. fowleri* [48], we screened two libraries of known bioactive compounds. The first was a library of 1,134 FDA-approved drugs assembled at the St Jude Children's Research Hospital. The second library was the MMV Pathogen Box; this collection contains 400 compounds with known activities against parasites that cause malaria, leishmaniasis, trypanosomiasis, and 10 other infectious diseases [118].

The initial screen of both compound libraries was conducted as single point assays of each compound at ~10 and ~1  $\mu$ M. Included in each plate were positive and negative growth controls. The quality control of the single point assay screens was  $Z'=0.95$  for 384-well plates and a  $Z'=0.93$  for 96-well plates. From the FDA-bioactive library, 24 hits were identified that produced  $\geq 70\%$  inhibition of growth of *N. fowleri* in the 72 hour assay (Figure 3.1). Several of the hits were identified more than once since different salts of some drugs were included in the compound library (e.g., azithromycin and azithromycin dihydrate). These hits were next evaluated in dose response assays to determine the 50% inhibitory concentrations ( $IC_{50}$ s). From these phenotypic screen data, 20 hits from multiple different classes of drugs were confirmed (Table 3.2). Among the most

potent were antibiotics that target protein synthesis. Azithromycin was the most potent compound with an  $IC_{50} = 20\text{nM}$  and several related antibiotics also were found to produce  $IC_{50}\text{s} \leq 440\text{nM}$ ; these included clarithromycin, erythromycin, and dirithromycin. Tilmicosin, a macrolide antibiotic for veterinary use, was among the most potent compounds ( $IC_{50} = 60\text{nM}$ ). For the first time, two pleuromutilin antibiotics, valnemulin and retapamulin, were found to be active against *N. fowleri*. Antifungals was the next major class that produced multiple hits. These included the known inhibitors itraconazole and ketoconazole, but also posaconazole was found to be potent ( $IC_{50} = 240\text{nM}$ ). In addition, a few nucleosides were identified as hits. The pyrimidine analog gemcitabine was a potent inhibitor ( $IC_{50} = 340\text{nM}$ ) and the purine nucleoside analogs fludarabine and clofarabine produced  $IC_{50}\text{s}$  of  $460\text{nM}$  and  $1.76\mu\text{M}$ , respectively.

The screen of the MMV Pathogen Box produced fewer hits ( $n=13$ ), yet posaconazole was confirmed again in this screen (Table 3.3). Posaconazole was the most potent compound identified in the Pathogen Box and was included in the library because it is used for the treatment of *Trypanosoma cruzi*, the causative agent of Chagas Disease. Interestingly, the majority of hits with  $IC_{50}\text{s}$  ranging from  $1\text{-}2\mu\text{M}$  were compounds with demonstrated activity against kinetoplastid parasites.

We also screened a small set of miscellaneous compounds with known activities against *Plasmodium falciparum* and other parasites (Table 3.4). The most potent compounds in this library were auranofin ( $8.37\mu\text{M}$ ), trans-mirinacamycin ( $9.29\mu\text{M}$ ), and tafenoquine succinate ( $9.56\mu\text{M}$ ). Most of the

compounds in this library were inactive at the concentrations screened (Table 3.4).

#### Rate of action studies

PAM is a rapidly fulminant disease with a short onset of symptoms most often followed by coma and death. Therefore, an important pharmacodynamic property of drugs to treat PAM is rapid onset of action. Few studies have addressed this issue and, more importantly, the current treatment drugs have been shown to require long exposure times ( $\geq 72$  hours) to produce dose response data in vitro [48]. In this study, we developed a new kinetic read assay which assesses the rate of action for the active compounds identified against *N. fowleri*. This assay is based upon metabolically active cells reducing a substrate followed by the binding to luciferase that is present in the media. The relative luminescence units produced were found to be proportional to metabolically active cells (Figure 3.2). To assess the rate of action, first the IC<sub>50</sub>s for each compound were determined and then we exposed amoebae to 1x-IC<sub>50</sub> (Figure 3.3) or 5x-IC<sub>50</sub> (Figure 3.4) concentrations and luciferase expression was monitored every hour for 72 hours. The results demonstrate that drugs currently used to treat PAM (miltefosine, amphotericin B, azithromycin, and fluconazole) have a slow onset of action in this assay. Interestingly, azithromycin had a lag phase of reduced activity for 30 hours before rapid onset of significant inhibition of amoebae growth (Figure 3.3A); increasing the dose of azithromycin to 5x-IC<sub>50</sub> did not abrogate the delayed onset of action (Figure 3.4A). At 1x-IC<sub>50</sub> of

miltefosine we did not see any shift differing from the control, however, at the higher concentration tested the miltefosine curve dropped below background; this may be due to solubility of drug in the growth media (Figure 3.4A). Importantly fluconazole, a drug that is included in the current treatment regimens because it is known to cross the blood-brain barrier, was not effective in the rate of action assay at either concentration (Figure 3.3A) and was not potent in standard in vitro drug susceptibility assays (data not shown).

Next, we examined the rate of action of hits identified in the library of FDA-approved drugs. As shown in Figure 3.3B, posaconazole and terbinafine exhibited the most rapid onset of action at the 1x-IC<sub>50</sub> concentration. At 5x-IC<sub>50</sub>, valnemulin and roxithromycin show a similar pattern to the lower dose of azithromycin (Figure 3.4B). A comparison of different conazoles identified both ketoconazole and posaconazole to be the most rapidly acting compounds in this study, at both the high and low drug concentrations used (Figures 3.3C and 3.4C).

### Drug combinations

Isobolograms from the fixed-ratio combinations between posaconazole and miltefosine, amphotericin B, or azithromycin showed additivity. Importantly no antagonistic activity, defined as  $\Sigma\text{FIC}>2$ , or synergistic activity ( $\Sigma\text{FIC}<0.5$ ) was seen with posaconazole in combination with any drug tested in this study (Figure 3.5).

### In vivo efficacy

Posaconazole was among the most potent drugs identified in the in vitro study, possessed a rapid onset of action, and was additive in in vitro combination assays with azithromycin, amphotericin B and miltefosine. Therefore, we next assessed the efficacy of posaconazole in the mouse model of PAM (Figure 3.6 and 3.7). We infected mice with NF69 strain on day 0 and dosed once daily on days 3, 4, and 5. Posaconazole at 20mg/kg (IV) showed significant results by curing 2 of 6 mice ( $p < 0.05$ ), whereas lower doses of posaconazole and miltefosine were not effective. Importantly, the model demonstrated the high degree of pathogenicity of *N. fowleri*, with all SHAM controls succumbing to disease by day 8. A repeat study with a less virulent challenge produced similar cure rates with 20mg/kg posaconazole (Figure 3.7). These data suggest that posaconazole is moderately effective when used alone, a result that suggests it is as potent as any drug ever reported when used in monotherapy in the mouse model of PAM.

To assess if posaconazole is more effective than fluconazole, the current conazole drug used in PAM treatments, we tested posaconazole (20mg/kg), ketoconazole (25mg/kg) and fluconazole (30mg/kg) alone and in combination with azithromycin (25mg/kg) in the PAM murine model. While the survival rate of azithromycin alone and vehicle were the same (30%), azithromycin alone prolonged survival for up to 5 days (Figure 3.8A). There was no significant difference in survival rate with posaconazole alone, but we observed prolonged survival of ~ 2.5 days. However, there was a significant increase in survival in the



group of animals treated with a combination of posaconazole and azithromycin as compared to SHAM-treated mice ( $p < 0.05$ ; Figure 3.8B). In contrast, prolonged survival in other combination treatments (azithromycin-fluconazole and azithromycin-ketoconazole) was no different than observed in mice treated with azithromycin alone (Figures 3.8B, 3.8C, and 3.8D).

#### Drug susceptibility across various *N. fowleri* strains

*N. fowleri* is ubiquitous in the environment, especially in warm climates, yet little is known about genetic heterogeneity and its affect on the response to chemotherapeutic drugs. Most previous studies of drug susceptibility with new drugs have included data for only one isolate; this has mainly included screening on the non-pathogenic *N. gruberi*. Therefore, we assessed the in vitro potency of amphotericin B, miltefosine, azithromycin and posaconazole for 5 patient isolates of *N. fowleri* that were obtained from the CDC and compared the data to our reference strain, NF69 (Figure 3.9). Using the Dunnett's multiple comparisons test, we found no significant differences in  $IC_{50}$ s between NF69 and the CDC isolates for any of the four most potent drugs tested ( $p > 0.05$ ). These data demonstrate that azithromycin and posaconazole are much more potent than the current treatment drugs (amphotericin B and miltefosine) against multiple *N. fowleri* isolates, further demonstrating the potential of posaconazole and azithromycin as effective combination drugs to be used in the treatment regimen of PAM.

## DISCUSSION

Phenotypic whole-cell screens have provided a major boost for discovery of new hits and leads for drug discovery against multiple parasitic protozoan diseases [119,120]. Similarly, screens of libraries of known bioactive compounds that have advanced into clinical development offer an advanced starting point for drug development. In particular the repurposing of already approved drugs for new indications is an attractive option for diseases such as PAM, a highly pathogenic disease that is understudied and is >97% fatal. In this study, we used a high-throughput assay to screen libraries of compounds and identified numerous new hits that can accelerate drug discovery as well as compounds that can be repurposed and used immediately for treatment of this neglected, nearly uniformly fatal disease.

Various antibiotics were identified in this study that provided nanomolar potency against *N. fowleri*. The most active compound identified was azithromycin, which already is a component of PAM treatments. Additionally, previous work with *N. fowleri* has shown azithromycin to have synergistic activity with amphotericin B [61]. We also found that clarithromycin, erythromycin, roxithromycin have nanomolar activity; these compounds have been previously identified to be active against *Naegleria* [110]. Interestingly, we identified two veterinary drugs that potentially could be used to treat animal infections with pathogenic free-living amoebae: valnemulin and tilmicosin. This is the first report of these compounds to have activity against *N. fowleri*. Valnemulin and tilmicosin

have been used to treat swine dysentery and bovine respiratory disease, respectively [121,122]. Further research should be conducted to see if these are viable candidates for treatment of CNS infections caused by pathogenic free-living amoebae. In addition to valnemulin, we identified another pleuromutilin antibiotic, retapamulin, to be potent in our assays.

By screening the MMV Pathogen Box, we identified 6 compounds with known anti-parasitic activity that had low micromolar potency against *N. fowleri*. MMV652003 is a benzoxaborole analog that targets leucyl-tRNA synthetase and has been found to be active against *T. b. brucei*, *P. falciparum*, and *C. elegans* [123–125]. MMV688180 is a pyrazole sulfonamide inhibitor of N-myristoyltransferase; it is known to be trypanocidal and cured all mice in the *T. b. brucei* and *T. b. rhodesiense* HAT models [126] and was effective, yet less potent against *T. cruzi* [127]. Importantly, MMV688180 (DDD85646) has recently been used as a scaffold to produce similar compounds with a lower molecular weight and polar surface area to increase BBB permeability [128]. MMV676602, a mammalian cyclin-dependent protein kinase inhibitor, has shown nanomolar activity in *Neospora caninum*, but found to be ineffective in the murine model [129]. MMV676602 as well as MMV676604 are known to be potent against *Toxoplasma gondii* tachyzoites [130]. Each of these hits provide starting points for new lead optimization studies for drugs active against amoebae.

We also found many antifungals to show potent activity. Itraconazole and posaconazole were two of the most active antifungals identified in this study. Posaconazole was identified as an active hit in both library screens; it was

initially developed for invasive *Candida* and *Aspergillus* infections in immunocompromised individuals [131]. The activity of the conazoles identified in this study confirms the activity pattern recently reported: itraconazole and posaconazole are considerably more active than ketoconazole and fluconazole [62]. Conazoles are of interest because they target CYP51, a key enzyme in sterol biosynthesis and verified target in *N. fowleri* [62]. Two amine antifungals were identified in our assay: butenafine and terbinafine. Butenafine is a benzyl amine derivative that is used to treat tinea pedis and *Candida albicans* [132]. Terbinafine is an allyl amine that is mainly used to treat fungal infections, but has also been used in combination successfully to treat osteo-cutaneous acanthamoebiasis [133].

Perhaps the most important result of our phenotypic screens was the identification of posaconazole as one of the most active compounds in two different chemical libraries. Of all the hits identified, posaconazole possessed the key pharmacodynamic properties required for a new drug to treat PAM. Since PAM is such a rapidly, fulminant disease that often is diagnosed just before (or after) a patient dies, we propose that rapidity of drug action is the most important property of a new PAM treatment drug. For this study, we validated a new rate of action method and demonstrated that posaconazole and ketoconazole are the fastest acting compounds thus far identified for inhibiting amoebae growth. In this assay, posaconazole inhibited amoebae growth significantly by 12 hours; in contrast, azithromycin did not begin to inhibit the amoebae until hour 30 and other drugs currently used to treat PAM had an even slower onset of action.

Another important pharmacodynamic property for a new PAM drug is the ability to use it in the cocktail of existing drugs currently used for treatment of PAM. We assessed synergistic and antagonistic potential for posaconazole with the current drugs that are given to PAM patients and found that posaconazole had additive activity in vitro with amphotericin B, miltefosine, and azithromycin. Although no synergy was observed, additive drug interactions are beneficial, especially since there is no indication posaconazole would reduce efficacy of the other drugs currently used.

Although *N. fowleri* infected mice are considered a good model for PAM and amoebae produce similar pathogenicity in mice and humans, very few drugs have shown efficacy in mouse models and none have produced high cure rates when used in monotherapy [81]. In this study, we used a stringent mouse model to assess drug efficacy. We waited 3 days after infection to dose and only dosed once per day for three days to assess prolonged survival and cure rates. Presumably more frequent dosing or starting treatment earlier could have increased efficacy, yet we aimed to test drugs in a model that is similar to current practice and that is often very late during an infection with amoebae. Posaconazole (IV) dosed at 20mg/kg cured 33% of infected mice, a cure rate as high as any other reported drug when used in monotherapy. Furthermore, the combination of posaconazole plus azithromycin was the most effective combination we tested in the murine model of PAM as evidenced by prolonged survival and increased cure rate in mice dosed with 25mg/kg azithromycin and

20mg/kg posaconazole. These data suggest that posaconazole is a potential combination partner for the treatment of PAM.

Interestingly, previous drug combination studies showed synergy between azithromycin and amphotericin B [61]. Additionally, Soltow and Brenner [61] showed a significant prolonged survival of mice given azithromycin than untreated controls or amphotericin B treated mice. We found that 25 mg/kg of azithromycin alone prolonged survival up to 5 days in comparison to untreated controls. In contrast, our data demonstrated very poor efficacy of fluconazole, both in vitro and in vivo. The rationale for including fluconazole in the current PAM treatment protocol is not documented. Presumably it was included due to its low molecular weight and low binding to plasma protein, thus fluconazole is known to cross the BBB more effectively than other conazoles [134]. Fluconazole was included in the cocktail of drugs used in one successful treatment of PAM and has since been used empirically in subsequent cases [31]. Importantly, there are no published data that fluconazole is effective against *N. fowleri* in vitro or in vivo in experimental models of PAM, thus bringing to question its usefulness in the current therapeutic regimen. Our studies demonstrate that posaconazole is much more potent than fluconazole, has rapid onset of action, is equally active against diverse strains, and produces greater efficacy in the murine model of PAM, both in monotherapy and in combination with azithromycin. Posaconazole may not cross the intact BBB well, yet during PAM the BBB is inflamed and leaky and that could be why we observed efficacy of the drug in vivo. In summary, our data suggest posaconazole is among the most

potent, rapidly acting drugs with potential for enhancing treatment of this usually fatal disease.

In a disease such as PAM, where clinical trials cannot be conducted to determine efficacy of a drug and pharmaceutical companies may not financially benefit from development of a novel therapeutic, drug repurposing is a promising approach for adjunctive therapeutics to treat PAM patients. There are only 4 well documented survivors of PAM in the United States and the current treatment regimen is based on these few successful treatments. Importantly, similar drug combinations have been used in many PAM patients without success, suggesting that new, more rapidly acting drugs need to be discovered. Thus far there has not been a path for progressing new drugs to add to the current cocktail of drugs used and due to the universally fatal outcomes encountered, physicians are reluctant to exclude any of the previously used drugs. Our data suggests the inclusion of fluconazole may not be warranted in the current PAM treatment regimen and that posaconazole could replace fluconazole in the treatment regimen for future PAM cases.

**Table 3.1:** Primary amoebic meningoencephalitis patient isolates

<b>Isolate</b>	<b>Sample Type</b>	<b>Year</b>	<b>Origin</b>
V067	CSF	1987	Arizona
V206	CSF	1990	Mexico
V413	CSF	1998	Texas
V414	CSF	1998	Florida
V596	CSF	2007	Nevada

CSF – Cerebrospinal fluid



**Table 3.2** Active FDA-approved compounds identified from the St. Jude Children's Research Hospital library

<b>Compound</b>	<b>IC<sub>50</sub> (μM)</b>	<b>Class</b>
Azithromycin <sup>a</sup>	0.02	Antibiotics
Azithromycin dihydrate <sup>a</sup>	0.02	
Clarithromycin	0.03	
Valnemulin hydrochloride	0.04	
Tilmicosin	0.06	
Erythromycin ethylsuccinate <sup>a</sup>	0.10	
(-)-Erythromycin <sup>a</sup>	0.12	
Roxithromycin	0.20	
Dirithromycin	0.39	
Retapamulin	0.44	
Itraconazole	0.08	Antifungals
Posaconazole	0.24	
Butenafine hydrochloride	0.42	
Ketoconazole	1.37	
Terbinafine hydrochloride <sup>a</sup>	3.00	
Liranaftate	5.42	
Terbinafine <sup>a</sup>	6.05	
Gemcitabine <sup>a</sup>	0.34	Nucleosides
Gemcitabine hydrochloride <sup>a</sup>	0.36	
Fludarabine phosphate	0.58	
Clofarabine	1.76	
Bortezomib	0.60	Proteasome inhibitor
Vorinostat	1.26	HDAC inhibitor
Pitavastatin	3.52	HMG-CoA reductase

<sup>a</sup>Different salts were included in compound library.

**Table 3.3** Active compounds from the Medicines for Malaria Venture (MMV) Pathogen Box

<b>Compound</b>	<b>Other Name</b>	<b>IC<sub>50</sub> (μM)</b>	<b>Disease Set<sup>a</sup></b>	<b>Sources</b>
MMV688774	Posaconazole	0.86	Reference	
MMV652003	AN3520	1.10	Kinetoplastids	[123,125]
MMV688180	DDD85646	1.44	Kinetoplastids	[126–128]
MMV024406		1.61	Kinetoplastids	
MMV676602	Milciclib	1.78	Kinetoplastids	[129,130]
MMV676604		2.17	Kinetoplastids	[130]
MMV688943	Difenoconazole	>10	Kinetoplastids	
MMV688942	Bitertanol	>10	Kinetoplastids	
MMV689244		>10	Kinetoplastids	
MMV689243		>10	Kinetoplastids	
MMV006741		>10	Malaria	
MMV1019989		>10	Malaria	
MMV1037162		>10	Malaria	

<sup>a</sup> Disease set refers to the group of organisms that have a known activity with the compounds in the collection as detailed by MMV.

**Table 3.4** Dose-response data from a collection of anti-parasitics (n=2).

<b>Compound<sup>a</sup></b>	<b>IC<sub>50</sub> <math>\mu</math>M</b>	<b>Collection</b>
Trans-mirincamycin	9.29	Antibiotics
Cis-mirincamycin	10.9	
Paromomycin	> 50	
Clindamycin	> 50	
Tafenoquine	9.56	Anti-parasitics
Pyronaridine	12.2	
JPC 2056	14.4	
PS 15 (WR 250417)	15.7	
Mefloquine hydrochloride	24.4	
Sitamaquine	26.7	
Amodiaquine	28.9	
Atovaquone	33.0	
Primaquine	41.6	
Dihydroartemisinin	> 50	
Chloroquine	> 50	
Artesunate	> 50	
Quinine	> 50	
Artemisinin	> 50	
Proguanil	> 50	
Cycloguanil	> 50	
Pyrimethamine	> 50	
WR 99210	> 50	
Lumefantrine	> 50	
Chlorpromazine	20.5	
Promethazine	26.6	Anti-histamine
Chlorpheniramine	> 50	Anti-histamine
Fluridon	> 50	Herbicides
Norflurazon	> 50	
Glyphosate	> 50	
Auranofin	8.37	Anti-rheumatic
Verapamil	34.7	Calcium-channel blocker
Desipramine	> 50	Antidepressant (NE reuptake inhibitor)
Furosemide	> 50	Diuretic

<sup>a</sup>Compounds were purchased commercially or from the Walter Reed Army Institute of Research information system library.

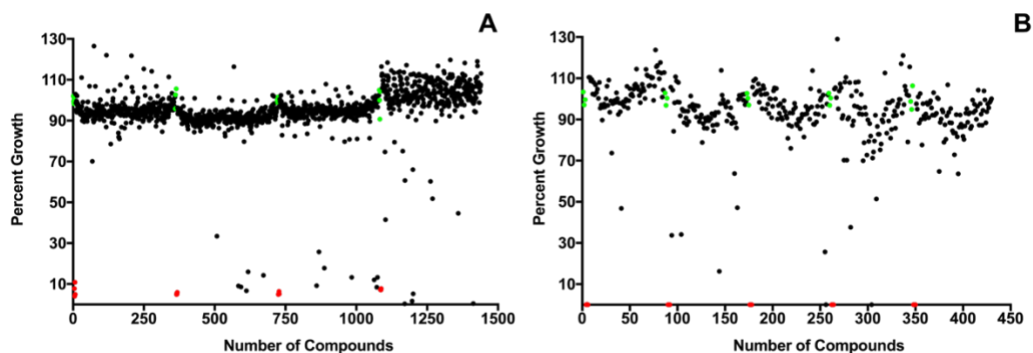


**Figure 3.1** Single point assays of FDA-approved compounds from the St. Jude Children's Hospital Library ranging from 1-17 $\mu$ M (A) and compounds from the Medicines for Malaria Venture (MMV) Pathogen Box at 1 $\mu$ M (B) were carried out using pathogenic *N. fowleri* (n=2). Each black point represents a compound that was screened, the red points are negative growth controls, and the green points are positive growth controls included on each plate. We identified 24 hits from the St. Jude Children's Research Hospital Library and 13 hits from the MMV Pathogen Box. Each hit was confirmed with a serial dilution to identify inhibitory concentrations.

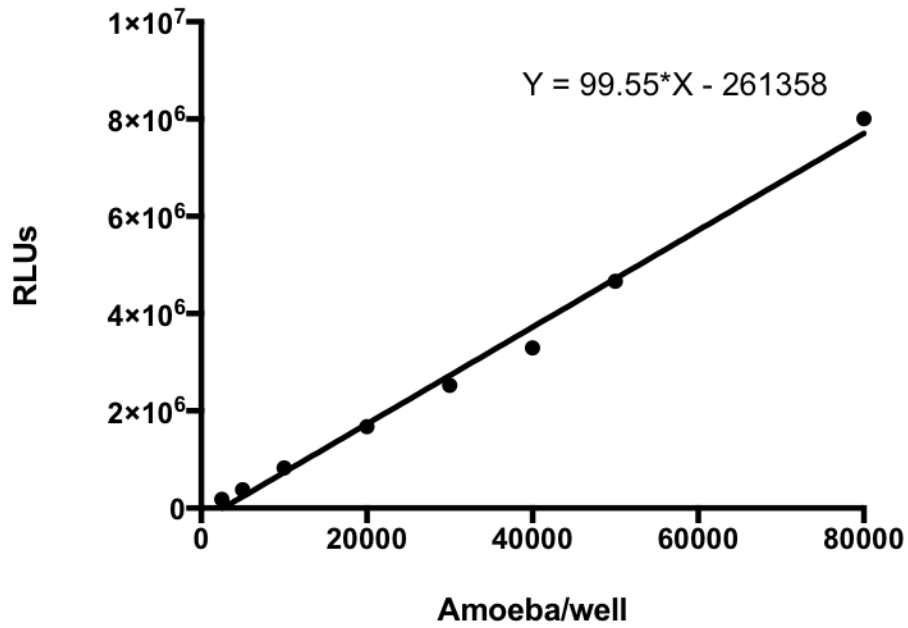


**Figure 3.2** Standard curve displaying the linearity between the number of amoebae per well and relative luminescent units (RLUs) for the RealTime-Glo Viability assay that was used to identify the rate of inhibition.

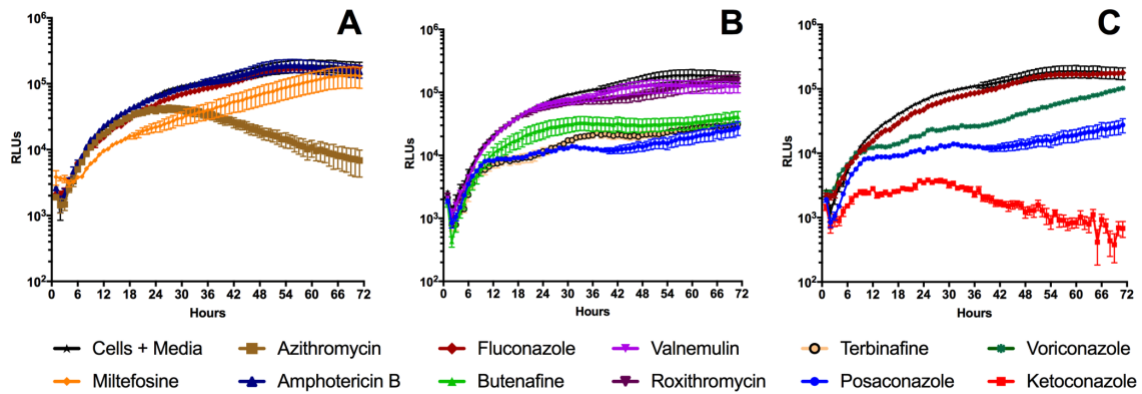


**Figure 3.3** Rate of inhibition at  $1x-IC_{50}$  for drugs in the current PAM treatment (A), FDA-approved compounds identified through the St. Jude screen (B), and known anti-fungals (C). These graphs are data from a single experiment with 4 replicates, but representative of independent biological repeats ( $n=3$ ).

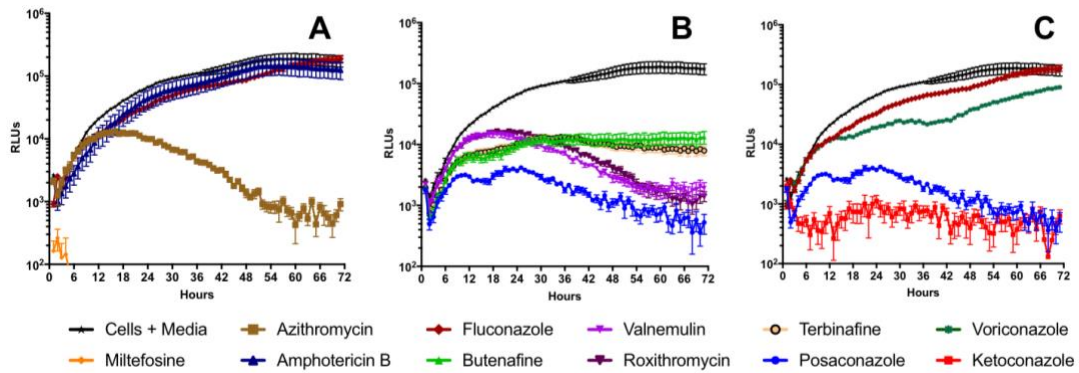


**Figure 3.4** Rate of inhibition at  $5 \times \text{IC}_{50}$  for drugs in the current PAM treatment (A), FDA-approved compounds identified through the St. Jude Children's Research Hospital screen (B), and known anti-fungals (C). These graphs are data from a single experiment with 4 replicates, but representative of independent biological repeats ( $n=3$ ).

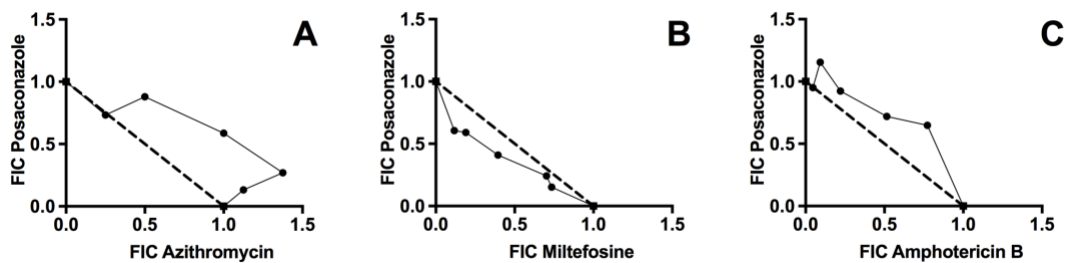


**Figure 3.5** Isobolograms of posaconazole with azithromycin (A), miltefosine (B), or amphotericin B (C). The dotted line in the graph represents the line of additivity. These graphs are data from a single experiment with replicates, but representative of independent biological repeats (n=3).



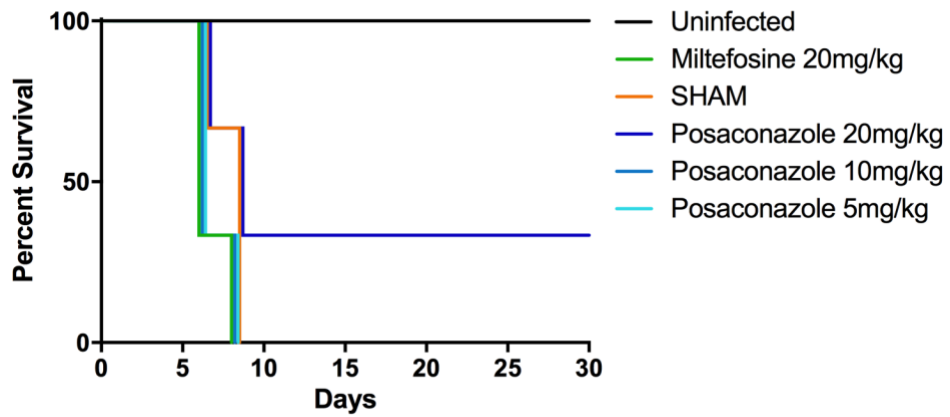


**Figure 3.6** Kaplan-Meier survival curves for female ICR mice (n=6) dosed intravenously with posaconazole at 20mg/kg, 10mg/kg and 5mg/kg, phosphate-buffered saline, or 20mg/kg miltefosine. 33% survival was observed with intravenous posaconazole (20mg/kg) treated mice (Logrank test for trend  $p < 0.05$ )

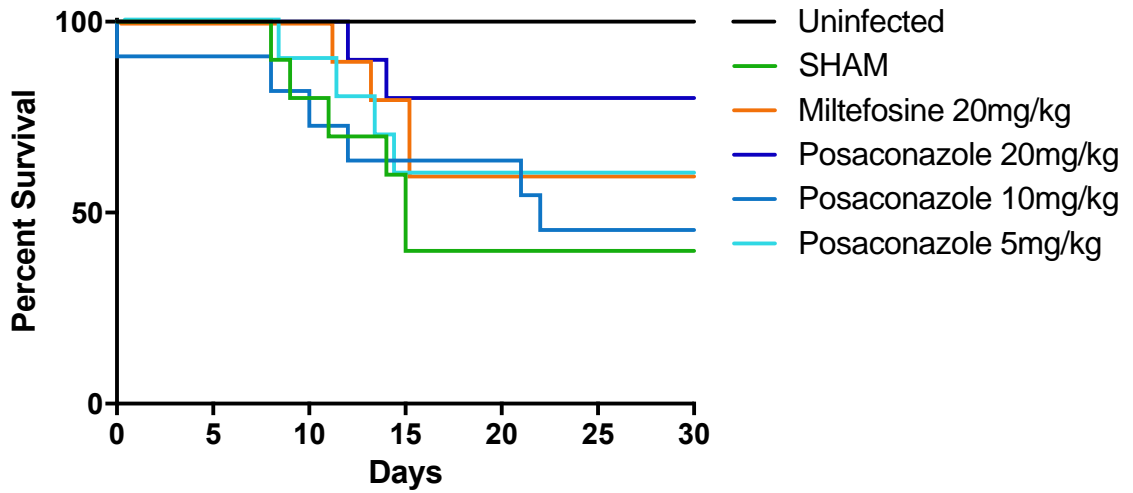


**Figure 3.7** Kaplan-Meier survival curves for female ICR mice (n=10) dosed intravenously with posaconazole at 20mg/kg, 10mg/kg and 5mg/kg, phosphate-buffered saline, or 20mg/kg miltefosine.

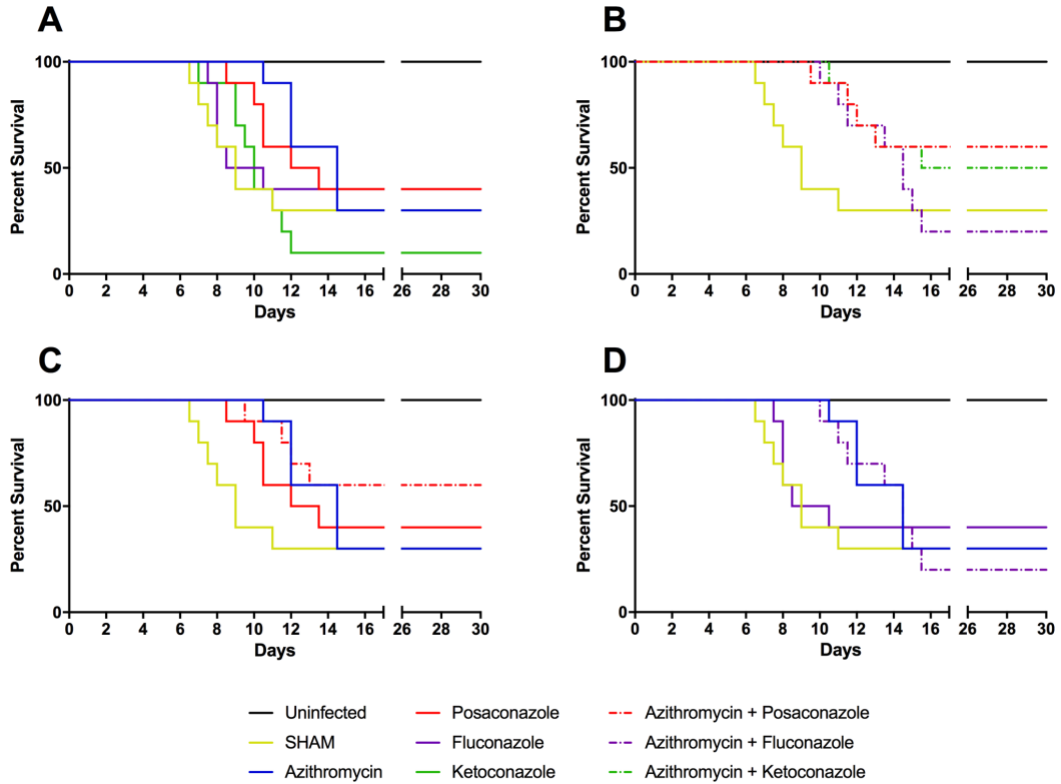


**Figure 3.8** Survival curves of mice infected with *N. fowleri* and dosed with combinations of azithromycin and conazoles. Female ICR mice (n=10) were dosed with (A) azithromycin at 25mg/kg, (B) posaconazole at 20mg/kg alone and in combination with azithromycin, (C) fluconazole 30mg/kg alone and in combination with azithromycin and (D) ketoconazole alone at 25mg/kg and in combination with azithromycin. Solid lines represent drug alone and dashed lines represent combination with azithromycin. Deaths are reported in half days.

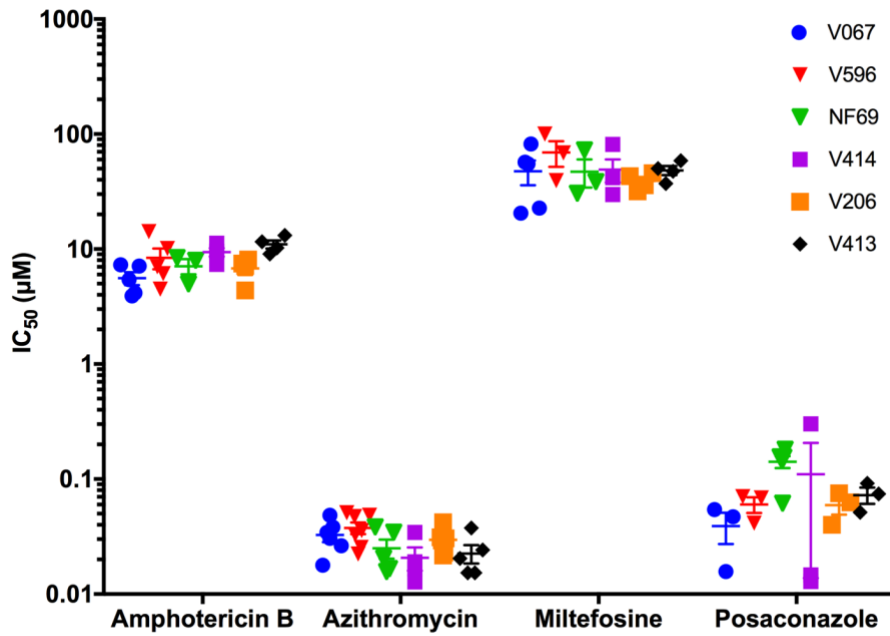


**Figure 3.9** IC<sub>50</sub>s of multiple CDC isolates and NF69 (reference strain). Each point represents one biological repeat with two replicates (n≥3). Error bars represent the standard error me

## CHAPTER 4

### DB 2518-RESISTANT *NAEGLERIA FOWLERI* ELUCIDATES POTENTIAL TARGETS FOR DRUG DISCOVERY

#### INTRODUCTION

Pentamidine is an aromatic diamidine that has been a longstanding treatment against infectious diseases. Pentamidine is currently listed as an essential medicine on the World Health Organization (WHO) Model List of Essential Medicines for the treatment of pneumocytosis and the primary stage of African trypanosomiasis [135]. Additionally, pentamidine isethionate has also been used in the treatment of granulomatous amoebic encephalitis caused by the free-living amoebae: *Acanthamoeba* spp., *Balamuthia mandrillaris*, and *Sappinia diploidea*. Moreover, propamidine isethionate and dibromopropamidine isethionate have been used for *Acanthamoeba* keratitis caused by various *Acanthamoeba* species. However, there are concerns with pentamidine toxicity, especially after extended treatment regimens. [2].

Due to the effectiveness of pentamidine with various infectious diseases, recent structure activity relationship studies with the pathogenic free-living amoebae, *Naegleria fowleri*, looked at various amidine classes to identify novel compounds that inhibit amoebic growth. This study identified both bis-benzimidazole amidines and diamidines to be among the most potent amidine

classes of those tested [48]. Other classes included the furamidine and arylimidamides, which have been shown to be active against trypanosomes and *Leishmania* spp., respectively [48,85,88,136]. Furamidines, such as DB 75, have been shown to be DNA binders with an affinity to bind to AT-rich areas [137]. However, additional evidence shows that DB 75 targets the mitochondria of *Trypanosoma brucei brucei* [138]. In contrast, the arylimidamide, DB 766, has been shown to target CYP5122A1 in *Leishmania donovani*, which is a key enzyme in ergosterol metabolism [139]. However, the mechanism by which bis-benzimidazole amidines or diamidines inhibit the growth of *Naegleria fowleri* is not known.

Many studies have used the development of drug-resistant parasites to identify potential targets for novel compounds [52,139,140]. In this study, we developed resistance to a bis-benzimidazole amidine, DB 2518, to identify potential targets for the novel compound. This is the first study in the field to develop drug-resistant *Naegleria fowleri*. Furthermore, we were able to clone the populations to further study phenotypic and genotypic differences among sensitive and resistant amoebae. First and foremost, the results of this study will be able to provide the free-living amoebae field with an additional reference genome. Additionally, identifying mutated genes within the resistant populations may elucidate a novel drug target that can be used to develop a new treatment for primary amoebic meningoencephalitis.

## **MATERIALS AND METHODS**

### Development of Resistance

*Naegleria fowleri* (ATCC 30215) were cultured in Nelson's culture medium (NCM) with 10% fetal bovine serum (FBS) at 34°C. To develop resistance, DB 2518 was added at 0.86µM (IC<sub>50</sub>) into the culture. Recovery periods were used to allow amoebae to grow to confluence before the re-addition of DB 2518. When amoebae consistently grew to confluence, drug pressure was increased to 8.6µM (10x-IC<sub>50</sub>). The step-wise increase of drug pressure continued until amoebae were able to grow at 100x IC<sub>50</sub>. Cells underwent cryopreservation on day 67 and still maintained the ability to grow under drug pressure when thawed (Figure 4.1).

### Drug Susceptibility

To identify if resistance was generated with step-wise increase of drug pressure and if there was any co-resistance to other drugs, we set up dose-response curves using the CellTiter-Glo (Promega) assay. Both drug-pressured and sensitive cell lines were counted with a hemocytometer and plated at 4,000 cells/well. Compounds were plated in replicate with a 1:2 dilution for 11 dilutions. Positive growth controls included 4,000 cells/well in complete NCM. To achieve maximum killing of amoebae, negative growth controls included 135µM of amphotericin B and 2,000 cells/well. DataAspects Plate Manager analysis software was used for curve fitting with nonlinear regression to detect IC<sub>50</sub>, IC<sub>90</sub>,

and slope values (Rice et al 2015). Values reported are from a minimum of three biological replicates.

### Cloning

After drug resistance was verified with dose-response curves, cultures were diluted to 0.5 amoeba/well and plated in a culture-treated 96-well plate to obtain clones of resistant and sensitive amoebae. Amoebae were grown in the wells in the absence of drug until confluent then transferred into flasks. Dose-response curves were performed to verify clones maintained a resistant phenotype.

### Growth Rate Assay

We observed growth rate differences between the resistant and sensitive cell lines during drug susceptibility testing. Therefore, we used the RealTime-Glo assay (RTG; Promega, Madison, WI) to quantify the differences in the rate of growth between both cell lines. Compounds were plated at 5x-IC<sub>50</sub> and 10x-IC<sub>50</sub> with three replicates per clone. The 96-well plates were prepared with 10µl of drug, 40µl with 4,000 cells and 50µl of RTG reagent containing enzyme and substrate. The positive growth controls were cells in media with RTG reagent and the negative controls were media and RTG reagent. The lab reference strain, NF69 was added as an additional control to identify any growth differences between sensitive clones and wildtype. Plates were incubated at 34°C for 72 hours in a SpectraMax i3x (Molecular Devices; Sunnyvale, CA). Relative



luminescence units (RLUs) were continually recorded every hour. Raw data was reshaped using Rstudio and analyzed with Prism (GraphPad Software; La Jolla, CA).

### Imaging

To quantify the differing sizes amongst the clones, DIC images were taken of trophozoites. Images were analyzed using the threshold and area measurement tools on FIJI.

One million amoebae for each clone were dispensed into wells of a chamber slide and incubated at 34°C for 15 minutes to allow for adherence. Amoebae were first stained with 1 µg/ml of Hoechst 33342 for 15 minutes at room temperature then washed with phosphate-buffered saline (PBS). In later experiments, 0.5 µg/ml of DAPI was used for 15 minutes because it stained the DNA of resistant clones more effectively. Cells were then stained with 50nM of LysoTracker Red DND-99 for 40 minutes in PBS at 34°C. Cells were washed with PBS and fixed with 2% paraformaldehyde in PBS. Images were taken on the Zeiss Axio Observer using ZEN 2.3.

### DNA Extraction

*N. fowleri* cells were first washed with phosphate-buffered saline (PBS) to remove any residual media components. Cell pellets were resuspended in 300 µL TELT buffer (50mM Tris at pH 8.0, 62.5mM EDTA at pH 8.0, 2.5M LiCl, 4% Triton X-100) to lyse cells. To separate nucleic acids from proteins and lipids,

300 $\mu$ L of 25:24:1 phenol/chloroform/isoamyl alcohol was added to samples and centrifuged at 16,830g for 5 minutes. The aqueous phase containing DNA was transferred into a new microcentrifuge tube. To precipitate DNA, 1mL of cold 100% ethanol was added to samples, inverted, and placed on ice for 5 minutes. Samples were centrifuged at 10,000g for 10 minutes at 4°C then washed with 1mL of cold 70% ethanol. Samples were centrifuged, resuspended in TE buffer (10mM Tris-HCL at pH 8.0 and 0.1mM EDTA) with 1 $\mu$ L of RNase A (PureLink) and incubated at 37°C for 30 minutes. Lastly, all samples were run on a 0.8% agarose gel to verify that base pair lengths were greater than 9kb.

### Whole Genome Sequencing and Assembly

Genomic DNA samples were sent to the Georgia Genomics and Bioinformatics Core (GGBC; Athens, GA) for library preparation and sequencing. The library was prepared using Hyper Prep kit with a insert size of ~630bp. Paired-end read sequence data from the Illumina NextSeq platform was quality tested using FastQC v0.11.5. All read sequences were trimmed using Trimmomatic v0.36 [141] based upon phred score >30 and minimum trimmed read length of 100; Illumina adapters were also checked and trimmed in this step.

For the *de novo* assembly, all reads were submitted to KmerGenie for a k-mer calculation for a diploid genome and an interval between consecutive k-mer sizes of 2. The ideal k-mer found was 23. Sequences were assembled using a multi-k genome assembler SPAdes v3.12.0 [142] using the best k-mer as a reference for the k-mer prediction. These results were submitted to an evaluation

using a Quality Assessment Tool for Genome Assemblies (QUAST). Reads were scaffolded using some of the available structure information from a different *N. fowleri* strain (ATCC 30863) reference genome using Chromosomer v0.1.4a [143]. These scaffolds were submitted to GapFiller v.2.1.1 [144] and Pilon v.1.22 [145] to fill in gaps, extend sequence lengths, and polish the base call by frequency on the Illumina alignment to improve the assembly.

### Genome Annotation and Analysis

The genome annotation was made using two gene prediction tools: GeneMark-ES [146] and AUGUSTUS [147]. GeneMark-ES is an unsupervised training prediction tool that is used to help to build an organism training file for the AUGUSTUS prediction. For the alignments, we submitted the Illumina reads to the Burrows-Wheeler Aligner (BWA-MEM) [148] and formatted the output with Picardtools.

The GATK HaplotypeCaller was used to identify variants. The variants were then filtered by quality and minimum depth coverage to decrease the chances of noise calls in the final results. All variant call files were then submitted to SnpEff [149] with a custom *N. fowleri* annotation database recovered from our results. All SNPs with some mutation effect in the mutated genomes were identified and ranked by type of effect. Functional analysis was carried out through Blast2GO to identify matches to known genes (Figure 4.2).

## RESULTS

### DB 2518 resistance

The inhibitory concentration was tested for *N. fowleri* cultures that were grown under 50x-IC<sub>50</sub> (43μM) of DB 2518 and the reference strain NF69 grown under normal conditions. We found the IC<sub>50</sub> of the DB 2518 culture to be 18x higher than NF 69 (Figure 4.3). Once clones were confluent, dose-response curves were generated to verify the resistant phenotype was not lost. An analysis of variance (ANOVA) on the IC<sub>50</sub>s identified a significant variation among the clones [F(5,11) =4325, p <0.0001]. A Dunnett's multiple comparisons post-hoc test identified that one clone, AB7 with an IC<sub>50</sub> of 198μM is significantly more resistant than the sensitive clones (DD8 and DE7; p > 0.0001). Additionally, CD12, CE5, and AA11 were found to be significantly more resistant than sensitive clones, DD8 and DE7. No significant differences in IC<sub>50</sub>s were identified between DD8 and DE7 (Figure 4.4).

The stability of resistance was indirectly identified by changes in morphology and verified with the addition of DB 2518 (43μM) to cultures. Even though cultures were tested for stability of resistance with a freeze-thaw cycle, two of the clones lost resistance without drug pressure within 3-4 weeks. The resistant clones AA11 and CE5 lost resistance, while AB7 and CD12 were able to survive the drug pressure in culture at week 4 (data not shown).

### Cross-resistance

After verifying that resistance was maintained post-cloning, we aimed to identify any cross-resistance with similar structured compounds (Table 4.1). We found that all of the clones maintained a degree of resistance with these compounds as shown through the resistance index (RI) calculated against DD8 (Table 4.2). Additionally, we show no significant differences in  $IC_{50}$  for any of the compounds among the sensitive clones, DD8 and DE7.

With DB 2518, AB7 has a RI approximately 23 times larger than the other clones; we do not see this significant difference across the other compounds (DB 2521, DB 2526, DB 2530, and DB 2541). Interestingly, this provides evidence that the location of the dimethylaminoethanol side chain of the terminal phenyl is important. In DB2518 the side chain is in the meta position, in DB 2526 the side chain is in the para position and we see a decrease of resistance in the resistant clones. Additionally, when comparing DB 2541 to DB 2526, we see the RI halved in AA11 and CE5. The only difference between these structures is the addition of a fluorine atom to DB 2541.

### Growth Rates

We used the RTG assay to identify any differences in growth between sensitive and resistant clones. We found that the sensitive clones, DD8 and DE7, grew faster than the reference strain, NF69, and resistant clones. Additionally, of the resistant clones, we found AB7 to show the least amount of growth within 72 hours (Figure 4.5).

## Imaging

The area of the resistant clones, AB7 and CD12, was found to be significantly smaller than the sensitive clones, DD8 and DE7 (Figure 4.6). As shown on the DIC images, the lack of vacuoles in the resistant clones may be an explanation for their decreased size.

In attempt to identify whether DB 2518 was co-localizing in the nucleus, we stained the resistant and sensitive clones with Hoechst 33342, a bisbenzimidazole, that is structurally similar to the bis-benzimidazole amidines used in this study (Table 4.1). Interestingly, in the resistant clones, the stain did not accumulate in the nucleus. Unlike in the sensitive clones where the same Hoechst stain was able to define the nucleus of each amoebae (Figure 4.7). However, when staining DNA with DAPI we were able to identify the nucleus in the resistant and sensitive amoebae (Figure 4.8). With the use of LysoTracker Red, a structurally different stain than DB 2518, we identified a different phenotypic difference among the resistant and sensitive clones. The resistant clones (AA11, AB7, CD12, and CE5) show a decreased amount of acidic vacuoles than the sensitive clones (Figure 4.8).

## Sequence analysis

The DD8 assembly (~25Mb) was found to be shorter than the reference genome for *N. fowleri* ATCC30863 (30Mb) that is publicly available on GenBank [150]. While both assemblies were similar, as compared on a synteny graph

(data not shown), DD8 was chosen as the reference assembly for variant analysis. Resistant and sensitive clones were assembled and initially compared to DD8. We were able to verify that there were an increased number of variants among the resistant clones in comparison to the sensitive clones. Additionally, we were able to verify that the variation between the runs was minimal (n=4). Resistant variants and sensitive variants were pooled separately and then compared for unique variants among the resistant clones. Due to the significant resistance seen in AB7, we pooled the remaining resistant clones and compared the mutations that were unique to AB7. These sequences were submitted to Blast2GO for analysis by comparing across all known protein sequences and motifs. There were 135 mutant sequences identified to be specific to AB7 with 129 of the sequences showing matches across known molecular function (F), cellular component (C), or biological process (P) of published genes (Table 4.3).

## **DISCUSSION**

This study was the first in the field to develop a drug-resistant amoebae population; furthermore, to use a resistant population to help identify a potential mechanism of action in the free-living amoebae field. In order to elucidate potential targets we first described phenotypic differences between the 4 resistant clones, AA11, AB7, CD12, and CE5, with the 2 sensitive clones, DD8 and DE7. Throughout the study we identified significant phenotypic differences in the resistant clones, AA11, AB7, CD12, and CE5 including an increased tolerance to DB-2518, slowed growth rates, smaller area, and fewer vacuoles.

Since AB7 showed significant phenotypic differences from wild type *N. fowleri* and the resistant clones, we used this population to identify mutations through whole-genome sequencing. In doing so, we identified 135 sequences that were mutated in comparison to any of the resistant and sensitive clones used in this study. From the 135 mutated sequences, we identified descriptions 129 to known sequences through gene ontology terms and known motifs.

The bis-benzimidazole amidine, DB 2518, was used to develop resistance in *N. fowleri*. One clone in particular, AB7, was over 100 times more resistant than sensitive clones. When testing similarly structured compounds against AB7, we did not identify the same degree of resistance. However, when using the structurally similar Hoechst stain we identified the inability of Hoechst to stain the DNA of AB7. Although Hoechst easily crosses the membrane of wild-type cells, the mechanism behind which Hoechst was unable to stain the DNA is still unknown. Due to the inability of resistant clones to also stain with LysoTracker Red, there was an initial concern that resistant clones were not allowing uptake or permeation of stains. However, with the use of DAPI, we were able to identify that the resistant clones were able to uptake stain, and therefore, selective to Hoechst most likely due to the similarity in structure to DB 2518.

In addition to the increased tolerance to DB 2518, AB7 also showed the slowest growth rate amongst all clones used in this study. While there was a definite decrease in growth seen while culturing, the growth rate of AB7 may actually be higher than shown in the RTG assay. Since AB7 is the most resistant clone, it is likely that mutations may have occurred decreasing its' ability to



metabolize the substrate in the assay, thereby showing no growth over the 72-hour time period. In order for the RTG assay to properly show growth over time, the substrate needs to be metabolized so that it may bind the enzyme and produce light units. To quantify the minimal growth seen with AB7 over time in cultures, it would be necessary to optimize an assay using a different mechanism or more reasonably to perform counts either manually or with flow cytometry over time. Additionally in this experiment, the sensitive clones, DE7 and DD8, showed an increased growth rate compared to the parental population NF69.

Unfortunately, this phenotype was selected for in the cloning process as populations were collected once they became confluent in the cloning plate. For future studies, it may be worth selecting sensitive clones at different times throughout the experiment and then and then testing their growth rate against NF69. By doing so, we would verify that the phenotype is representative of the wildtype population and have a more accurate comparison of growth rates between sensitive and resistant clones.

Interestingly, the size of the resistant amoebae and sensitive amoebae was significantly different. This morphological difference was readily noticed post-cloning and quantified through DIC imaging. One could hypothesize that the smaller amoebae are less able to phagocytose nutrients due to their reduced area and therefore less capable of growing at the same rates. To test this hypothesis, future work may include inducing phagocytosis in the resistant and sensitive clones by plating amoebae with heat-inactivated fluorescently tagged bacteria and tracking cells over time to measure phagocytosis events.

The structure of LysoTracker Red is dissimilar to DB 2518, therefore, the lack of acidic vacuole staining in the resistant clones becomes an interesting morphological distinction to further study. Using LysoTracker Red we found a decreased amount of vacuoles in the resistant amoebae than the sensitive amoebae. In amoebae, lysosomes are important acidic organelles that release enzymes upon merging with phagosomes for digestion [151]. The reduced number of lysosomes seen in the resistant clones supports the hypothesis that there is a reduction in phagocytosis among the resistant clones. It is also possible that the decrease in vacuoles within the amoebae is the reason for the smaller area seen in the resistant clones. To verify that the decreased area of the amoebae is due solely to the lack of vacuoles, a cytoplasm stain can be used to quantify the area within both sensitive and resistant amoebae.

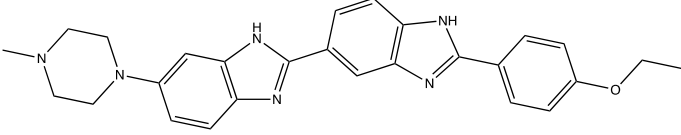
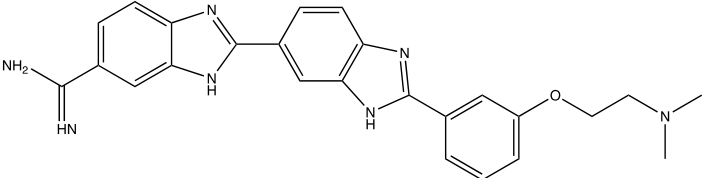
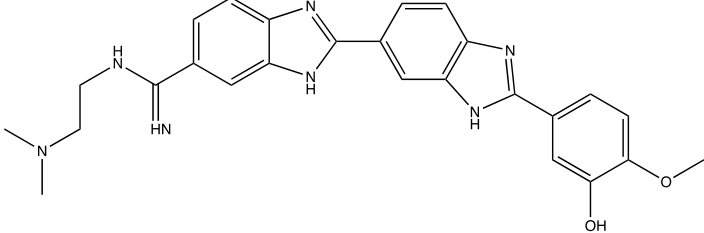
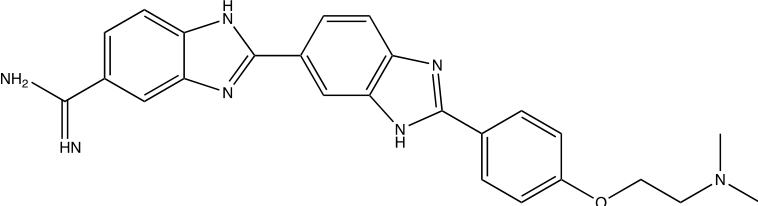
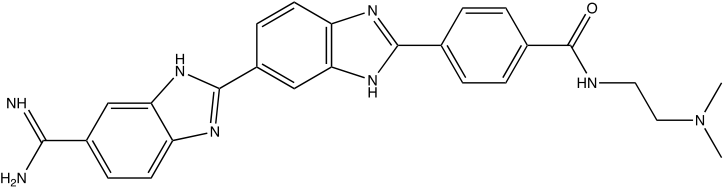
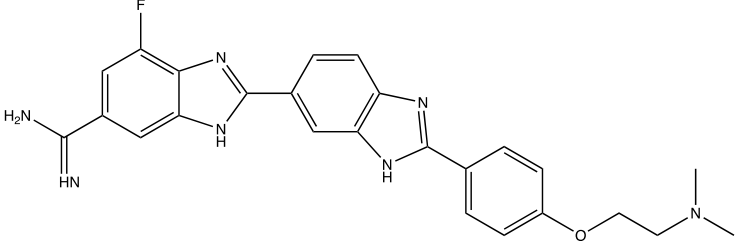
Future work needs to be done to further understand the phenotypic differences among the resistant clones. For instance, the loss of resistance seen with the AA11 and CE5 clones suggests there may be a fitness cost associated with the drug-resistance. Future studies looking at the competitive growth in the presence and absence of drug may be able to provide evidence for a fitness cost in the mutants.

Since AB7 showed significant differences among the other clones, whole genome sequencing analysis identified the mutated sequences only found in AB7. Our analysis identified 135 sequences to be mutated and 129 of those sequences shared motifs or found to be similar to known proteins based of gene ontology analysis. Due to the vacuolar phenotype seen amongst resistant clones, *cgd8\_4790* (vacuolar ATP synthase), *g8718* (vacuolar protein sorting 9 domain-

containing protein 1-like) and g5766 (vacuolar protein sorting-associated protein 16) are of particular interest. Interestingly, vacuolar protein sorting protein and vacuolar ATP synthase mutants in yeast have been shown to have growth and organelle acidification defects [152]. Future work is needed to confirm the target of DB 2518. These experiments would include designing primers to sequence these mutated regions in AB7 to verify the mutations are present. It is possible that the amoebae may be using the vacuoles to break down DB 2518 from the cell causing the diminished lysosome phenotype and is therefore a result of the amoebae becoming resistant and not necessarily the direct target of DB 2518. Ideally, to verify that these regions are the target of DB 2518, it would be useful to knockout these genes individually in the wildtype *N. fowleri* and test for DB 2518 susceptibility.

Lastly, many of the non-vacuolar sequences identified to be mutated in AB7 are nucleoside-related. To identify if these are a target of DB 2518, we could screen the nucleoside analogs, gemcitabine, fludarabine, and clofarabine, which we have found to be active in NF69 (Table 3.2), against AB7 and determine if there is cross-resistance. The results from these experiments could help elucidate the mechanism by which DB 2518 is inhibiting the amoebae. In this study we identified trends through the gene ontology analysis that may be the target or downstream effect of DB 2518. Future work is still needed to validate the target, however the analysis from our mutant sequences can be used to elucidate additional novel targets for the treatment of primary amoebic meningoencephalitis.

**Table 4.1** Comparison of the structurally similar bis-benzimidazole amidines with Hoechst stain.

Compound	Structure
Hoechst 33342	
DB 2518	
DB 2521	
DB 2526	
DB 2530	
DB 2541	

**Table 4.2** Cross-resistance among resistant clones

Clones	DB 2518		DB 2521		DB 2526		DB 2530		DB 2541	
	IC <sub>50</sub> (μM) ± SD	RI	IC <sub>50</sub> (μM) ± SD	RI	IC <sub>50</sub> (μM) ± SD	RI	IC <sub>50</sub> (μM) ± SD	RI	IC <sub>50</sub> (μM) ± SD	RI
DD8	1.44 ± 0.4	1.0	0.40 ± 0.08	1.0	0.58 ± 0.07	1.0	0.75 ± 0.10	1.0	1.12 ± 0.25	1.0
DE7	1.38 ± 0.5	0.96	0.37 ± 0.03	0.9	0.58 ± 0.15	1.0	0.82 ± 0.15	1.1	1.01 ± 0.12	0.9
AA11	8.09 ± 2.2	5.6	2.12 ± 0.78	5.3	2.44 ± 0.33	4.2	4.03 ± 0.87	5.4	3.08 ± 0.79	2.8
CE5	9.72 ± 1.8	6.8	1.92 ± 0.10	4.8	2.80 ± 0.77	4.8	3.15 ± 0.87	4.2	2.47 ± 0.52	2.2
CD12	11.07 ± 1.7	7.7	1.75 ± 1.03	4.4	1.70 ± 0.59	2.9	3.34 ± 1.74	4.5	2.88 ± 1.99	2.6
AB7	198.74 ± 3.3	138.0	2.69 ± 0.47	6.7	2.66 ± 0.17	4.6	3.61 ± 2.38	4.8	4.47 ± 3.03	4.0

**Table 4.3** Mutated sequences identified in the resistant clone, AB7

<b>Sequence Name</b>	<b>Description</b>	<b>GO hits*</b>	<b>Enzyme Names</b>
g641	sorting nexin-20	F	
g8729	fibronectin, type-like protein	F, C	
g4407	predicted protein	C, P	
g5637	predicted protein	F	
g9116	predicted protein	F, C, P	
g681	predicted protein	F	
g5110	calcium uniporter protein, mitochondrial isoform X1	F, C, P	
g9600	progesterone-induced-blocking factor 1 isoform X1	C, P	
g9174	integral membrane protein	F, C	
g642	predicted protein	F, P	
g4455	predicted protein	F, C, P	
cgd1_3140	UMP-CMP kinase	F, P	Nucleoside-phosphate kinase; UMP/CMP kinase
g4384	kinesin-like protein KIN-7N	F, C, P	Adenosinetriphosphatase; Nucleoside-triphosphate phosphatase
g9421	Ribosomal large subunit pseudouridine synthase B	F, P	
g1449	alternative oxidase	F, C, P	
g1458	DnaJ domain protein	F	
g4266	predicted protein	F	
cgd1_870	peptidylprolyl isomerase	F, P	Peptidylprolyl isomerase
cgd5_1470	nucleoside-diphosphate kinase	F, P	Nucleoside-diphosphate kinase
g9048	ankyrin repeat domain-containing protein	F	
cgd8_4790	vacuolar ATP synthase 22 kDa proteolipid subunit, putative	F, C	
g4513	predicted protein		
g6077	regulator of chromosome condensation RCC1	F, C, P	

g4382	S-adenosyl-L-methionine-dependent methyltransferase	F, P	
g4399	X-linked retinitis pigmentosa GTPase regulator		
g73	predicted protein	F, P	
g5057	predicted protein	F, C, P	
g3339	predicted protein		
g5767	Origin recognition complex subunit 2	C	
g8288	glutathione S-transferase T1-like	F	
g5765	predicted protein	C	
g2983	KH domain protein	F, C, P	
g6912	charged multivesicular body protein 1	C, P	
g8020	predicted protein	F	
g9100	C2 and GRAM domain-containing protein At1g03370 isoform X1	F, C, P	
g8330	protein RKD5-like	F, C, P	
g3650	predicted protein	F, C, P	Protein-serine/threonine phosphatase; 4-nitrophenylphosphatase
g4380	centromere protein J-like	F, C, P	
g3136	Phosphatidylglycerol/phosphatidylinositol transfer protein	C, P	
g7032	nucleoporin GLE1	C, P	
g2831	predicted protein	C	
g4456	ornithine decarboxylase antizyme	F	
g6080	histone H2A	F, C, P	
g8285	predicted protein	C	
g4370	predicted protein	F, P	
g8942	Stk1 family PASTA domain-containing Ser/Thr kinase	F, P	
g4367	predicted protein	C	
g1425	SRPBCC domain-containing protein		
g9120	chromosome segregation protein SMC	F, C, P	

g2858	predicted protein	F, C, P	
g2727	N-acetylglucosamine-1-phosphodiester alpha-N-acetylglucosaminidase	C	
g6369	predicted protein	C	
cgd4_3260	RNA polymerases N / 8 kDa subunit family protein	F, P	DNA-directed RNA polymerase
g3208	predicted protein	F, C	
g479	predicted protein		
g9122	predicted protein	F	
g8284	ribosomal protein L35	F, C, P	
g4497	predicted protein		
g5775	predicted protein		
g4398	predicted protein	F, P	
g6886	predicted protein		
g4270	predicted protein		
g5051	trypsin domain containing protein	F, C, P	
g8283	Cell cycle control protein		
g3652	silent information regulator family protein	F	
g4371	predicted protein	F, C, P	
g3653	predicted protein		
g4452	cilia- and flagella-associated protein 53-like	P	
g2981	predicted protein	F, C, P	
g9564	predicted protein	F, C, P	
g5634	cysteine proteinase		
g4275	hypothetical protein NAEGRDRAFT_79172		
g5759	hypothetical protein VF21_09252	F, P	
g9115	nuclear pore complex protein Nup160	F, C, P	
g5038	pentatricopeptide repeat-containing protein At1g63330-like	F	
g5056	nuclear pore complex protein NUP96	F, C, P	



g4377	mitochondrial intermediate peptidase	F, C, P	
g5106	rap/ran GTPase-activating protein	F, P	
g4518	abc transporter B family protein	F, C, P	
g9044	cytokinin dehydrogenase 6-like	F, P	
g5752	Ded_cyto domain-containing protein	F, C, P	
g6866	Eukaryotic translation initiation factor 2A	F, P	
g5068	DUF214 family protein	F, C	
g6091	predicted protein	F, C	Adenosinetriphosphatase; Nucleoside-triphosphate phosphatase
g6858	predicted protein	F	
g4392	nucleolar complex protein 3 homolog isoform X1	F, C, P	
g3125	leucine rich repeat protein	F	
g7050	transmembrane protein, putative	C	
g8728	predicted protein	F, P	
g8717	predicted protein	F	
g5292	adenylyl cyclase-associated protein 1	P	
g5104	predicted protein	F	
g5052	peptide-N4-(N-acetyl-beta-glucosaminy)asparagine amidase	F, C, P	
g6085	growth hormone-regulated TBC protein 1-A-like	F, C, P	
g8718	VPS9 domain-containing protein 1-like	C	
g5766	vacuolar protein sorting-associated protein 16	C, P	
g9630	predicted protein	F, P	
g5108	outer dynein arm docking complex protein oda-dc	C	
g4386	dynein intermediate chain 2	F	
g5036	predicted protein	F	

g6076	predicted protein	F, P	
g3846	valine--tRNA ligase, mitochondrial 1-like isoform X2	F, C, P	Valine--tRNA ligase; Carboxylesterase
g2813	chromodomain-helicase-DNA- binding protein 7	F, P	Nucleoside-triphosphate phosphatase
g6608	Serine/threonine-protein kinase HT1	F, P	
g9218	predicted protein	F,P	
g6083	midasin	F, C, P	Adenosinetriphosphatase; Nucleoside-triphosphate phosphatase
g477	guanine nucleotide-binding protein alpha-1 subunit	F, P	Nucleoside-triphosphate phosphatase
g9488	Unconventional myosin-le	F, C, P	Nucleoside-triphosphate phosphatase
g4394	transmembrane protein 60-like	F, C	
cgd1_890	eIF2 kinase IF2K-A (incomplete catalytic triad)	F, C, P	
cgd4_3400	long-chain-fatty-acid--CoA ligase 5	F	
g4401	GTPase ObgE	F	
g8723	predicted protein	F, P	
g9616	lysyl-tRNA synthetase	F, C, P	Lysine--tRNA ligase
g8720	predicted protein	F, P	
cgd6_120	protein disulfide isomerase	F, C, P	Protein disulfide- isomerase
g4499	predicted protein	F, C, P	Transferring phosphorus- containing groups; Mannosyl-oligosaccharide 1,2-alpha-mannosidase; Alpha-mannosidase
g4381	histone H3-like centromeric protein CSE4	F, C, P	
cgd7_1490	tryptophanyl-tRNA synthetase (TrpRS2)	F, C, P	Tryptophan--tRNA ligase
g5647	predicted protein	F, C, P	Adenosinetriphosphatase; Nucleoside-triphosphate phosphatase

g541	CMGC/MAPK protein Kinase	F, C, P	Transferring phosphorus-containing groups; Mitogen-activated protein kinase
cgd5_2190	DNA/RNA non-specific endonuclease family protein	F, C, P	
cgd8_2330	transhydrogenase	F, C, P	NAD(P)(+) transhydrogenase (Si-specific)
cgd2_4320	thioredoxin reductase	F, C, P	Thioredoxin-disulfide reductase
g5764	acetyl-CoA hydrolase	F, P	
g4387	tubulin alpha-3 chain-like	F, P	Nucleoside-triphosphate phosphatase
cgd7_5100	Thioredoxin family protein	F, C, P	
g4595	beta-tubulin	F, C, P	Nucleoside-triphosphate phosphatase
g4833	extracellular solute-binding protein		
g2825	Not identified		
g5264	Not identified		
g5651	Not identified		
g5778	Not identified		
g6090	Not identified		
g9055	Not identified		

\* Gene ontology hits: molecular function – F, cellular component – C, biological process – P

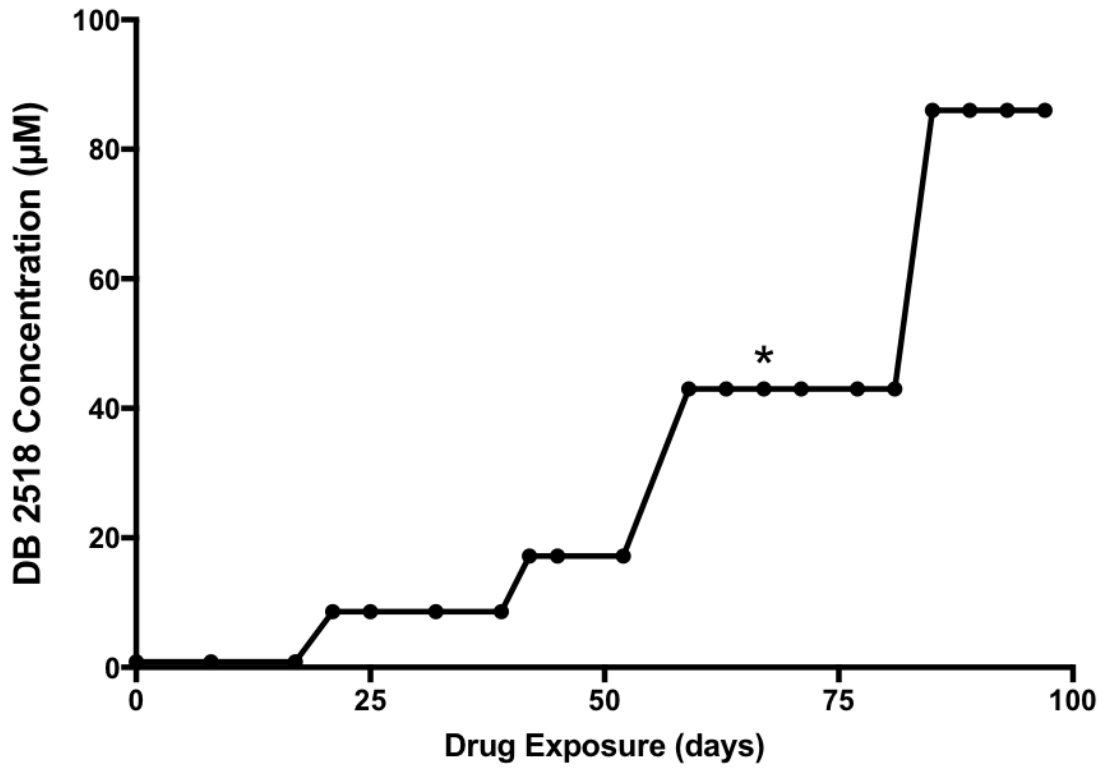


**Figure 4.1** Development of resistance for *N. fowleri* to DB 2518. Each black point marks the addition of DB 2518 to culture flasks. The asterisk represents the point when cultures were frozen and rethawed.

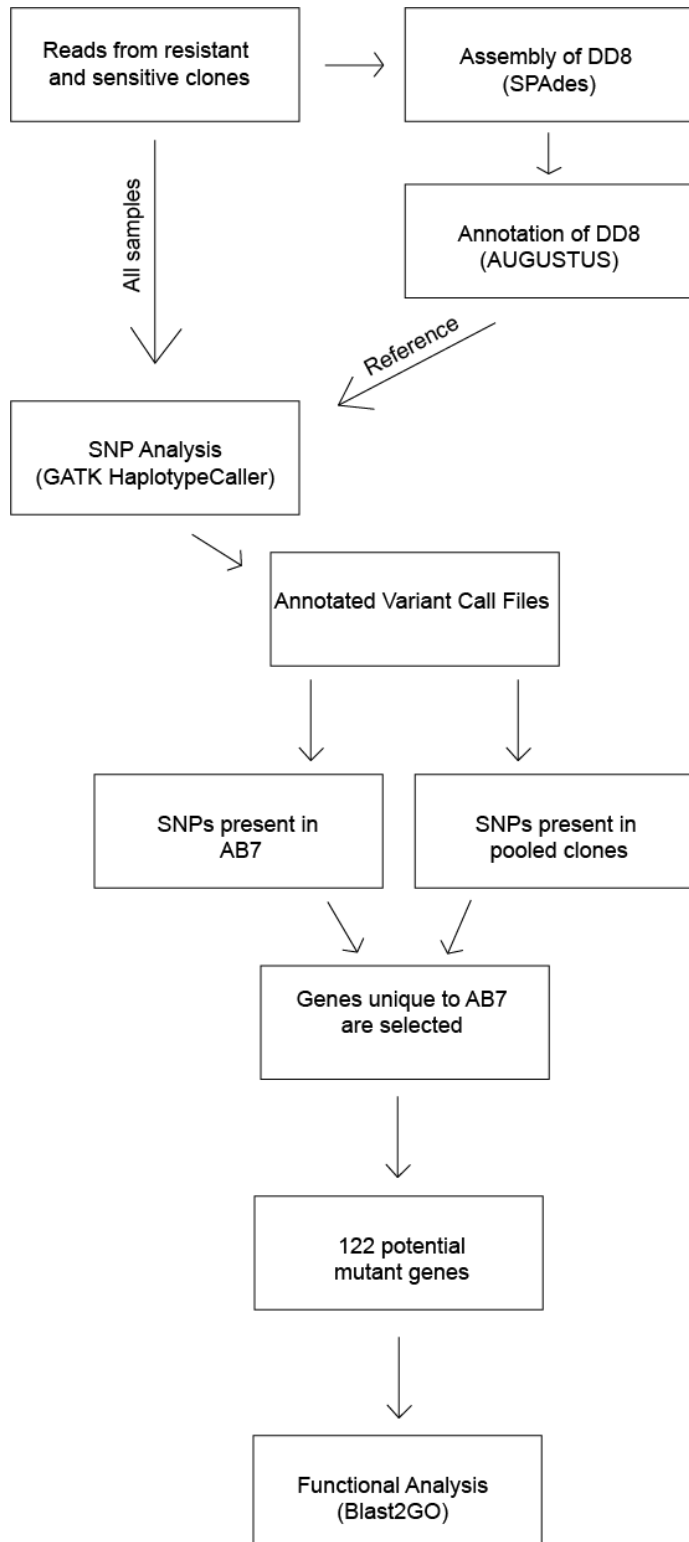


**Figure 4.2** Work flow describing the identification of potential genes that are mutated in AB7 in comparison to DD8 and the remaining clones.

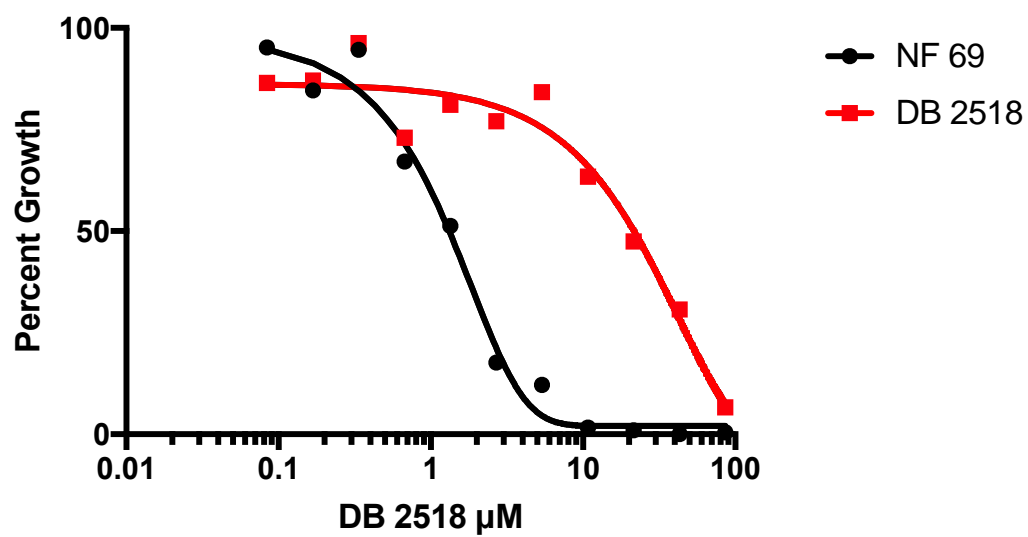


**Figure 4.3** Dose-response curves for DB 2518 with NF69 (reference strain) and NF69 cultures grown with 50x-IC<sub>50</sub> (43µM) of DB 2518.

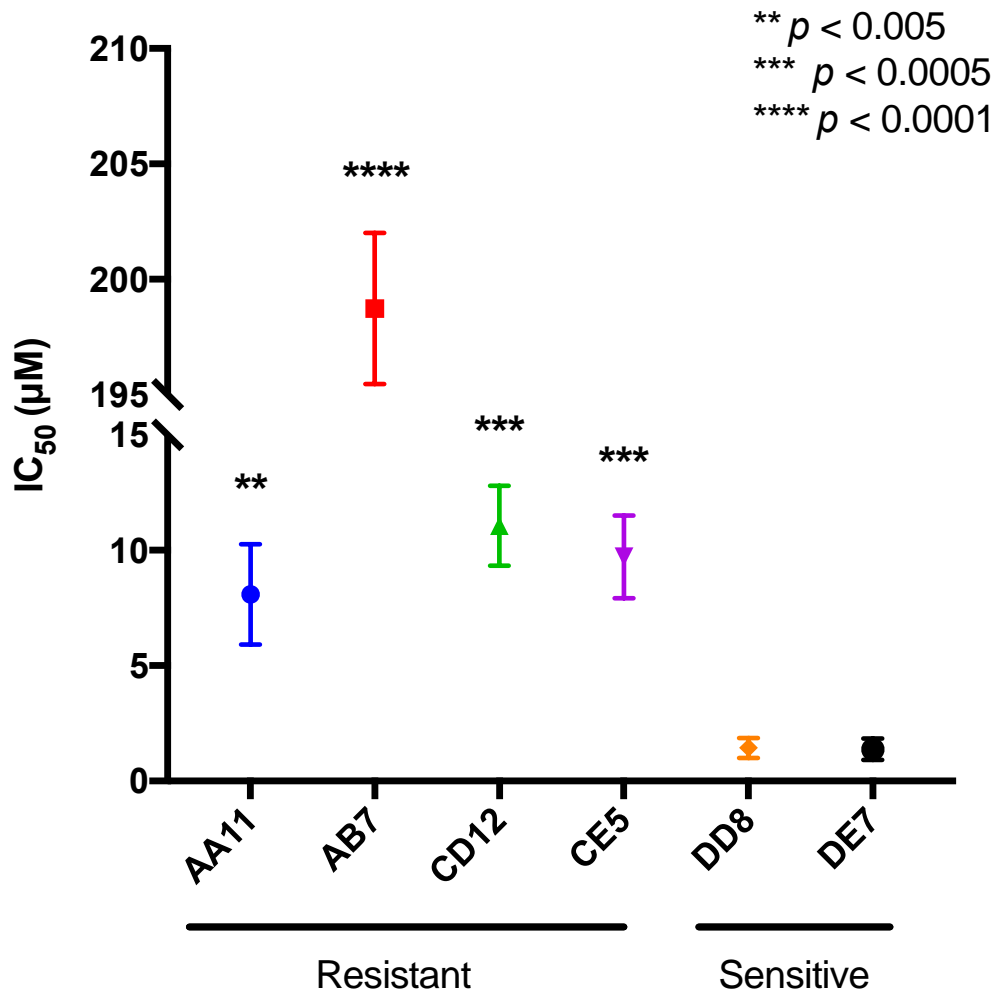


**Figure 4.4** Half maximum inhibitory concentrations (IC<sub>50</sub>) of DB 2518 with clones of *N. fowleri* grown under DB 2518 drug pressure (AA11, AB7, CD12, and CE5) and grown under normal conditions (DD8 and DE7). Clones were grown for 2 weeks without drug pressure prior to being tested (n=3).

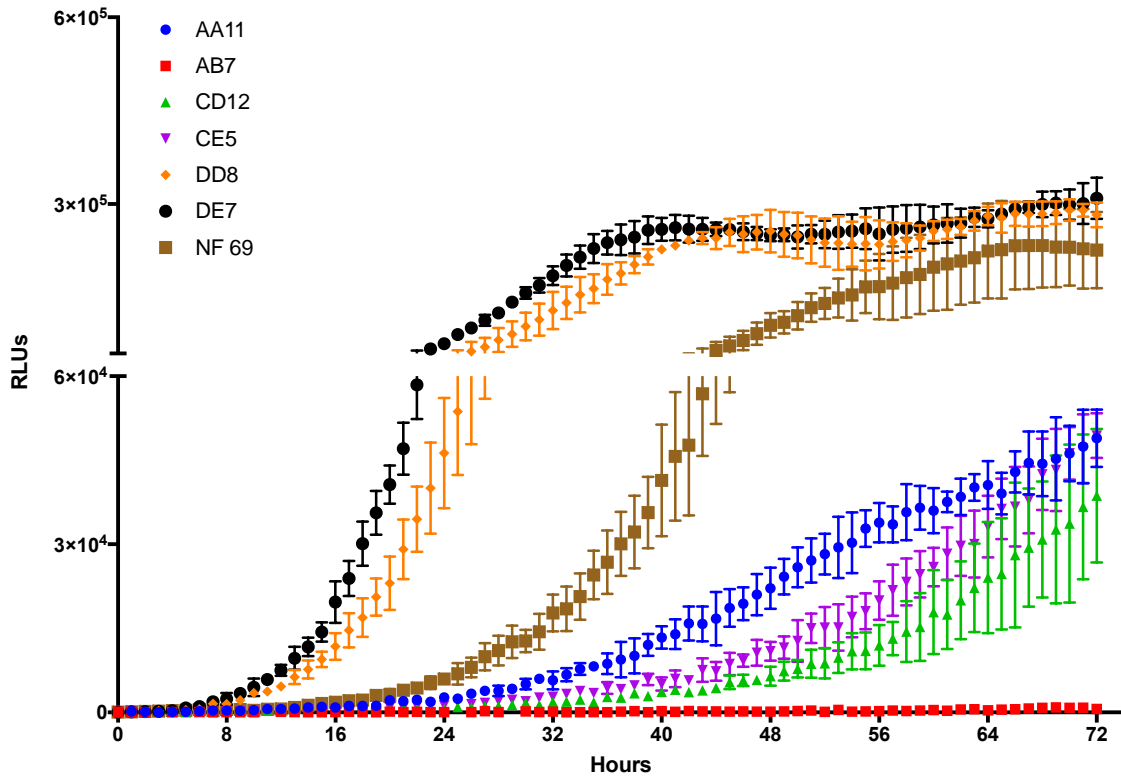


**Figure 4.5** Growth rate differences between DB 2518-resistant clones (AA11, AB7, CD12, CE5), sensitive clones (DD8 and DE7), and the reference strain (NF69). Clones were removed from drug pressure for at least 2 weeks before being tested. This data is representative of two biological replicates.



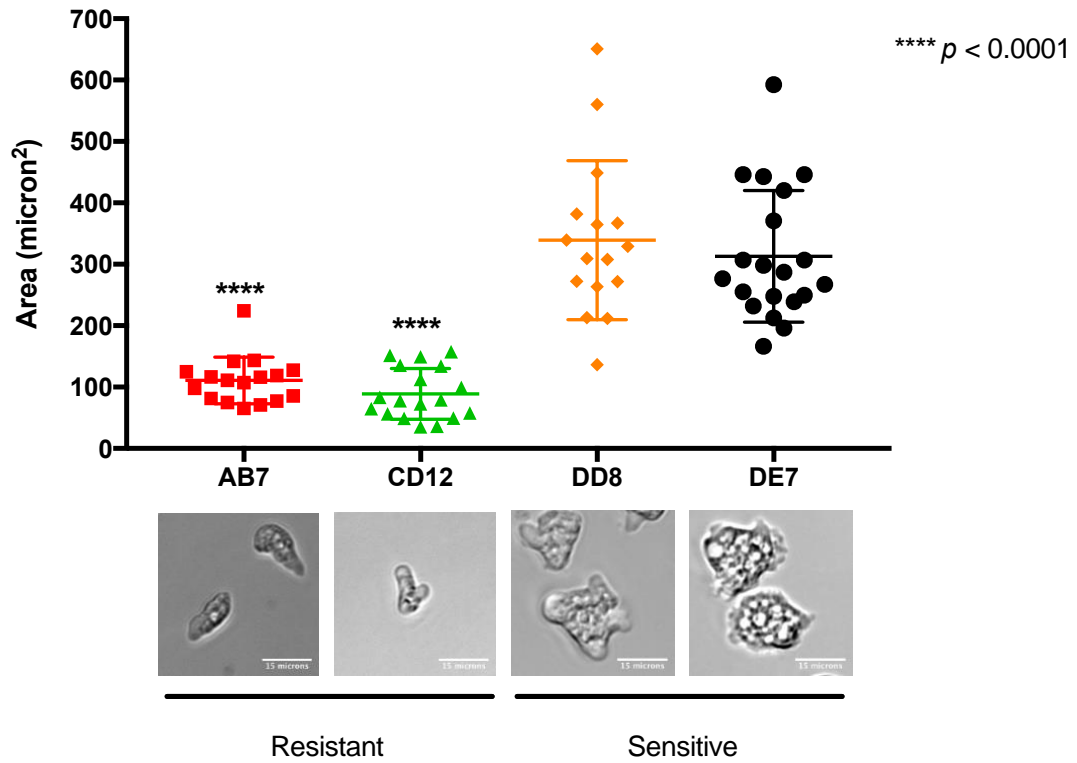


**Figure 4.6** Area of trophozoites from resistant clones, AB7 and CD12, and sensitive clones, DD8 and DE7 (n>15). AA11 and CE5 are not shown due to instability of resistance. Below are DIC images of representative trophozoites from the corresponding clonal population.

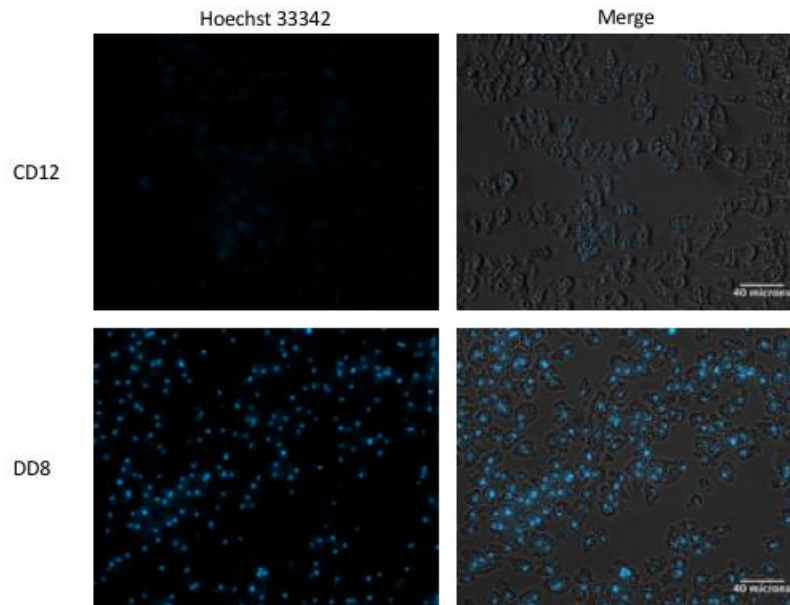


**Figure 4.7** Nuclear staining with Hoechst 33342 of resistant clone, CD12, and sensitive clone, DD8. These images are representative of the remaining resistant clones and sensitive clone (40x).

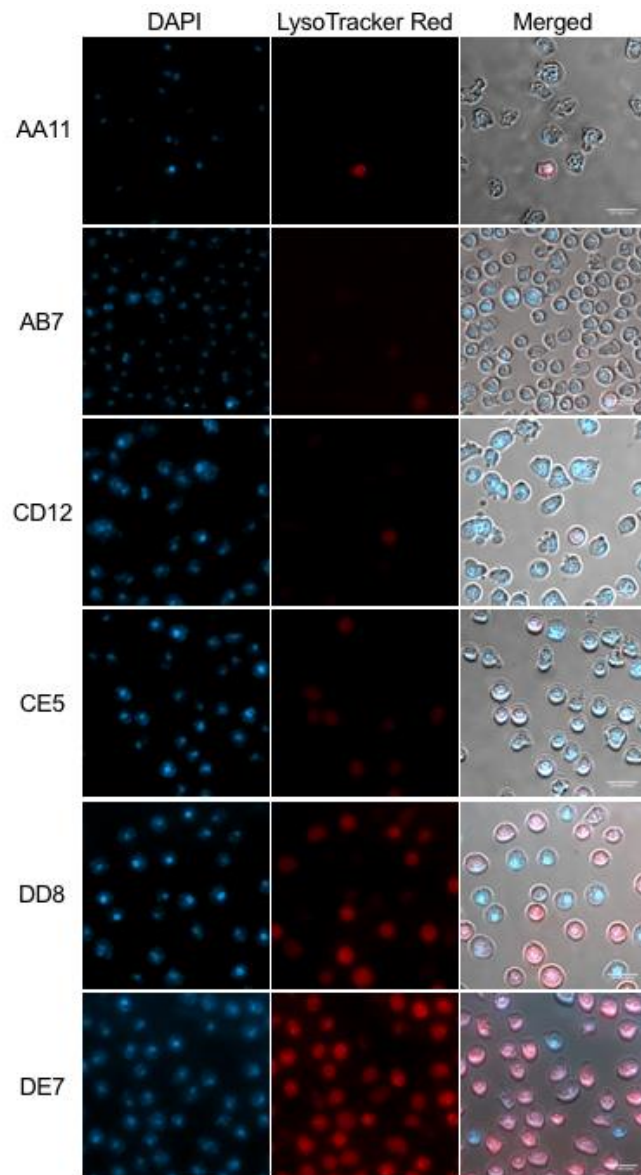


**Figure 4.8** Fluorescent imaging with DAPI and LysoTracker Red identifies a decrease in acidic vacuoles in resistant clones (40x).

## CHAPTER 5

### CONCLUSION

Primary amoebic meningoencephalitis (PAM) is a fulminant disease that is greater than 97% fatal in healthy individuals. Symptoms of disease manifest days after the free-living amoebae, *Naegleria fowleri*, is introduced into the nasal cavity. Moreover, patients succumb to death only days after symptoms such as headache, fever, nausea and vomiting, photophobia, seizures, and stiff neck arise [31]. The fast nature of the disease and the lack of effective treatments available urges the need for effective high-throughput drug discovery methods to be developed against the pathogenic amoebae.

This project aimed to bridge the gap in the free-living amoebae field with modern drug discovery techniques to assess compounds to identify the best potential treatment for PAM patients. We did this by creating a high-throughput phenotypic assay using the pathogenic *N. fowleri* to identify active compounds. Secondly, after identifying active compounds through structure-activity relationship studies or complete library screens, we further characterized compounds by their ability to work in combination with the current PAM therapeutics: azithromycin, amphotericin B and miltefosine. Lastly, we developed resistance to a novel nanomolar potent compound, DB 2518, and performed whole genome sequencing to identify mutations and elucidate a potential drug target.

With the development of two high-throughput methods against *N. fowleri*, we were able to identify two classes of compounds, bis-benzimidazole amidines and diamidines, to be potent *N. fowleri* inhibitors. This was the first identification of activity for these classes against pathogenic free-living amoebae. Importantly, the assay we developed focused on identifying compounds that showed quick inhibition, within 72 hours of drug exposure. Additionally, we screened furamide analogues, diarylbenzimidazole diamidines, diarylindole diamidines, and arylimidamides and found these scaffolds to be largely inactive. Continuing structure-activity relationship studies, we optimized monoamidino compounds and diamidino compounds to reach nanomolar potency and avoid cytotoxicity in a murine macrophage cell line. Of the bis-benzimidazole amidine class, DB 173 was found to be the most potent with an IC<sub>50</sub> of 177nM and selectivity index of 44.6. DB 1734 was the most active bis-benzimidazole diamidine with an IC<sub>50</sub> of 385nM and selectivity index of 8.4. These compounds were found to be 500 times more potent than pentamidine, which is a drug of choice for many amoebic infections [48].

In addition to structure-activity studies of active scaffolds, we identified active compounds through a large library screen of FDA-approved compounds and from the Medicines for Malaria Venture (MMV) Pathogen Box collection. We identified azithromycin to be the most potent compound from these libraries with an IC<sub>50</sub> of 20nM. Additionally we identified clarithromycin, erythromycin, and roxithromycin to be potent inhibitors, which is similar to findings in the field [110]. We also discovered valnemulin and tilmicosin to be inhibitors of *N. fowleri*, which

could be useful for veterinary PAM cases. Expectedly, we saw itraconazole, posaconazole, and ketoconazole to possess activity against *N. fowleri*. These conazoles have been shown to inhibit CYP51, an enzyme in *Naegleria fowleri* sterol biosynthesis [62]. Importantly, we also identified posaconazole to be a potent hit in the MMV Pathogen Box collection. Interestingly, the additional active compounds identified from the MMV Pathogen Box belong to the kinetoplastid disease set. Of these hits, MMV652003 was the most potent compound with an  $IC_{50}$  of  $1.1\mu\text{M}$ . MMV652003 is a leucyl-tRNA synthetase inhibitor, which has shown inhibition against *T. b. brucei* and *P. falciparum* parasites. For the first time in the free-living amoebae field, we described how quickly compounds are inhibiting the amoebae by measuring relative luminescent units hourly. Using this method, we discovered a lag of approximately 30 hours before azithromycin begins inhibiting the amoebae. In contrast, posaconazole and ketoconazole were seen to inhibit amoebae growth within the first 12 hours of exposure. Additionally, we evaluated the combinatorial activity of hits with the current PAM therapeutics: azithromycin, miltefosine, and amphotericin B. We found that posaconazole was additive when combined with each of the aforementioned compounds. Lastly, we identified posaconazole to cure 33% of *N. fowleri* infected mice with 3 doses of 20mg/kg. Moreover, when posaconazole was used in combination with azithromycin, we identified 40% more mice survived than fluconazole treated mice, which is the current conazole included in the PAM combination therapy.

In addition to high-throughput phenotypic screening, we developed a bis-benzimidazole resistant *N. fowleri* population to elucidate the potential target(s).

By analyzing the resulting mutated genes from the resistant clones in comparison to the sensitive clones, we identified potential genes that can be used to develop novel compounds to treat PAM. Moreover, we compared various phenotypic differences between the resistant and sensitive clones. We found that resistant amoebae were smaller in area, grew slower, and showed cross-resistance when tested across similarly structured compounds. This is the first study in the free-living amoebae field to develop drug-resistant amoebae to study phenotypic and genotypic variations. Importantly, the work done in this study will be able to provide the field with a reference genome.

## REFERENCES

1. Page F. An illustrated key to freshwater and soil amoebae, with notes on cultivation and ecology. Freshwater Biological Association; 1976.
2. Visvesvara GS, Moura H, Schuster FL. Pathogenic and opportunistic free-living amoebae: *Acanthamoeba* spp., *Balamuthia mandrillaris*, *Naegleria fowleri*, and *Sappinia diploidea*. FEMS Immunol. Med. Microbiol. 2007. p. 1–26.
3. Jonckheere JF De. A century of research on the amoeboflagellate genus *Naegleria*. Acta Protozool. **2002**; 41(4):309–342.
4. Heuser M, Razavi L. Amebo-flagellates as Research Partners: The Laboratory Biology of *Naegleria* and *Tetramitus*. Methods Cell Biol. 1970. p. 379–388.
5. Culbertson C. Pathogenic *Naegleria* sp.—study of a strain isolated from human cerebrospinal fluid. J Protozool **1968**; 15(2):353–363.
6. Carter RF. Description of a *Naegleria* sp. isolated from two cases of primary amoebic meningo-encephalitis, and of the experimental pathological changes induced by it. J Pathol. **1970**; 100(4):217–244.
7. Page FC. Re-Definition of the Genus *Acanthamoeba* with Descriptions of Three Species. J Protozool. **1967**; 14(4):709–724.
8. Culbertson CG, Smith JW, Minner JR. *Acanthamoeba*: Observations on animal pathogenicity. Science. **1958**; 127(3313):1506.
9. Culbertson CG, Smith JW, Cohen HK, Minner JR. Experimental Infection of Mice and Monkeys by *Acanthamoeba*. Am J Pathol. **1959**; 35(1):185–197.
10. Visvesvara GS. Epidemiology of infections with free-living amebas and laboratory diagnosis of microsporidiosis. Mt Sinai J Med. **1993**; 60(4):283–8.
11. Marciano-Cabral F, Cabral G. *Acanthamoeba* spp. as agents of disease in humans. Clin. Microbiol. Rev. **2003**; 273–307.



12. Visvesvara GS, Schuster FL, Martinez AJ. Balamuthia Mandrillaris, N. G., N. Sp., Agent of Amebic Meningoencephalitis In Humans and Other Animals. *J Eukaryot Microbiol.* **1993**; 40(4):504–514.
13. Chimelli L. A morphological approach to the diagnosis of protozoal infections of the central nervous system. *Patholog Res Int.* **2011**; 2011:290853.
14. Brondfield MN, Reid MJA, Rutishauser RL, et al. Disseminated Acanthamoeba infection in a heart transplant recipient treated successfully with a miltefosine-containing regimen: Case report and review of the literature. *Transpl Infect Dis.* **2017**; 19(2).
15. Barete S, Combes A, Jonckheere JF De, et al. Fatal disseminated Acanthamoeba lenticulata infection in a heart transplant patient. *Emerg Infect Dis.* **2007**; 13(5):736–738.
16. Visvesvara GS, Stehr-Green JK. Epidemiology of free-living ameba infections. *J Protozool.* **1990**; 37(4):25S–33S.
17. Moore MB, McCulley JP, Luckenbach M, et al. Acanthamoeba keratitis associated with soft contact lenses. *Am J Ophthalmol.* **1985**; 100(3):396–403.
18. Beattie TK, Tomlinson A, McFadyen AK, Seal D V, Grimason AM. Enhanced attachment of Acanthamoeba to extended-wear silicone hydrogel contact lenses: A new risk factor for infection? *Ophthalmology.* **2003**; 110(4):765–771.
19. Pérez-Santoja JJ, Kilvington S, Hughes R, Tufail A, Matheson M, Dart JKG. Persistently culture positive Acanthamoeba keratitis: In vivo resistance and in vitro sensitivity. *Ophthalmology.* **2003**; p. 1593–1600.
20. Khan NA. Acanthamoeba: Biology and increasing importance in human health. *FEMS Microbiol. Rev.* **2006**; p. 564–595.
21. Singhal T, Bajpai A, Kalra V, et al. Successful treatment of Acanthamoeba meningitis with combination oral antimicrobials. *Pediatr Infect Dis J.* **2001**; 20(6):623–627.
22. Seijo Martinez M, Gonzalez-Mediero G, Santiago P, et al. Granulomatous amebic encephalitis in a patient with AIDS: isolation of acanthamoeba sp. Group II from brain tissue and successful treatment with sulfadiazine and fluconazole. *J Clin Microbiol.* **2000**; 38(10):3892–5.
23. Slater CA, Sickel JZ, Visvesvara GS, Pabico RC, Gaspari AA. Successful

- Treatment of Disseminated Acanthamoeba Infection in an Immunocompromised Patient. *N Engl J Med.* **1994**; 331(2):85–87.
24. Oliva S, Jantz M, Tiernan R, Cook DL, Judson MA. Successful treatment of widely disseminated acanthamoebiasis. *South Med J.* **1999**; 92(1):55–7.
  25. Larkin DF, Kilvington S, Dart JK. Treatment of Acanthamoeba keratitis with polyhexamethylene biguanide. *Ophthalmology.* **1992**; 99(2):185–91.
  26. Gray TB, Gross KA, Cursons RT, Shewan JF. Acanthamoeba keratitis: a sobering case and a promising new treatment. *Aust N Z J Ophthalmol.* **1994**; 22(1):73–6.
  27. Illingworth CD, Cook SD, Karabatsas CH, Easty DL. Acanthamoeba keratitis: risk factors and outcome. *Br J Ophthalmol.* **1995**; 79(12):1078–82.
  28. Murdoch D, Gray TB, Cursons R, Parr D. Acanthamoeba keratitis in New Zealand, including two cases with in vivo resistance to polyhexamethylene biguanide. *Aust N Z J Ophthalmol.* **1998**; 26(3):231–6.
  29. Lindquist TD. Treatment of Acanthamoeba keratitis. *Cornea.* **1998**; 17(1):11–6.
  30. Seal D, Hay J, Kirkness C, et al. Successful medical therapy of Acanthamoeba keratitis with topical chlorhexidine and propamidine. *Eye.* **1996**; 10(4):413–421.
  31. Capewell LG, Harris AM, Yoder JS, et al. Diagnosis, clinical course, and treatment of primary amoebic meningoencephalitis in the United States, 1937-2013. *J Pediatric Infect Dis Soc.* **2015**; 4(4):68–75.
  32. Shakoor S, Beg MA, Mahmood SF, et al. Primary amoebic meningoencephalitis caused by Naegleria fowleri, Karachi, Pakistan. *Emerg Infect Dis.* **2011**; 17(2):258–261.
  33. Yoder JS, Eddy BA, Visvesvara GS, Capewell L, Beach MJ. The epidemiology of primary amoebic meningoencephalitis in the USA, 1962-2008. *Epidemiol Infect.* **2010**; 138(7):968–975.
  34. Yoder JS, Straif-Bourgeois S, Roy SL, et al. Primary amoebic meningoencephalitis deaths associated with sinus irrigation using contaminated tap water. *Clin Infect Dis.* **2012**; 55(9).
  35. Rojas-Hernández S, Jarillo-Luna A, Rodríguez-Monroy M, Moreno-Fierros L, Campos-Rodríguez R. Immunohistochemical characterization of the initial stages of Naegleria fowleri meningoencephalitis in mice. *Parasitol*

Res. **2004**; 94(1):31–36.

36. Martinez AJ, Nelson EC, Jones MM, Duma RJ, Rosenblum WI. Experimental Naegleria meningoencephalitis in mice. An electron microscope study. *Lab Investig.* **1971**; 25(5):465–75.
37. Martinez AJ, Nelson EC, Duma RJ. Animal model of human disease. Primary amebic meningoencephalitis, Naegleria meningoencephalitis, CNS protozoal infection. *Am J Pathol.* **1973**; 73(2):545–8.
38. Marciano-Cabral F, Cabral GA. The immune response to Naegleria fowleri amebae and pathogenesis of infection. *FEMS Immunol Med Microbiol.* **2007**; 51(2):243–259.
39. Martínez-Castillo M, Ramírez-Rico G, Serrano-Luna J, Shibayama M. Iron-Binding Protein Degradation by Cysteine Proteases of Naegleria fowleri. *Biomed Res Int.* **2015**; 2015:1–8.
40. Ortíz-Estrada G, Calderón-Salinas V, Shibayama-Salas M, León-Sicairos N, La Garza M De. Binding and endocytosis of bovine hololactoferrin by the parasite entamoeba histolytica. *Biomed Res Int.* **2015**; 2015.
41. Linam WM, Ahmed M, Cope JR, et al. Successful Treatment of an Adolescent With Naegleria fowleri Primary Amebic Meningoencephalitis. *Pediatrics.* **2015**; 135(3):744–748.
42. Andriole VT, Kravetz HM. The Use of Amphotericin B in Man. *JAMA.* **1962**; 180(4):269.
43. Baginski M, Sternal K, Czub J, Borowski E. Molecular modelling of membrane activity of amphotericin B , a polyene macrolide antifungal antibiotic. *Int Rev Conf Biotechnol.* **2004**; (1100):1–4.
44. Laniado-Laborín R, Cabrales-Vargas MN. Amphotericin B: side effects and toxicity. *Rev Iberoam Micol.* **2009**; 26(4):223–227.
45. Seidel JS, Harmatz P, Visvesvara GS, Cohen A, Edwards J, Turner J. Successful Treatment of Primary Amebic Meningoencephalitis. *N Engl J Med.* **1982**; 306(6):346–348.
46. Carter RF. Sensitivity to amphotericin B of a Naegleria sp. isolated from a case of primary amoebic meningoencephalitis. *J Clin Pathol.* **1969**; 22(4):470–474.
47. Goswick SM, Brenner GM. Activities of azithromycin and amphotericin B against Naegleria fowleri in vitro and in a mouse model of primary amebic

- meningoencephalitis. *J Parasitol.* **2003**; 89(2):837–842.
48. Rice CA, Colon BL, Alp M, Göker H, Boykin DW, Kyle DE. Bis-benzimidazole hits against *Naegleria fowleri* discovered with new high-throughput screens. *Antimicrob Agents Chemother.* **2015**; 59(4):2037–2044.
  49. Smorenburg C, Seynaeve C, Bontenbal M, Planting A, Sindermann H, Verweij J. Phase II study of miltefosine 6% solution as topical treatment of skin metastases in breast cancer patients. *Anti Cancer Drugs.* **2000**; 11(10):825–828.
  50. Dorlo TPC, Balasegaram M, Beijnen JH, Vries PJ de. Miltefosine: a review of its pharmacology and therapeutic efficacy in the treatment of leishmaniasis. *J Antimicrob Chemother.* **2012**; 67(11):2576–2597.
  51. Monge-Maillo B, Lopez-Velez R. Miltefosine for Visceral and Cutaneous Leishmaniasis: Drug Characteristics and Evidence-Based Treatment Recommendations. *Clin Infect Dis.* **2015**; 60(9):1398–1404.
  52. Rakotomanga M, Saint-Pierre-Chazalet M, Loiseau PM. Alteration of fatty acid and sterol metabolism in miltefosine-resistant *Leishmania donovani* promastigotes and consequences for drug-membrane interactions. *Antimicrob Agents Chemother.* **2005**; 49(7):2677–2686.
  53. Moreira W, Leprohon P, Ouellette M. Tolerance to drug-induced cell death favours the acquisition of multidrug resistance in *Leishmania*. *Cell Death Dis.* **2011**; 2(9).
  54. Centers for Disease Control and Prevention (CDC). Investigational Drug Available Directly from CDC for the Treatment of Infections with Free-Living Amebae. *MMWR. Morb. Mortal. Wkly. Rep.* 2013.
  55. Cope JR, Conrad DA, Cohen N, et al. Use of the Novel Therapeutic Agent Miltefosine for the Treatment of Primary Amebic Meningoencephalitis: Report of 1 Fatal and 1 Surviving Case. *Clin Infect Dis.* **2015**; 62(6):774–776.
  56. Cope JR, Ali IK. Primary Amebic Meningoencephalitis: What Have We Learned in the Last 5½ Years? *Curr. Infect. Dis. Rep.* **2016**; p. 31.
  57. Parnham MJ, Erakovic Haber V, Giamarellos-Bourboulis EJ, Perletti G, Verleden GM, Vos R. Azithromycin: mechanisms of action and their relevance for clinical applications. *Pharmacol Ther.* **2014**; 143(2):225–45.
  58. Champney WS, Burdine R. Azithromycin and clarithromycin inhibition of

- 50S ribosomal subunit formation in *Staphylococcus aureus* cells. *Curr Microbiol.* **1998**; 36(2):119–123.
59. Jaruratanasirikul S, Hortiwakul R, Tantisarasart T, Tussanasunthornwong S. Distribution of azithromycin into brain tissue , cerebrospinal fluid , and aqueous humor of the Distribution of Azithromycin into Brain Tissue , Cerebrospinal Fluid , and Aqueous Humor of the Eye. *Antimicrob Agents Chemother.* **1996**; 40(3):825–827.
60. Schuster FL, Visvesvara GS. Efficacy of novel antimicrobials against clinical isolates of opportunistic amebas. *J Eukaryot Microbiol.* **1998**; 45(6):612–618.
61. Soltow SM, Brenner GM. Synergistic activities of azithromycin and amphotericin B against *Naegleria fowleri* in vitro and in a mouse model of primary amebic meningoencephalitis. *Antimicrob Agents Chemother.* **2007**; 51(1):23–27.
62. Debnath A, Calvet CM, Jennings G, et al. CYP51 is an essential drug target for the treatment of primary amoebic meningoencephalitis (PAM). *PLoS Negl Trop Dis.* **2017**; 11(12).
63. Heeres J, Meerpoel L, Lewi P, Heeres J, Meerpoel L, Lewi P. Conazoles. *Molecules.* **2010**; 15(6):4129–4188.
64. Vargas-Zepeda J, Gómez-Alcalá A V, Vázquez-Morales JA, Licea-Amaya L, Jonckheere JF De, Lares-Villa F. Successful treatment of *Naegleria fowleri* meningoencephalitis by using intravenous amphotericin B, fluconazole and rifampicin. *Arch Med Res.* **2005**; 36(1):83–86.
65. Duma RJ, Finley R. In vitro susceptibility of pathogenic *Naegleria* and *Acanthamoeba* species to a variety of therapeutic agents. *Antimicrob Agents Chemother.* **1976**; 10(2):370–376.
66. Tiewcharoen S, Junnu V, Chinabut P. In vitro effect of antifungal drugs on pathogenic *Naegleria* spp. *Southeast Asian J Trop Med Public Health.* **2002**; 33(1):38–41.
67. Tiewcharoen S, Junnu V, Suvoutho S. Effect of antifungal drugs on pathogenic *Naegleria* spp isolated from natural water sources. *J Med Assoc Thai.* **2003**; 86(9):876–82.
68. Schuster FL, Guglielmo BJ, Visvesvara GS. In-vitro activity of miltefosine and Voriconazole on clinical isolates of free-living amebas: *Balamuthia mandrillaris*, *Acanthamoeba* spp., and *Naegleria fowleri*. *J Eukaryot Microbiol.* **2006**; 53(2):121–126.

69. Debnath A, Tunac JB, Galindo-Gomez S, et al. Corifungin, a new drug lead against *Naegleria*, identified from a high-throughput screen. *Antimicrob Agents Chemother.* **2012**; 56(11):5450–5457.
70. Ondarza RN, Iturbe A, Hernández E, Hernandez E. In vitro antiproliferative effects of neuroleptics, antimycotics and antibiotics on the human pathogens *Acanthamoeba polyphaga* and *Naegleria fowleri*. *Arch Med Res.* **2006**; 37(6):723–729.
71. Kim J-HH, Jung S-YY, Lee Y-JJ, et al. Effect of therapeutic chemical agents in vitro and on experimental meningoencephalitis due to *Naegleria fowleri*. *Antimicrob Agents Chemother.* **2008**; 52(11):4010–4016.
72. Sateriale A, Bessoff K, Sarkar IN, Huston CD. Drug repurposing: mining protozoan proteomes for targets of known bioactive compounds. *J Am Med Informatics Assoc.* **2014**; 21(2):238–244.
73. Merchant M, Thibodeaux D, Loubser K, Elsey RM. Amoebacidal effects of serum from the American Alligator (*Alligator mississippiensis*). *J Parasitol.* **2004**; 90(6):1480–1483.
74. Hobson RP. The effects of diffusates from the spores of *Aspergillus fumigatus* and *A. terreus* on human neutrophils, *Naegleria gruberi* and *Acanthamoeba castellanii*. *Med Mycol.* **2000**; 38(2):133–41.
75. Nagington J, Richards JE. Chemotherapeutic compounds and *Acanthamoebae* from eye infections. *J. clin. Path.* 1976.
76. Fowler M, Carter RF. Acute pyogenic meningitis probably due to *Acanthamoeba* sp.: a preliminary report. *Br Med J.* **1965**; 2(5464):740–742.
77. Siddiqui R, Khan NA. Primary amoebic meningoencephalitis caused by *Naegleria fowleri*: an old enemy presenting new challenges. *PLoS Negl Trop Dis.* **2014**; 8(8)
78. Kadlec V, Skvarova J, Cerva L, Nebazniva D. Virulent *Naegleria fowleri* in indoor swimming pool. *Folia Parasitol (Praha).* **1980**; 27(1):11–17.
79. Martinez J, Duma RJ, Nelson EC, Moretta FL. Experimental naegleria meningoencephalitis in mice. Penetration of the olfactory mucosal epithelium by *Naegleria* and pathologic changes produced: a light and electron microscope study. *Lab Invest.* **1973**; 29(2):121–133.
80. Ondarza RN, Iturbe A, Hernandez E. The effects by neuroleptics, antimycotics and antibiotics on disulfide reducing enzymes from the human

- pathogens *Acanthamoeba polyphaga* and *Naegleria fowleri*. *Exp Parasitol* **2007**; 115(1):41–47.
81. Visvesvara GS. Amebic meningoencephalitis and keratitis: Challenges in diagnosis and treatment. *Curr. Opin. Infect. Dis.* **2010**; p. 590–594.
  82. Schuster FL, Visvesvara GS. Opportunistic amoebae: challenges in prophylaxis and treatment. *Drug Resist Updat* **2004**; 7(1):41–51.
  83. Perrine D, Chenu JP, Georges P, Lancelot JC, Saturnino C, Robba M. Amoebicidal efficiencies of various diamidines against two strains of *Acanthamoeba polyphaga*. *Antimicrob Agents Chemother.* **1995**; 39(2):339–342.
  84. Wenzler T, Yang S, Patrick DA, et al. In vitro and in vivo evaluation of 28DAP010, a novel diamidine for treatment of second-stage African sleeping sickness. *Antimicrob Agents Chemother.* **2014**; 58(8):4452–4463.
  85. Wang MZ, Zhu X, Srivastava A, et al. Novel arylimidamides for treatment of visceral leishmaniasis. *Antimicrob Agents Chemother.* **2010**; 54(6):2507–2516.
  86. Hu L, Kully ML, Boykin DW, Abood N. Optimization of the central linker of dicationic bis-benzimidazole anti-MRSA and anti-VRE agents. *Bioorg Med Chem Lett.* **2009**; 19(13):3374–3377.
  87. Farahat AA, Paliakov E, Kumar A, et al. Exploration of larger central ring linkers in furamidine analogues: synthesis and evaluation of their DNA binding, antiparasitic and fluorescence properties. *Bioorg Med Chem.* **2011**; 19(7):2156–2167.
  88. Souza EM de, Oliveira GM, Boykin DW, et al. Trypanocidal activity of the phenyl-substituted analogue of furamidine DB569 against *Trypanosoma cruzi* infection in vivo. *J Antimicrob Chemother.* **2006**; 58(3):610–614.
  89. Souza EM De, Lansiaux A, Bailly C, et al. Phenyl substitution of furamidine markedly potentiates its anti-parasitic activity against *Trypanosoma cruzi* and *Leishmania amazonensis*. *Biochem Pharmacol.* **2004**; 68(4):593–600.
  90. Czarny A, Wilson WD, Boykin DW. Synthesis of mono-cationic and dicationic analogs of Hoechst 33258. *J Heterocycl Chem.* **1996**; 33(4):1393–1397.
  91. Chaires JB, Ren J, Hamelberg D, et al. Structural selectivity of aromatic diamidines. *J Med Chem.* **2004**; 47(23):5729–5742.

92. Brendle JJ, Outlaw A, Kumar A, et al. Antileishmanial activities of several classes of aromatic dications. *Antimicrob Agents Chemothe*. **2002**; 46(3):797–807.
93. Stephens CE, Tanious F, Kim S, et al. Diguanidino and “reversed” diamidino 2,5-diarylfurans as antimicrobial agents. *J Med Chem*. **2001**; 44(11):1741–1748.
94. Paine MF, Wang MZ, Generaux CN, et al. Diamidines for human African trypanosomiasis. *Curr Opin Investig Drugs*. **2010**; 11(8):876–883.
95. Lansiaux A, Tanious F, Mishal Z, et al. Distribution of furamidine analogues in tumor cells: targeting of the nucleus or mitochondria depending on the amidine substitution. *Cancer Res*. **2002**; 62(24):7219–7229.
96. Ismail MA, Brun R, Easterbrook JD, Tanious FA, Wilson WD, Boykin DW. Synthesis and antiprotozoal activity of aza-analogues of furamidine. *J Med Chem*. **2003**; 46(22):4761–4769.
97. Ismail MA, Batista-Parra A, Miao Y, et al. Dicationic near-linear biphenyl benzimidazole derivatives as DNA-targeted antiprotozoal agents. *Bioorg Med Chem*. **2005**; 13(24):6718–6726.
98. Ismail MA, Arafa RK, Brun R, et al. Synthesis, DNA affinity, and antiprotozoal activity of linear dications: Terphenyl diamidines and analogues. *J Med Chem*. **2006**; 49(17):5324–5332.
99. Hu LX, Kully ML, Boykin DW, Abood N. Synthesis and structure-activity relationship of dicationic diaryl ethers as novel potent anti-MRSA and anti-VRE agents. *Bioorg Med Chem Lett*. **2009**; 19(16):4626–4629.
100. Hu LX, Kully ML, Boykin DW, Abood N. Synthesis and in vitro activity of dicationic bis-benzimidazoles as a new class of anti-MRSA and anti-VRE agents. *Bioorg Med Chem Lett*. **2009**; 19(5):1292–1295.
101. Wenzler T, Yang S, Braissant O, Boykin DW, Brun R, Wang MZ. Pharmacokinetics, *Trypanosoma brucei gambiense* efficacy, and time of drug action of DB829, a preclinical candidate for treatment of second-stage human African trypanosomiasis. *Antimicrob Agents Chemother*. **2013**; 57(11):5330–5343.
102. Yang S, Wenzler T, Miller PN, et al. Pharmacokinetic comparison to determine the mechanisms underlying the differential efficacies of cationic diamidines against first- and second-stage human African trypanosomiasis. *Antimicrob Agents Chemother*. **2014**; 58(7):4064–4074.



103. Thuita JK, Wang MZ, Kagira JM, et al. Pharmacology of DB844, an orally active aza analogue of pafuramidine, in a monkey model of second stage human African trypanosomiasis. *PLoS Negl Trop Dis.* **2012**; 6(7).
104. Schorer M, Debache K, Barna F, et al. Di-cationic arylimidamides act against *Neospora caninum* tachyzoites by interference in membrane structure and nucleolar integrity and are active against challenge infection in mice. *Int J Parasitol Drugs Drug Resist.* **2012**; 2:109–120.
105. McBride J, Ingram PR, Henriquez FL, Roberts CW. Development of colorimetric microtiter plate assay for assessment of antimicrobials against *Acanthamoeba*. *J Clin Microbiol.* **2005**; 43(2):629–634.
106. Alp M, Goker H, Brun R, Yildiz S. Synthesis and antiparasitic and antifungal evaluation of 2'-arylsubstituted-1H,1'-H-[2,5']bisbenzimidazolyl-5-carboxamidines. *Eur J Med Chem.* **2009**; 44(5):2002–2008.
107. Hu L, Patel A, Bondada L, et al. Synthesis and antiprotozoal activity of dicationic 2,6-diphenylpyrazines and aza-analogues. *Bioorg Med Chem.* **2013**; 21(21):6732–6741.
108. Jimenez-Diaz MB, Ebert D, Salinas Y, et al. (+)-SJ733, a clinical candidate for malaria that acts through ATP4 to induce rapid host-mediated clearance of *Plasmodium*. *Proc Natl Acad Sci U S A.* **2014**; 111(50):E5455-62.
109. Guiguemde WA, Shelat AA, Bouck D, et al. Chemical genetics of *Plasmodium falciparum*. *Nature.* **2010**; 465(7296):311–315.
110. Kim JH, Lee YJ, Sohn HJ, et al. Therapeutic effect of rokitamycin in vitro and on experimental meningoencephalitis due to *Naegleria fowleri*. *Int J Antimicrob Agents.* **2008**; 32(5):411–417.
111. Poeta M Del, Schell WA, Dykstra CC, et al. In vitro antifungal activities of a series of dication-substituted carbazoles, furans, and benzimidazoles. *Antimicrob Agents Chemother.* **1998**; 42(10):2503–10.
112. Martinez AJ. Free-living amoebas; natural history, prevention, diagnosis, pathology and treatment of disease. Boca Raton, FL: CRC Press; 1985.
113. Centers for Disease Control and Prevention. *Naegleria fowleri* — Primary Amebic Meningoencephalitis (PAM) — Amebic Encephalitis. 2014.
114. Matanock A, Mehal JM, Liu L, Blau DM, Cope JR. Estimation of undiagnosed *Naegleria fowleri* primary amebic meningoencephalitis, United States. *Emerg. Infect. Dis. Centers for Disease Control and Prevention*; 2018. p. 162–164.

115. Irazuzta JE, Pretzlaff R, Rowin M, Milam K, Zemlan FP, Zingarelli B. Hypothermia as an adjunctive treatment for severe bacterial meningitis. *Brain Res. Elsevier*; **2000**; 881(1):88–97.
116. Polderman KH, Herold I. Therapeutic hypothermia and controlled normothermia in the intensive care unit: Practical considerations, side effects, and cooling methods. *Crit. Care Med.* **2009**; 1101–1120.
117. Zyserman I, Mondal D, Sarabia F, McKerrow JH, Roush WR, Debnath A. Identification of cysteine protease inhibitors as new drug leads against *Naegleria fowleri*. *Exp Parasitol.* **2018**; 188:36–41.
118. Medicines for Malaria Venture. The Pathogen Box | Catalysing neglected disease drug discovery. *Med. Malar. Ventur.* 2016.
119. Lotharius J, Gamo-Benito FJ, Angulo-Barturen I, et al. Repositioning: The fast track to new anti-malarial medicines? *Malar J. BioMed Central*; **2014**; 13(1):143.
120. Voorhis WC Van, Adams JH, Adelfio R, et al. Open Source Drug Discovery with the Malaria Box Compound Collection for Neglected Diseases and Beyond. *PLoS Pathog.* **2016**; 12(7).
121. Šperling D, Čížek A, Smola J. Effect of zinc chelate and valnemulin for the treatment of swine dysentery in an experimental challenge study. *Res Vet Sci.* **2014**; 96(1):30–32.
122. Gorham PE, Carroll LH, McAskill JW, et al. Tilmicosin as a single injection treatment for respiratory disease of feedlot cattle. *Can Vet J.* **1990**; 31(12):826–9.
123. Nare B, Wring S, Bacchi C, et al. Discovery of novel orally bioavailable oxaborole 6-carboxamides that demonstrate cure in a murine model of late-stage central nervous system African trypanosomiasis. *Antimicrob Agents Chemother.* **2010**; 54(10):4379–4388.
124. Duffy S, Sykes ML, Jones AJ, et al. Screening the medicines for malaria venture pathogen box across multiple pathogens reclassifies starting points for open-source drug discovery. *Antimicrob Agents Chemother.* **2017**; 61(9).
125. Partridge FA, Brown AE, Buckingham SD, et al. An automated high-throughput system for phenotypic screening of chemical libraries on *C. elegans* and parasitic nematodes. *Int J Parasitol Drugs Drug Resist.* **2018**; 8(1):8–21.

126. Frearson JA, Brand S, McElroy SP, et al. N-myristoyltransferase inhibitors as new leads to treat sleeping sickness. *Nature*. **2010**; 464(7289):728–732.
127. Roberts AJ, Torrie LS, Wyllie S, Fairlamb AH. Biochemical and genetic characterization of *Trypanosoma cruzi* N-myristoyltransferase. *Biochem J*. **2014**; 459(2):323–332.
128. Bayliss T, Robinson DA, Smith VC, et al. Design and Synthesis of Brain Penetrant Trypanocidal N-Myristoyltransferase Inhibitors. *J Med Chem*. **2017**; 60(23):9790–9806.
129. Müller J, Aguado A, Laleu B, Balmer V, Ritler D, Hemphill A. In vitro screening of the open source Pathogen Box identifies novel compounds with profound activities against *Neospora caninum*. *Int J Parasitol*. **2017**; 47(12):801–809.
130. Spalenka J, Escotte-Binet S, Bakiri A, et al. Discovery of new inhibitors of *Toxoplasma gondii* via the pathogen box. *Antimicrob Agents Chemother*. **2018**; 62(2).
131. Greer ND. Posaconazole (Noxafil): a new triazole antifungal agent. *Proc (Bayl Univ Med Cent)*. **2007**; 20(2):188–96.
132. Iwatani W, Arika T, Yamaguchi H. Two mechanisms of butenafine action in *Candida albicans*. *Antimicrob Agents Chemother*. **1993**; 37(4):785–8.
133. Sharma M, Sudhan SS, Sharma S, Megha K, Nada R, Khurana S. Osteocutaneous acanthamoebiasis in a non-immunocompromised patient with a favorable outcome. *Parasitol Int*. **2017**; 66(6):727–730.
134. Kethireddy S, Andes D. CNS pharmacokinetics of antifungal agents. *Expert Opin Drug Metab Toxicol*. **2007**; 3(4):573–581.
135. WHO Model List of Essential Medicines. 2017. Available from: <http://www.who.int/medicines/publications/essentialmedicines/en/>
136. Thuita JK, Karanja SM, Wenzler T, et al. Efficacy of the diamidine DB75 and its prodrug DB289, against murine models of human African trypanosomiasis. *Acta Trop*. **2008**; 108(1):6–10.
137. Boykin DW. Antimicrobial activity of the DNA minor groove binders furamidine and analogs. *J Braz Chem Soc. Brazilian Chemical Society*; **2002**; 13(6):763–771.
138. Lanteri CA, Tidwell RR, Meshnick SR. The Mitochondrion Is a Site of

Trypanocidal Action of the Aromatic Diamidine DB75 in Bloodstream Forms of *Trypanosoma brucei* Downloaded from. *Antimicrob Agents Chemother.* **2008**; 52(3):875–882.

139. Pandharkar T, Zhu X, Mathur R, et al. Studies on the Antileishmanial Mechanism of Action of the Arylimidamide DB766: Azole Interactions and Role of CYP5122A1. *Antimicrob Agents Chemother.* **2014**; 58(8):4682–4689.
140. Basselin M, Denise H, Coombs GH, Barrett MP. Resistance to pentamidine in *Leishmania mexicana* involves exclusion of the drug from the mitochondrion. *Antimicrob Agents Chemother.* **2002**; 46(12):3731–3738.
141. Bolger AM, Lohse M, Usadel B. Trimmomatic: a flexible trimmer for Illumina sequence data. *Bioinformatics.* **2014**; 30(15):2114–2120.
142. Bankevich A, Nurk S, Antipov D, et al. SPAdes: a new genome assembly algorithm and its applications to single-cell sequencing. *J Comput Biol.* **2012**; 19(5):455–77.
143. Tamazian G, Dobrynin P, Krasheninnikova K, Komissarov A, Koepfli K-P, O'Brien SJ. Chromosomer: a reference-based genome arrangement tool for producing draft chromosome sequences. *Gigascience.* **2016**; 5(1):38.
144. Boetzer M, Pirovano W. Toward almost closed genomes with GapFiller. *Genome Biol.* **2012**; 13(6):R56.
145. Walker BJ, Abeel T, Shea T, et al. Pilon: an integrated tool for comprehensive microbial variant detection and genome assembly improvement. *PLoS One.* **2014**; 9(11):e112963.
146. Borodovsky M, Lomsadze A. Eukaryotic gene prediction using GeneMark.hmm-E and GeneMark-ES. *Curr Protoc Bioinforma.* **2011**; Chapter 4(1):Unit 4.6.1-10.
147. Stanke M, Morgenstern B. AUGUSTUS: a web server for gene prediction in eukaryotes that allows user-defined constraints. *Nucleic Acids Res.* **2005**; 33.
148. Li H, Durbin R. Fast and accurate short read alignment with Burrows-Wheeler transform. *Bioinformatics.* **2009**; 25(14):1754–60.
149. Cingolani P, Platts A, Wang LL, et al. A program for annotating and predicting the effects of single nucleotide polymorphisms, SnpEff: SNPs in the genome of *Drosophila melanogaster* strain w1118; iso-2; iso-3. *Fly.* **2012**; 6(2):80–92.

150. Zysset-Burri DC, Müller N, Beuret C, et al. Genome-wide identification of pathogenicity factors of the free-living amoeba *Naegleria fowleri*. *BMC Genomics*. **2014**. (15)1:496.
151. Oates PJ, Touster O. In vitro fusion of *Acanthamoeba* phagolysosomes. II Quantitative characterization of in vitro vacuole fusion by improved electron microscope and new light microscope techniques. *J Cell Biol*. **1978**; 79(1):217–34.
152. Sambade M, Alba M, Smardon A, et al. A genomic screen for yeast vacuolar membrane ATPase mutants. *Genetics*. **2005**; 170(4): 1539-51.

AMERICAN  
SOCIETY FOR  
MICROBIOLOGY**Title:** Bis-Benzimidazole Hits against Naegleria fowleri Discovered with New High-Throughput Screens**Author:** Christopher A. Rice, Beatrice L. Colon, Mehmet Alp et al.**Publication:** Antimicrobial Agents and Chemotherapy**Publisher:** American Society for Microbiology**Date:** Apr 1, 2015

Copyright © 2015, American Society for Microbiology

**LOGIN**

If you're a **copyright.com user**, you can login to RightsLink using your copyright.com credentials.

Already a **RightsLink user** or want to [learn more?](#)

**Permissions Request**

Authors in ASM journals retain the right to republish discrete portions of his/her article in any other publication (including print, CD-ROM, and other electronic formats) of which he or she is author or editor, provided that proper credit is given to the original ASM publication. ASM authors also retain the right to reuse the full article in his/her dissertation or thesis. For a full list of author rights, please see: [http://journals.asm.org/site/misc/ASM\\_Author\\_Statement.xhtml](http://journals.asm.org/site/misc/ASM_Author_Statement.xhtml)

[BACK](#)[CLOSE WINDOW](#)

**OXFORD UNIVERSITY PRESS LICENSE  
TERMS AND CONDITIONS**

Nov 03, 2018

This Agreement between Ms. Beatrice Colon ("You") and Oxford University Press ("Oxford University Press") consists of your license details and the terms and conditions provided by Oxford University Press and Copyright Clearance Center.

License Number	4461380951029
License date	Nov 03, 2018
Licensed content publisher	Oxford University Press
Licensed content publication	Journal of Infectious Diseases
Licensed content title	Phenotypic screens reveal posaconazole as rapidly cidal combination partner for treatment of Primary Amoebic Meningoencephalitis
Licensed content author	Colon, Beatrice L; Rice, Christopher A
Licensed content date	Oct 24, 2018
Type of Use	Thesis/Dissertation
Institution name	
Title of your work	Phenotypic screens reveal posaconazole as rapidly cidal combination partner for treatment of Primary Amoebic Meningoencephalitis
Publisher of your work	University of Georgia
Expected publication date	Dec 2018
Permissions cost	0.00 USD
Value added tax	0.00 USD
Total	0.00 USD
Title	Phenotypic screens reveal posaconazole as rapidly cidal combination partner for treatment of Primary Amoebic Meningoencephalitis
Institution name	University of Georgia
Expected presentation date	Dec 2018
Requestor Location	Ms. Beatrice Colon 500 DW Brooks Drive Ste 370  ATHENS, GA 30606 United States Attn: Ms. Beatrice Colon
Publisher Tax ID	GB125506730
Billing Type	Invoice
Billing Address	Ms. Beatrice Colon 500 DW Brooks Drive Ste 370  ATHENS, GA 30606 United States Attn: Ms. Beatrice Colon
Total	0.00 USD
Terms and Conditions	

**STANDARD TERMS AND CONDITIONS FOR REPRODUCTION OF MATERIAL  
FROM AN OXFORD UNIVERSITY PRESS JOURNAL**

1. Use of the material is restricted to the type of use specified in your order details.
2. This permission covers the use of the material in the English language in the following territory: world. If you have requested additional permission to translate this material, the terms and conditions of this reuse will be set out in clause 12.
3. This permission is limited to the particular use authorized in (1) above and does not allow you to sanction its use elsewhere in any other format other than specified above, nor does it apply to quotations, images, artistic works etc that have been reproduced from other sources which may be part of the material to be used.
4. No alteration, omission or addition is made to the material without our written consent. Permission must be re-cleared with Oxford University Press if/when you decide to reprint.
5. The following credit line appears wherever the material is used: author, title, journal, year, volume, issue number, pagination, by permission of Oxford University Press or the sponsoring society if the journal is a society journal. Where a journal is being published on behalf of a learned society, the details of that society must be included in the credit line.
6. For the reproduction of a full article from an Oxford University Press journal for whatever purpose, the corresponding author of the material concerned should be informed of the proposed use. Contact details for the corresponding authors of all Oxford University Press journal contact can be found alongside either the abstract or full text of the article concerned, accessible from [www.oxfordjournals.org](http://www.oxfordjournals.org) Should there be a problem clearing these rights, please contact [journals.permissions@oup.com](mailto:journals.permissions@oup.com)
7. If the credit line or acknowledgement in our publication indicates that any of the figures, images or photos was reproduced, drawn or modified from an earlier source it will be necessary for you to clear this permission with the original publisher as well. If this permission has not been obtained, please note that this material cannot be included in your publication/photocopies.
8. While you may exercise the rights licensed immediately upon issuance of the license at the end of the licensing process for the transaction, provided that you have disclosed complete and accurate details of your proposed use, no license is finally effective unless and until full payment is received from you (either by Oxford University Press or by Copyright Clearance Center (CCC)) as provided in CCC's Billing and Payment terms and conditions. If full payment is not received on a timely basis, then any license preliminarily granted shall be deemed automatically revoked and shall be void as if never granted. Further, in the event that you breach any of these terms and conditions or any of CCC's Billing and Payment terms and conditions, the license is automatically revoked and shall be void as if never granted. Use of materials as described in a revoked license, as well as any use of the materials beyond the scope of an unrevoked license, may constitute copyright infringement and Oxford University Press reserves the right to take any and all action to protect its copyright in the materials.
9. This license is personal to you and may not be sublicensed, assigned or transferred by you to any other person without Oxford University Press's written permission.
10. Oxford University Press reserves all rights not specifically granted in the combination of (i) the license details provided by you and accepted in the course of this licensing transaction, (ii) these terms and conditions and (iii) CCC's Billing and Payment terms and conditions.
11. You hereby indemnify and agree to hold harmless Oxford University Press and CCC, and their respective officers, directors, employs and agents, from and against any and all claims arising out of your use of the licensed material other than as specifically authorized pursuant to this license.
12. Other Terms and Conditions:

v1.4

**Questions? [customercare@copyright.com](mailto:customercare@copyright.com) or +1-855-239-3415 (toll free in the US) or +1-978-646-2777.**